Studies on the Cellular and Molecular Regulation of Cardiovascular Development

By

Elise Rachel Pfaltzgraff

Dissertation

Submitted to the Faculty of the

Graduate School of Vanderbilt Univeristy

in partial fulfillment of the requirements

for the degree of

DOCTOR OF PHILOSOPHY

in

Cell and Developmental Biology

August, 2014

Nashville, Tennessee

Approved:

Jeff Reese, M.D.

David M. Bader, Ph.D.

Ellen Dees, M.D.

Chee C. Lim, Ph.D.

Ryoma Ohi, Ph.D.

To my parents,

Allyson and George Pfaltzgraff,

for your constant love and support.

ACKNOWLEDGEMENTS

This work was made financially possible with the support of the Program in Developmental Biology Training Grant and the Certificate Program for Molecular Medicine. My research was funded by an American Heart Association predoctoral fellowship and grant in aid. I am additionally grateful for the Program in Developmental Biology and Cell and Developmental Biology Department leaders and staff for fostering a great environment for trainees.

My graduate school mentors, Dr. Trish Labosky and Dr. David Bader both provided excellent environments in which to grow as a scientist. I thank them both for letting me into their labs and mentoring me along my time in graduate school. To Trish, thank you for taking me in as an undergrad and being patient with me as I learned my way around the lab. Those summers were critical both for me to decide to attend graduate school and to get my feet under myself when it came to bench research. Dr. Bader, thank you for giving me a second lab home and allowing me to complete my thesis work in your lab. I also greatly appreciate the freedom I have been given to pursue projects outside of basic research under my tenure in the Bader lab. Being able to experience two very different lab environments over a long period of time has helped me refine my own research interests and management styles.

I would also like to thank the members of my committee, Jeff Reese, Ellen Dees, Chee Lim, Ryoma Ohi, and Lawrence Prince. Not only did my committee provide critical guidance for my science, many of the techniques I have used in my research were learned

in the laboratories of my committee members. As collaborators they have been generous both with their time and their resources.

Vanderbilt Univeristy has been a great place to grow as scientist. One of the great aspects of Vanderbilt is the high quality CORE facilities and staff. Two of the most important facilities are the CISR and the Epithelial Biology Core, particularly Sean Schaffer and Joseph Roland. These two were instrumental in teaching me how to capture quality images and properly analyze my data.

Next I need to thank all the wonderful people I have worked with in my different lab homes. First, I appreciate all the people I worked with in the Labosky lab: Tong Wang, Audrey Frist, Alison LeGrone, Jenny Plank, Brian Nelms, Nathan Mundell, and Michael Suflita. Many of these people not only helped me decide I wanted to go to graduate school in the first place, but also helped me get comfortable at the bench. Alison was instrumental in helping me learn how to manage a mouse colony. I feel like I never fully appreciated everything she did until she was gone. Next, the Bader lab has been a great second home for me. Cheryl Seneff, Niki Winters, Becca Thomason, Paul Miller, Sam Reddy, and Elaine Shelton all helped me feel welcome and a full member of the Bader lab. My current bay mate, Annabelle Williams, and our adopted lab, Annie Gintzig and Scott Borinstein, have continued to make lab a productive and fun place to grow as a scientist. Finally, I want to thank my CPMM home. My time in the CPMM helped me discover my passion for clinical and translation research. Ellen Dees, my clinical mentor, and the leaders of the CPMM, Lou Muglia, Mark de Caestecker, Abigail Brown, and Nadia Ehtesham, allowed me to have the opportunity to explore the world of clinical

research open to Ph.D.'s. The friendships I made through the CPMM have made the years of research go by a little smoother, and I thank them for that.

I also need to thank Mrs. Peterson, Mr. Beversdorf, Mr. Jacobson, and Professor Wall for challenging me and preparing me for this path I have taken in life. Your strong influence in my life has inspired my interest in teaching.

Last but not least I need to thank my family. I ventured as far from home as I dared to pursue my graduate work. Thank you for putting up with me being so far away. Mom and Dad, thank you for raising me surrounded by inquiry and learning. It was not only a great way to grow up, but it also helped me be the scientist I am today. I could not have done this without your support. And finally, thank you to my husband and our own little family. Jason, every day you show me strength, support, and patience that have carried me through the highs and lows of graduate school. I love you and I am excited to see what the future holds for us.

TABLE OF CONTENTS

Page

LIST OF TABLES

LIST OF FIGURES

LIST OF ABBREVIATIONS

aAo	Aortic Arch
Ach	Acetylcholine
ANOVA	Analysis of Variance
AHA	American Heart Association
bFGF	Basic Fibroblast Growth Factor
bc	Brachiocephalic Artery
BDM	2,3 Butanedione-monoxime
B-H	Benjamini and Hochberg
$CaCl_2$	Calcium Chloride
CENP-F	Centromere Protein F
CO_2	Carbon Dioxide
°C	Celsius
da	ductus arteriosus
dAo	Descending Aorta
DAPI	4’,6-diamidino-2-phenylindole
DAVID	Database for Annotation, Visualization and Integrated Discovery
DIC	Differential Interference Contrast
DMEM	Dulbecco’s Modified Eagle Medium
DMSO	Dimethyl Sulfoxide
DNA	Deoxyribonucleic Acid
dpc	Days Post Coitum
dPBS	Dulbecco’s Phosphate Buffered Saline
EDTA	Ethylenediaminetetraacietic Acid
EKG	Electrocardiogram
EMT	Epithelial to Mesenchymal Transition
EP4	Prostaglandin E Receptor 4
ET-1	Endothelin-1
EtOH	Ethanol
FA	Focal Adhesion
FACS	Fluorescence Activated Cell Sorting
FBS	Fetal Bovine Serum
FRAP	Fluorescence Recovery After Photobleaching
FN	Fibronectin
GEO	Gene Expression Omnibus
GFAP	Glial Fibrillary Acidic Protein
GO	Gene Ontology
H	Heart
HIPPA	Health Insurance Portability and Accountability Act
HPRT	Hypoxanthine-Guanine Phosphoribosyltransferase
hr	Hour
Hz	Hertz
IACUC	Institutional Animal Care and Use Committee
IGF1	Insulin-like Growth Factor 1

Immorto	*Tg(H2-K1-tsA58^{11kio})*
KCl	Potassium Chloride
KH_2PO4	Monopotassium Phosphate
KO	Knockout
lcc	Left Common Carotid Artery
lsc	Left Subclavian Artery
MEF	Mouse Embryonic Fibroblast
MIAME	Minimum Information About a Microarray Experiment
min	Minute
MITF	Microphthalmia-Associated Transcription Factor
MgSO4	Magnesium Sulfate
mmHg	Millimeters Mercury
MT	Microtubule
NaCl	Sodium Chloride
$NaHCO_3$	Sodium Bicarbonate
NaH_2PO4	Monosodium Phosphate
NaOH	Sodium Hydroxide
N_2	Nitrogen
NC	Neural Crest
NIH	National Institutes of Health
NOC	Nocodazole
O_2	Oxygen
PAP	Papaverine
PBS	Phosphate Buffered Saline
PDA	Patent Ductus Arteriosus
PDB	Program for Developmental Biology
PE	Phenylephrine
PFA	Paraformaldehyde
PGP9.5	Protein Gene Product 9.5
Phal	Phalloidin
qRT-PCR	Quantitative Reverse Transcription Polymerase Chain Reaction
R26R^{YFP}	*Gt(ROSA)26Sor$^{tm1(EYFP)Cos}$*
REDCap	Research Electronic Data Capture
RMA	Robust Multi-chip Average
RNA	Ribonucleic acid
ROI	Region of Interest
RT	Room Temperature
SDB	Society for Developmental Biology
SEM	Standard Error of the Mean
SMA	Smooth Muscle Actin
SM-MHC	Myosin Heavy Chain
SNP	Sodium Nitroprusside
SNPs	Single Nucleotide Polymorphisms
SR	Self Renewal
t ½	Half Time
UPGMA	Unweighted Pair Group Method of Average Linkage

VSMC	Vascular Smooth Muscle Cell
vin	Vinculin
Wnt1-Cre	*Tg(Wnt1-Cre)11Rth*
WT	Wild type
YFP	Yellow Fluorescent Protein

CHAPTER I

INTRODUCTION

Life requires a constant ebb and flow of nutrients and waste to and from cells. Unicellular organisms can simply take in nutrients and release cellular wastes across the phospholipid membrane. Once an organism becomes multi-cellular, however, mere diffusion is often insufficient to facilitate basic metabolic needs. These needs become particularly apparent during development. A developing vertebrate embryo can only subsist for a finite time without a vasculature. One of the earliest organ systems to develop is the vascular system to allow for continued rapid maturation of complex multicellular organisms. Failure of the cardiovascular system to develop results in early termination of the embryo.

While continual maturation occurs postnatally, the majority of patterning for the cardiovascular system is established during the prenatal period. Multiple lines of evidence support the hypothesis that embryonic origin plays an important role in vascular biology. By reviewing vascular structure and development, I will highlight the importance of understanding the implications of development on the physiology of an adult organ system.

Current surgical treatments of cardiovascular ailments are fairly crude. Surgical repairs fix structural problems but no care is taken to replicate the underlying characteristics of the vessel in the mended region. When artificial vascular grafts are used, the grafts, while tubular, fail to replicate regional vascular properties. Any surgical

procedure used to treat heart failure can leave damaging scar tissue in the heart. While these interventions work to fix the problem at hand, underlying biological issues have not been addressed. By understanding the implications of development and underlying biology of the cardiovascular system we can formulate better interventions for cardiovascular diseases.

Together my thesis research demonstrates the need to understand the implications of development and cell biology for vascular function and repair. Through my interest in investigating these fields, I have also focused my efforts on establishing methods for both experimental techniques (Chapters IV and V) and educating developmental biology students (Chapter VI). The focus of discussion in this dissertation, however, will be on the laboratory outcomes related to vascular development and disease. First, a thorough evaluation of characteristics of vascular smooth muscle cells (VSMCs) from the regions of the adult and embryonic aorta revealed differences between the regions of the embryonic aorta are not conserved in the adult. These data have important implications for vascular development and disease. The second story examines the cell biological implications of the loss of centromere protein F (CENP-F). A cardiac specific deletion of CENP-F results in dilated cardiomyopathy. By knowing how CENP-F alters cell biology in a model cell line, we can better comprehend how loss of CENP-F modifies cardiac biology. Ultimately, these studies further our understanding of vascular biology and disease.

Vascular Structure

The cardiovascular system is generally organized in three basic layers: an outer vascularized layer, a middle muscular layer, and an inner single cell protective layer. In the heart, these layers are called the epicardium, the myocardium, and the endocardium (Figure 1.1). The epicardium provides a protective outer layer to the heart while also containing the coronary arteries that dive into the myocardium to provide oxygenated blood and nutrients to the muscle (Komiyama et al., 1987; Lie-Venema et al., 2007). The epicardium can also be activated in times of cardiac injury (Zhou and Pu, 2011). The myocardial compartment consists of the cardiomyocytes, fibroblasts, and extracellular matrix. This functional compartment is what physically pumps the blood through the circulatory system. The inner endocardial layer modulates the development and homeostasis of the heart based on its direct contact with the circulation (Stankunas et al., 2008; Wagner and Siddiqui, 2007). These three layers function together to support both embryonic development and adult cardiovascular homeostasis.

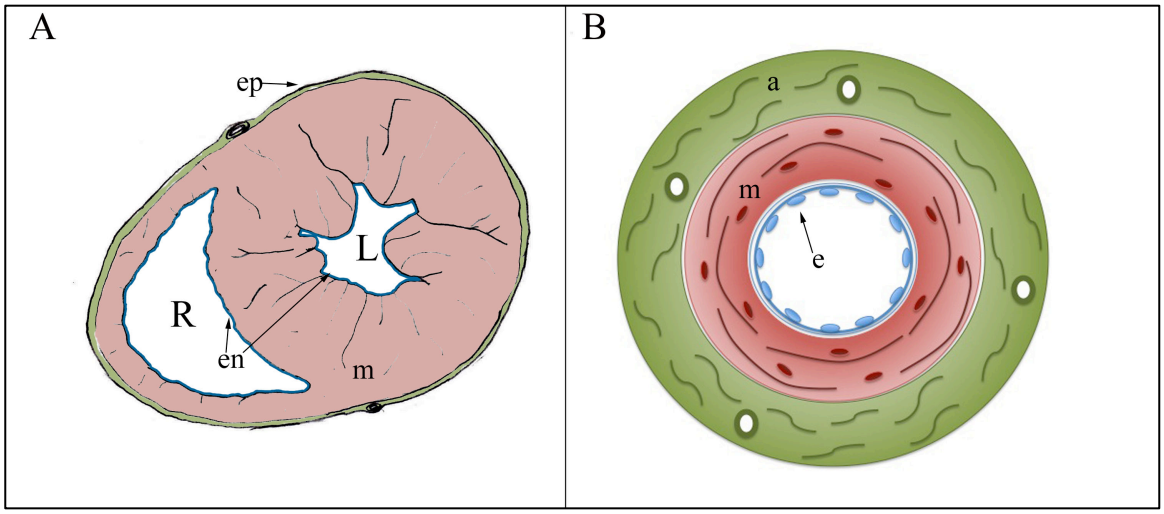

Figure 1.1 Basic structure of the cardiovascular system consists of three layers. A) In the heart the layers are the endocardium (en, blue), the myocardium (m, red), and the epicardium (ep, green). The left (L) and right (R) ventricles of the heart differ in both function and morphology. Since the left ventricle must pump blood to the body the muscular wall is much thicker than the right ventricle. The right ventricle is also at a lower pressure than left ventricle since it pumps blood into the lungs. B) In the vasculature, the first layer is the *tunica intima* (e, blue). This layer is adjacent to the lumen of the vessel and contains endothelial cells. The middle layer is the *tunica media* (m, red). This layer consists of VSMCs and extra-cellular matrix. The outer layer is the *tunica adventitia* and is composed of matrix, fibroblasts, and vascular progenitor cells (a, green).

In the vasculature these layers are referred to as the *tunica adventitia*, the *tunica media*, and the *tunica intima.* Like the epicardium, the adventitia is a protective layer that is critical for oxygenating the muscular layer of the organ. The adventitia contains the vasa vasorum, the source of oxygenated blood for the media of large vessels (Kawabe and Hasebe, 2014). While rich in connective tissue, the adventitia of the major vessels also contains a $Sca1^{+}$ cell population capable of giving rise to VSMCs (Passman et al., 2008). While the embryonic origin of these cells is unknown, they appear in the perivascular space between the aortic arch and pulmonary trunk between 15.5 and 18.5

days post coitum (dpc) in mice. The adventitia has a critical role in vascular maintenance and repair.

The *tunica media* is the main contractile layer of the vascular system containing vascular smooth muscle cells (VSMCs) and extracellular matrix that is arranged in concentric layers of muscle alternating with elastin or matrix. The VSMCs of the media provide tonic contractions that allow for the perpetuation of blood flow (Owens et al., 2004). Those same VSMCs deposit the elastin and collagen contributing to the extracellular matrix of the media (Owens et al., 2004). This extracellular matrix provides the elasticity critical to proper vascular function (Rosenquist et al., 1990; Ruckman et al., 1994; Thieszen et al., 1996).

VSMCs are a very plastic population of cells with the ability to modulate their phenotype based on environmental cues (Owens et al., 2004). Depending on these cues, VSMCs can exhibit a differentiated contractile phenotype or a synthetic proliferative phenotype (Figure 1.2). These phenotypic switching cues can come from within the tunica media, from cell to cell contact, or from autocrine factors (Owens, 1995). The tunica intima as well as the adventitia can also have a powerful impact on the phenotype switching of VSMCs. Growth factors, contractile agonists, NO, and modulation of vascular permeability all influence phenotype switching. The VSMCs also integrate mechanical signals from the surrounding tissue and extracellular matrix when establishing phenotypic plasticity (Owens, 1995). The contractile and synthetic phenotypes are extremes on either end of a spectrum. VSMCs fluidly exist anywhere along the continuum of this spectrum. The embryonic origins of VSMCs varies based on the vessel in question and will be further examined in the following section.

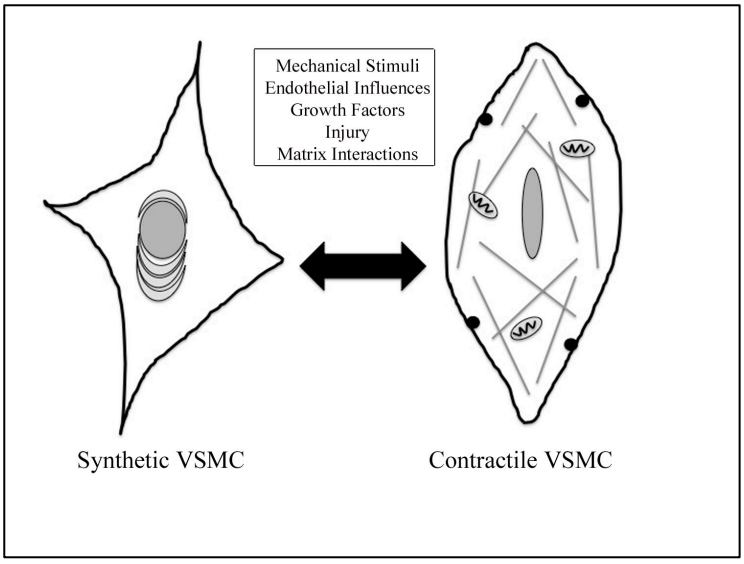

Figure 1.2 VSMCs exhibit phenotypic plasticity. VSMCs exist along a continuum between mature cells expressing the contractile VSMC markers to the synthetic VSMC which is proliferative and migratory, and can secrete extracellular matrix into the media. Any single VSMC can move along this continuum and both phenotypes are necessary for homeostatic vascular function.

While there is no definitive marker for VSMCs, these cells do express different markers depending on their differentiation or phenotypic state. Alpha-smooth muscle actin (αSMA) is an early marker of VSMC commitment (Owens, 1995). It is also expressed during development by other myogenic lineages. SM22 is a marker of early differentiated VSMCs but it is also widely expressed in other developing myogenic lineages (Li et al., 1996a). Smooth muscle myosin heavy chain (smMHC) is a marker of mature contractile VSMCs (Manabe and Owens, 2001; Owens, 1995). Calponin is a member of the calmodulin family of proteins and is another late stage marker of VSMCs (Gimona et al., 1990). All of these markers are highly expressed in contractile VSMCs but are down-regulated in synthetic VSMCs (Owens, 1995; Owens et al., 2004). An

isoform of non-muscular myosin heavy chain, NM-B MHC, is highly expressed in embryonic VSMCs but has also been identified as one of the best markers of synthetic VSMCs (Kuro-o et al., 1991; Rensen et al., 2007). An array of molecular markers must be used to identify VSMCs from other mesenchymal cells. Identification of regionally specific VSMC markers would further facilitate *in vivo* and *in vitro* studies of VSMC characteristics.

The intimal layer is a single cell layer of endothelial cells that can modulate the activity of the VSMCs based on interactions with flowing blood. The endothelial cells of the intima sit on a basal lamina with an internal elastic lamina, which together provides both stability and flexibility to the endothelial layer. Since they are in direct contact with the lumen of the vessel, endothelial cells are poised to play a critical role in tissue homeostasis (Andersen and Stender, 2000; Arnal et al., 1999; Baldwin and Thurston, 2001; Bazigou and Makinen, 2013; Chien et al., 1998; Cines et al., 1998; Traub and Berk, 1998; Woo et al., 2011). It is not clear to what extent there are regional differences in endothelial cell characteristics or whether origin influences vascular function.

Vascular Development

In mammals the development of a healthy cardiovascular system depends upon the coordination of cells from diverse embryonic origins. Vasculogenesis begins with specification of angioblasts (Ren et al., 2010; Sato et al., 2008; Vokes and Krieg, 2002). Derived from the mesoderm, angioblasts form an endothelial plexus throughout the developing embryo and the yolk sac (Schmidt et al., 2007). The vasculature begins

forming by the condensation of this endothelial plexus. Cell-cell junctions form and endothelial cells rearrange to generate patent lumens (Houser et al., 1961; Jin et al., 2005). These primitive vessels remodel, branch, and recruit mural cells (fibroblasts and VSMCs).

VSMC progenitors arise from distinct embryonic sources including splanchnic mesoderm (Wilm et al., 2005), somitic mesoderm (Esner et al., 2006; Wasteson et al., 2008), neural crest (NC) (Jiang et al., 2000; Le Lievre and Le Douarin, 1975), mesothelia, (Que et al., 2008) and others (Gittenberger-de Groot et al., 1999; Rinkevich et al., 2012). In the aorta, splanchnic mesodermal cells are first recruited and differentiate into VSMCs. Before the splanchnic mesoderm cells completely encircle the dorsal aorta, the cells are displaced by somitic mesodermal cells. Differentiation of these somitic mesoderm cells begins in the ventral anterior end of the vessel. Differentiation then proceeds around the circumference of the vessel (ventral to dorsal), and down the length of the aorta toward the diaphragm (anterior to posterior).

Meanwhile, the outflow tract of the aorta begins as the aortic sac feeding a series of six paired pharyngeal arch arteries surrounded by the pharyngeal arch mesoderm. The cardiac NC migrates down the pharyngeal arches to invade the aortic sac. A subset of the cardiac NC participates in septation of the truncus arteriosus into the aortic arch and the pulmonary trunk (Kirby, Gale et al. 1983). The rest of the cardiac NC remains in the pharyngeal arch arteries and becomes the VSMCs of the aortic arch and the arteries of the head and neck (Le Lievre and Le Douarin, 1975). The border that forms between the NC-derived VSMCs of the ascending aortic arch (aAo) and mesoderm-derived VSMCs of the descending aorta (dAo) is maintained throughout development and into adulthood (Jiang

et al., 2000; Le Lievre and Le Douarin, 1975). Arch arteries one, two and five bilaterally resorb while arch artery three become sections of the vessels of the head and neck. Arch artery four on the left unilaterally becomes the aortic arch while the right side resorbs. Arch artery six contribute to the pulmonary trunk and ductus arteriosus.

Once cells encircle the aorta and differentiate into VSMCs, they undergo a closely regulated process of layer formation within the media. Different regions of the vasculature consistently form different numbers of layers in the media. Lumen diameter is the best predictor for the number of layers that exist in the media (Wolinsky and Glagov, 1964, 1967). However, studies of transgenic mice that manipulate animal's mass or vascular matrix components demonstrate that there are regional mechanisms that can compensate for increased vascular demands without changing the number of vascular layers (Dilley and Schwartz, 1989; Faury et al., 2003; Hoglund and Majesky, 2012; Wagenseil and Mecham, 2009).

Much of the initial patterning of the vasculature occurs rapidly and before the heart even begins beating. Once the heart beats, perfusing vessels with blood, the vasculature begins growing and remodeling through angiogenesis (Blatnik et al., 2005; Chen and Tzima, 2009; Culver and Dickinson, 2010). Hemodynamic force is one of the most powerful forces in vascular remodeling and is required for complete vascular and embryonic development.

Cardiac Development

In the mouse, heart development begins by the specification of mesodermal cardiac progenitors in the bilateral primary heart fields soon after gastrulation, around 7.0 dpc (Kinder et al., 2001). By 7.5 dpc these heart fields converge at the midline of the embryo forming the cardiac crescent. This crescent undergoes tubulogenesis with an inner layer of endothelial cells and a single layer of myocardial cells (Saga et al., 1999). The most anterior portion of this tube is specified to become the outflow tract and the ventricles while the posterior portion is fated to become the atria and sinus venosus (Yutzey et al., 1994). The tube elongates and begins rightward looping. The second heart field migrates into the anterior portion of the heart tube investing part of the prospective right ventricle, atria, and out flow tract (Galli et al., 2008; Kelly et al., 2001; Zaffran et al., 2004). With this, the primitive chambers of the heart are patterned.

Physical formation of the chambers of the heart begins by development of the atrioventricular (AV) canal between the presumptive atrial and ventricular regions. Endocardial cushions form within the AV canal and the outflow tract through an epithelial to mesenchymal transition of endocardium into the cardiac jelly (Kinsella and Fitzharris, 1980; Markwald et al., 1977). These endocardial cushions mature into the four valves of the heart (aortic, pulmonary, tricuspid and mitral valves). Trabeculation and septation of the atria and ventricles begins at 9.5 dpc.

In order to support the thickening myocardium, the heart requires a vascular system to deliver oxygenated blood throughout the organ. The vasculature of the heart is developed from the epicardium (Komiyama et al., 1987; Lie-Venema et al., 2007; Mikawa and Gourdie, 1996; Perez-Pomares et al., 2002; Tomanek, 2005; Winters et al.,

2014). The proepicardium forms from the splanchnic mesoderm as a cluster of cells dorsal to the looped heart (Komiyama et al., 1987; Lie-Venema et al., 2007). From this position, the proepicardium migrates over the sinus venosus to cover the heart in a single cell epithelium (Komiyama et al., 1987). The heart is unique among the thoracoabdominal organs in that it recruits a mesothelium external to the organ (Winters et al., 2014). Some of the epicardial cells dive into the myocardium and form the coronary vessels. This capillary plexus remodels into two major coronary arteries once the coronary ostia forms in the aorta just anterior to the aortic valve (Eralp et al., 2005; Tomanek, 2005).

Heterogeneity in Cardiac Physiology and Disease

Heterogeneity is also a characteristic of the structure and function of the heart. While the different chambers of the heart are made up of the same basic cell types, there are distinct morphological and functional differences between the chambers. For example, the right and left ventricles of the heart are organized to be efficient in performing certain functions. The right ventricle, in the embryo must pump blood through the ductus arteriosus into the aorta thus pumping blood to the entire embryo. Prostaglandins expressed in both the ductus and the placenta help keep the ductus open (Olley and Coceani, 1981). With the ductus open, and pressure higher in the lungs than the aorta, blood flows from the right ventricle to the systemic circulation. Soon after birth, the ductus down-regulates prostaglandin receptor expression and the ductus closes and eventually becomes the ligamentum arteriosus (Clyman et al., 1999). With the ductus

closed and the umbilical supply of blood halted, the right atrium receives deoxygenated blood from the vena cava and the right ventricle is poised to pump blood into the lungs through the pulmonary arteries. Blood returns to the left atrium through the pulmonary veins. Blood is then pumped into the left atrium, which must now pump blood into the systemic circulation. Because of these different functions performed by the right and left ventricles they have very dissimilar morphology (Fig 1.1a) and are subject to different maladies.

For example, pulmonary hypertension strains the right ventricle of the heart, as the right ventricle must contract harder against increasing pressure in the lungs (Rich and Brundage, 1987; Steudel et al., 1998). This increased strain results in hypertrophy of the muscle and a decrease in the volume of blood that fills the heart. Obstruction or resistance in the systemic circulation has a similar hypertrophying reaction in the left ventricle (Drozdz and Kawecka-Jaszcz, 2013) (Figure 1.3A). Dilated cardiomyopathy can also occur with hypertension or after cardiac infarction when myocytes can no longer keep up with an increased workload. The wall of the heart thins, the lumen diameter increases, and ejection fraction decreases (Luk et al., 2009) (Figure 1.3B). Both dilated and hypertrophic cardiomyopathy can also be caused by drug toxicity (Felker et al., 1999; Mizia-Stec et al., 2008; Piano, 2002; Steinherz et al., 1991; Swain et al., 2003), and by genetic mutations which result in myocytes needing to work harder to generate force (Dees et al., 2012a; Durand et al., 1995; Kamisago et al., 2000; Muretta and Thomas, 2013).

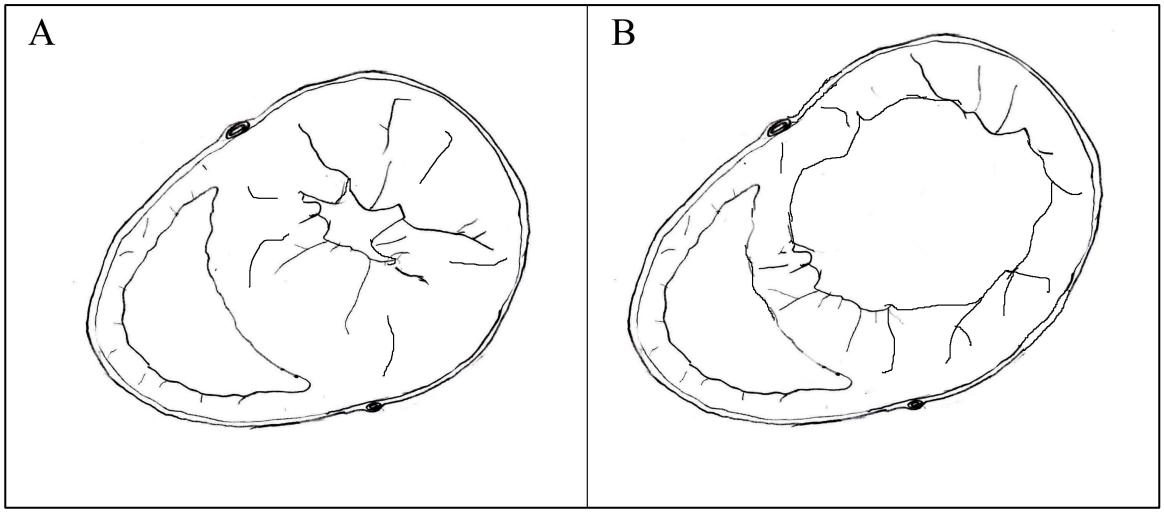

Figure 1.3 Left ventricle cardiomyopathy. A) Hypertrophic cardiomyopathy. B) Dilated cardiomyopathy.

When regional defects in the heart need to be repaired, many treatments do not address the underlying defect in the tissue. While surgical myomectomy can be performed to reduce obstructive cardiomyopathy, the underlying cause is not addressed and the remaining muscle could still fail to function properly and relapse may occur (Minakata et al., 2005). Another form of treatment is alcohol ablation that delivers alcohol straight into the afflicted muscle with a catheter. While this method destroys the hypertrophic muscle, it also introduces scar tissue into the myocardium (Dimitrow et al., 2001; Ivens, 2004). This remodeling can have unpredictable consequences on the efficiency of the heart. A more complete understanding of the underlying problems that give rise to cardiomyopathy will shed light on preventative measures or treatments.

Heterogeneity of Vascular Physiology and Disease

Heterogeneity of blood vessels is intrinsic and critical to cardiovascular function. Different regions of the vasculature require different physical properties in order to meet distinct physiological requirements. The outflow tract of the heart is an elastic artery that contains multiple elastic lamina able to withstand the pulsatile force produced by the beating heart (Shirwany and Zou, 2010). While the descending aorta is also considered an elastic artery, the extracellular components differ greatly from the ascending aorta and the blood velocity has decreased substantially compared to the aortic arch (Gadson et al., 1993; Ruckman et al., 1994). As the blood moves further out in the vasculature tree, the vessels become more muscular and contain fewer elastic lamina (Figure 1.4). These vessels must maintain vascular tone in order to deliver blood to their target tissues and organs (Shirwany and Zou, 2010). The capillary bed contains pericytes that function to regulate capillary blood flow and permeability. The venous system, while patterned similarly to the arteriole system, has distinct differences. To return to the heart blood relies on a series of valves in the veins to keep blood moving against gravity and at a lower pressure than in the arteries, particularly in the limbs (Bazigou and Makinen, 2013; Meissner et al., 2007). While there are pericyte cells associated with veins, they do not play a contractile role as they do in muscular arteries. Rather, veins rely in part on skeletal muscle contractions to act like peripheral muscle pumps to return blood to the heart (Alimi et al., 1994). There is a large amount of variation in structure and function along the vascular tree.

Differences in vascular structure are also reflected within the three lamina. For example, regional variation in endothelial cells of the tunica intima regulates vessel permeability (Katora and Hollis, 1976), while great variability in connective tissue

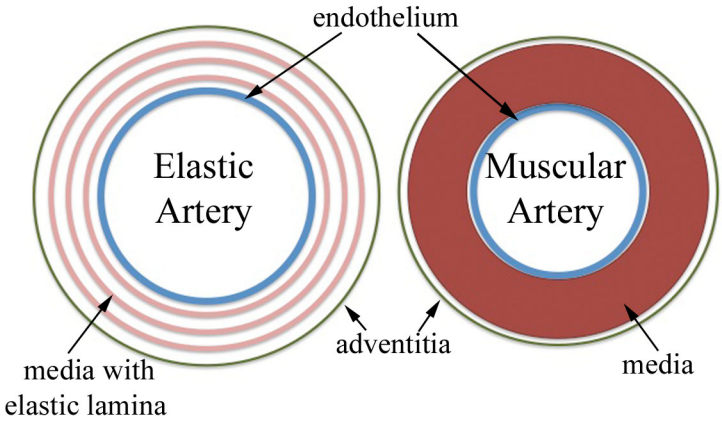

Figure 1.4 Structural differences between elastic and muscular arteries. The media of elastic arteries, such as the aorta, consist of multiple organized layers of VSMCs interspersed with layers of elastin. Muscular arteries, such as the mesenteric artery, have fewer elastic lamina within the media.

elements has been noted along the entirety of the vascular tree (Gadson et al., 1993; Ruckman et al., 1994). Significant heterogeneity in structure and function has been noted for the tunica media (Stenmark and Mecham, 1997; van Meurs-van Woezik et al., 1983), whose major cellular components are VSMCs or pericytes. In the large conducting arteries of the cardiac outflow tract, this layer contains significant amounts of elastin contributing to the distensible properties that are essential for reacting to blood volume and pressure changes during the cardiac cycle (Fawcett et al., 1994). Conversely, medium-sized muscular arteries (e.g. coronary and mesenteric vessels) contain less elastin but are enriched in VSMCs critical for regulation of vessel diameter and

distribution of blood to specific tissues of the body. Capillaries consist of an endothelium wrapped by a single pericyte. In addition to differences in their basic morphology, these vessels have regionally distinct expression of matrix and signaling pathway components often linked to the tunica media (Andersen and Stender, 2000; Cheung et al., 2012; Flaim et al., 1985; Gadson et al., 1997; Gadson et al., 1993; Ko et al., 2001; Leroux-Berger et al., 2011; Reslan et al., 2013; Ruckman et al., 1994; Subbiah et al., 1981; Sufka et al., 1990; Thieszen et al., 1996; Trigueros-Motos et al., 2013).

Not only does the physiology of these different vascular regions differ, but the regions of the vasculature are differentially susceptible to vascular disease. First, atherosclerosis does not plague the entire vasculature equally. Branch points and places with higher turbulent flow, including the aortic arch, develop plaques more frequently than other regions (Van Assche et al., 2011; VanderLaan et al., 2004). Even when these atherosclerotic prone vessels are transplanted into a region that does not develop plaques, atherosclerosis still occurs (Haimovici and Maier, 1971). Secondly, under calcifying conditions similar to those seen in cases of kidney failure, the ascending aorta calcifies much more rapidly compared to the descending aorta (Leroux-Berger et al., 2011). In fact, VSMCs isolated from the ascending aorta retain this propensity to calcify, linking this condition to VSMC biology. These data support our hypothesis that VSMCs from different regions of the vasculature are intrinsically different and have the potential to contribute to disease.

This begs the question, what determines these differences in physiological and pathological states? These characteristics could be dependent on environmental factors or embryonic origins of the cells that constitute the vessels. We hypothesize that a

combination of vascular environment and embryonic origin account for regional variation in physiology and disease in the cardiovascular system (Figure 1.5). We explore this hypothesis in the second chapter.

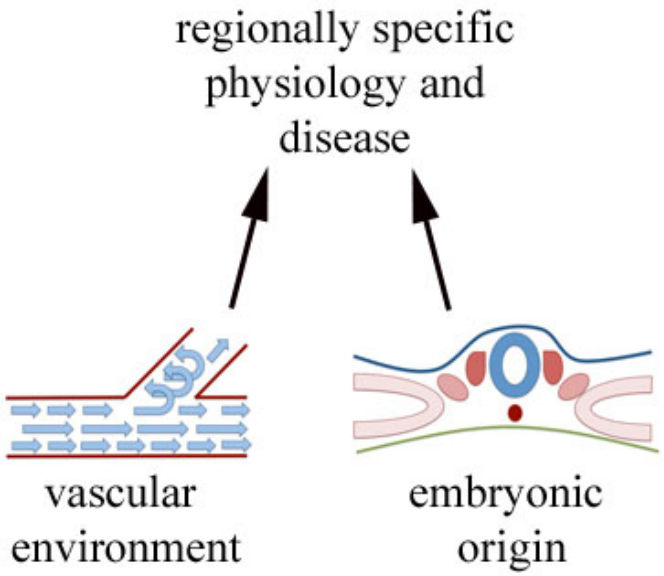

Figure 1.5 Both vascular environment and embryonic origin of the vascular components play a role in establishing regionally specific vascular physiology and disease.

There is abundant evidence that embryonic origin of VSCMs plays an important role in vascular biology. Differences in VSMC characteristics such as gene expression have been attributed to their embryonic origin (Zhang et al., 2012). Studies also suggest that when vessels prone to atherosclerosis are placed in a vascular region that does not typically develop atherosclerosis, they retain their predisposition to disease (Haimovici and Maier, 1971). Additionally, differentiation of VSMCs from embryonic stem cells through NC- or mesoderm-lineages provide evidence that VSMC characteristics are programmed based on embryonic origin (Cheung et al., 2012). These studies suggest that

individual VSMC characteristics are strongly determined by embryonic origin. However, definitive evidence that embryonic origin dictates vascular phenotype has not been provided (Gittenberger-de Groot et al., 1999).

Congenital cardiovascular defects also occur at the boundaries between vascular regions of different embryonic origins. Two examples of these conditions are coarctation of the aorta and interruption of the aortic arch (Jacobs et al., 1995; Tanous et al., 2009). Building a better understanding of the embryonic origin and patterning of the vasculature could lead to greater comprehension of how to prevent or effectively repair these conditions. Current surgical means of repair, while they correct the structural defect, fail to address the underlying patterning problems. Many patients who have had coarctation repairs as older children or adults develop hypertension without re-coarctation suggesting that there is an underlying cause of the structural defect has not been addressed by surgery (O'Sullivan et al., 2002). This is additional evidence that regional differences in vascular biology need to be understood to be able to properly address vascular diseases.

Summary

The cardiovascular system is a carefully orchestrated mosaic of cell types from a diversity of developmental origins. It is not hard to imagine then, how embryonic origin could play a large role in physiology and disease in the adult. A better understanding of the similarities and differences between these different vascular regions can help us understand how to prevent and treat these vascular disease in a more elegant way that actually addresses the underlying biology of the system.

The proximal aorta is particularly interesting because its VSMCs arise from two distinct embryonic origins: NC and somitic mesoderm (Jiang et al., 2000; Wasteson et al., 2008). This juxtaposition of VSMCs from different embryonic origins in the aorta affords the opportunity to test the hypothesis that embryonic origin of VSMCs relates to the vascular function of distinct regions within a single vessel. The second chapter of this book investigates basic cell biological differences between the arch of the aorta and the descending aorta. I identify distinct differences between these regions in the embryonic aorta that assimilate in the adult.

The third chapter of this volume begins to investigate the biological process through which CENP-F, a protein thought to only be expressed during mitosis, can cause dilated cardiomyopathy when deleted from a population of largely post-mitotic cells: cardiomyocytes. It has been previously shown that cardiac specific deletion of CENP-F leads to adult onset dilated cardiomyopathy. How loss of CENP-F results in cardiomyopathy is unknown. To begin to understand the role CENP-F plays in the heart, we first examined CENP-F in mouse embryonic fibroblasts (MEFs).

Ultimately the focus of this dissertation is to investigate the cell biological characteristics of both physiological and pathological features of the cardiovascular system.

CHAPTER II

EMBRYONIC DOMAINS OF THE AORTA DERIVED FROM DIVERSE ORIGINS EXHIBIT DISTINCT PROPERTIES THAT CONVERGE INTO A COMMON PHENOTYPE IN THE ADULT

This chapter was published under this title in *The Journal of Molecular and Cellular Cardiology* in April 2014 (Pfaltzgraff et al., 2014).

Abstract

Vascular smooth muscle cells are derived from distinct embryonic origins. Vessels originating from differing smooth muscle cell populations have distinct vascular and pathological properties involving calcification, atherosclerosis, and structural defects such as aneurysm and coarctation. We hypothesized that domains within a single vessel, such as the aorta, vary in phenotype based on embryonic origin. Gene profiling and myographic analyses demonstrated that embryonic ascending and descending aortic domains exhibited distinct phenotypes. *In vitro* analyses demonstrated that VSMCs from each region were dissimilar in terms of cytoskeletal and migratory properties, and retention of different gene expression patterns. Using the same analysis, we found that these same two domains are indistinguishable in the adult vessel. Our data demonstrate that VSMCs from different embryonic origins are functionally distinct in the embryonic mouse, but converge to assume a common phenotype in the aorta of healthy adults. These

findings have fundamental implications for aortic development, function and disease progression.

Introduction

Heterogeneity of blood vessels is intrinsic and critical to cardiovascular function. Differences in vascular structure are reflected in the three layers comprising definitive arteries and veins (from lumen outward): the tunica intima, media, and adventitia. For example, regional variation in endothelial cells of the tunica intima regulates vessel permeability (Katora and Hollis, 1976), while great variability in connective tissue elements has been noted along the entirety of the vascular tree (Gadson et al., 1993; Ruckman et al., 1994). Significant heterogeneity in structure and function has been noted for the tunica media (Stenmark and Mecham, 1997; van Meurs-van Woezik et al., 1983), whose major cellular components are vascular smooth muscle cells (VSMCs) or pericytes. In the large conducting arteries of the cardiac outflow tract, this layer contains significant amounts of elastin contributing to the distensible properties that are essential for reacting to blood volume and pressure changes during the cardiac cycle (Fawcett et al., 1994). Conversely, medium-sized muscular arteries (e.g. coronary and mesenteric vessels) contain less elastin but are enriched in VSMCs critical for regulation of vessel diameter and distribution of blood to specific tissues of the body. In addition to differences in their basic morphology, these vessels have distinct susceptibility to diseases often linked to the tunica media (Andersen and Stender, 2000; Cheung et al., 2012; Flaim et al., 1985; Gadson et al., 1997; Gadson et al., 1993; Ko et al., 2001;

Leroux-Berger et al., 2011; Reslan et al., 2013; Ruckman et al., 1994; Subbiah et al., 1981; Sufka et al., 1990; Thieszen et al., 1996; Trigueros-Motos et al., 2013).

VSMC progenitors arise from distinct embryonic sources including splanchnic mesoderm (Wilm et al., 2005), somitic mesoderm (Wasteson et al., 2008), neural crest (NC) (Jiang et al., 2000; Le Lievre and Le Douarin, 1975), mesothelia, (Que et al., 2008) and others (Gittenberger-de Groot et al., 1999; Rinkevich et al., 2012). Interestingly, differences in VSMC characteristics such as gene expression have been attributed to their embryonic origin (Zhang et al., 2012). Also, studies suggest that when vessels prone to atherosclerosis are placed in a vascular region that does not typically develop atherosclerosis, they retain their predisposition to disease (Haimovici and Maier, 1971). Additionally, differentiation of VSMCs from embryonic stem cells through NC- or mesoderm-lineages provide evidence that VSMC characteristics are programmed based on embryonic origin (Cheung et al., 2012). These studies suggest that individual VSMC characteristics are strongly determined by embryonic origin. However, definitive evidence that embryonic origin dictates vascular phenotype has not been provided (Gittenberger-de Groot et al., 1999).

While different vessels arise from distinct embryonic origins, the proximal aorta is particularly interesting because its VSMCs arise from two distinct embryonic origins: NC and somitic mesoderm (Jiang et al., 2000; Wasteson et al., 2008). In the mouse, at 9.5 days post coitum (dpc), NC cells migrate from the dorsal neural tube and contribute to the pharyngeal arch arteries and aortic sac. At 12.5 dpc, NC facilitates a complex septation and remodeling of the outflow tract and pharyngeal arteries resulting in the pulmonary trunk and the aorta (Kirby et al., 1983). After outflow tract septation and remodeling, a

separate population of NC cells invest the vessel and differentiate into VSMCs (Le Lievre and Le Douarin, 1975). At 9.0 dpc, cells from lateral plate mesoderm begin to migrate around the ventral side of descending aorta (Wasteson et al., 2008). By 9.5 dpc, cells from somitic mesoderm begin populating the dorsal side of the descending aorta (Wasteson et al., 2008). At 11.5 dpc, the entire descending aorta is ensheathed by VSMCs derived from the somitic mesoderm. The border that forms between the NC-derived VSMCs of the ascending aortic arch (aAo) and mesoderm-derived VSMCs of the descending aorta (dAo) is maintained throughout development and into adulthood (Jiang et al., 2000; Le Lievre and Le Douarin, 1975). This juxtaposition of VSMCs from different embryonic origins in the aorta affords the opportunity to test the hypothesis that embryonic origin of VSMCs relates to the vascular function of distinct regions within a single vessel.

Not only are the embryonic origins of these VSMC populations distinct, but the regions of the vasculature are differentially susceptible to vascular disease, namely atherosclerosis and calcification of the aorta. Transplantation studies in which an atherosclerotic-prone vessel was placed in a region of the vasculature that does not develop atherosclerosis demonstrated that the propensity to develop atherosclerosis is intrinsic to the vessel itself (Haimovici and Maier, 1971). Furthermore, under *ex vivo* calcifying conditions, the ascending aorta calcified much more rapidly compared to the descending aorta (Leroux-Berger et al., 2011). Even if VSMCs were isolated from the ascending aorta, they retained this propensity to calcify, linking this condition to VSMC biology. These data support our hypothesis that VSMCs from different regions of the vasculature are intrinsically different and have the potential to contribute to disease.

Additionally, in human patients, the aortic border between the NC- and somitic mesoderm-derived VSMCs is the location of several cardiovascular defects: coarctation of the aortic arch, interrupted aortic arch type A, and aortic aneurism. Coarctation of the aorta is a narrowing of the aorta at the level of the ductus arteriosus (Tanous et al., 2009). Interrupted aortic arch type A is a complete discontinuation of the aortic lumen distal to the left subclavian artery. Aortic aneurisms are dilations of the aorta, which can occur in different regions of the aorta, but are typically found at borders between VSMCs of different embryonic origins (Majesky et al., 2011). Regardless of the defect, typical treatment involves surgical repair of the aorta. Understanding the biology of these different VSMC populations and their juxtaposition can inform the study and treatment of these human conditions.

Using gene profiling, myography, and cell biological strategies, we demonstrate that NC- and somitic mesoderm-derived VSMCs of the embryonic aorta are significantly different throughout development. Surprisingly, using the same modalities, we demonstrate that the two domains are indistinguishable in the normal, healthy adult. Thus, this unexpected result demonstrates that embryonic origin does not dictate adult phenotype in the specific case of the aorta and has major implications for our understanding of vascular development and disease.

Materials and Methods

Animals

Mice were from a mixed genetic background and maintained in accordance with protocols approved by the Vanderbilt University Institutional Animal Care and Use Committee (IACUC). Timed matings were performed to obtain embryos at specific stages of development. Noon on the day a vaginal plug was observed was considered day 0.5 dpc. The *Tg(Wnt1-Cre)11Rth* (called *Wnt1-Cre*) transgenic mouse line was used to lineage-map NC cells with *Gt(ROSA)26Sor*$^{tm1(EYFP)Cos}$ (called *R26R*^{YFP}). The *Tg(H2-K1-tsA58*^{11Kio}*)* line (called Immorto) was used to conditionally immortalize isolated VSMCs. This line expresses a temperature sensitive SV-40 large T antigen in the presence of interferon gamma.

Microarray

For the microarray conducted on adult tissues, the aAo, dAo, coronary artery, and mesenteric arteries were isolated from three individual 8 week-old female mice. Tissue was flash frozen prior to homogenization and RNA isolation. Samples were run on the Affymetrix mouse Gene 1.0 ST arrays.

The embryonic microarray was conducted using tissue from 13.5 dpc embryos. To obtain enough tissue without the need to amplify the RNA sample, two biological samples were pooled for each experimental sample. A total of three experimental samples were run on Affymetrix Mouse Exon/Gene (WT) arrays.

Microarray images were scanned with an Affymetrix high resolution GenePix 4000B scanner in the Vanderbilt Functional Shared Resource (http://www.thefgsr.com/). Raw .CEL files were subsequently uploaded into Partek Genomics Suite version 6.6 (Partek Incorporated, St. Louis, MO) and processed using Robust Multi-chip Average (RMA) normalization (Bolstad et al., 2003; Irizarry et al., 2003).

Following RMA normalization, Partek analysis software was used to perform pairwise comparisons of average group values and one-way ANOVA for analysis of aAo, dAo, superior mesenteric artery, and coronary artery tissues. Only probes that resulted in a fold-change of at least 1.5 with a Benjamini and Hochberrg (B-H) multiple hypothesis corrected *p* value of less than 0.05 were considered significantly altered. All six possible individual pairwise comparisons were performed with an expectation of 1.5-fold difference between each comparison. Data were uploaded to the Gene Expression Omnibus (GEO) repository and complied with MIAME standards. The GEO accession numbers are: GSE50250 and GSE50251. To generate the heat map, hierarchical clustering was performed using UPGMA (unweighted pair-group method of average linkage) and Euclidian distance as the dissimilarity measure in Partek.

Real Time PCR

Quantitative reverse transcription PCR (qRT-PCR) was completed to validate the expression of genes identified from the microarray. RNA samples were harvested from the aAo and dAo of 13.5, 15.5, and 17.5 dpc embryos, 8 week-old adults and cell lines. In all cases, RNA was isolated using Qiagen RNeasy Mini Kits (74104). Ambion Turbo DNase (AM2238) was used to remove any DNA from the samples. Reverse transcription

was done with the Invitrogen SuperScript III First-Strand Synthesis System (18080-051). qRT-PCR was performed using Promega Gotaq qPCR master Mix (A6001) on Bio-Rad CFX96 Detection System. Primers are displayed in Table 2.1. All experiments were run in duplicate, and the relative amount of RNA was determined by comparison with *Hypoxanthine guanine phosphoribosyl transferase* (*Hprt*) mRNA. Student's paired t-tests were used to determine statistical significance. N=5.

Gene Name	Forward Primer 5'-3'	Reverse Primer 5'-3'
Desmocollin 3	TTGACCAAGAGGGTAAATCA	GAATTATCTCTGGTGCGTTG
Foxd1	TGTCCAGTGTGGAGAACTTT	GGAGTCCTACCTTCGCTCT
Integrin beta-8	TGGTGTGTTCAAGAGGATTT	CCTTTGCTTATCAAACTGGA
Mesothelin	AGACAAATGGACCTTGTGAA	GGGTAGGTCTTGTCCAGTTT
Myelin protein zero like 2	ACTGGCTTTCCCTGATGTAT	GTAGGACAAAGGGCTGTGA
Robo4	GAGCCAGTGTGTGGAGAAG	AAGGTCTGGAAGAGTTGAGG
HPRT	TACGAGGAGTCCTGTTGATGTTGC	GGGACGCAGCAACTGACATTTCTA

Table 2.1 Real time forward and reverse primer sequences.

Myography

For fetal studies, pregnant females were anesthetized by intraperitoneal injection of 0.4 ml 2.5% Avertin (2,2,2-tribromoethanol in tert-amyl alcohol; Sigma-Aldrich, St Louis, MO), followed by isoflurane inhalation (Baxter, Deerfield, IL) to facilitate fetal anesthesia.

Anesthetized fetuses were submerged in ice-cold, deoxygenated (95% N_2, 5% CO_2) Krebs buffer. Krebs buffer was modified (109 mM NaCl, 34 mM $NaHCO_3$, 4.7 mM KCl, 0.9 mM $MgSO_4$, 1.0 mM KH_2PO_4, 11.1 mM dextrose, and 2.5 mM $CaCl_2$) to maintain stable pH (7.30–7.35) and relative hypoxia in the vessel bath (dissolved oxygen

content = 1.5–1.8%; measured pO_2 = 38–45 Torr). Aortae were dissected from 15.5 dpc (n=8) and 19.5 dpc fetuses (n=10) and transferred to custom microvessel perfusion chambers (Instrumentation and Model Facility, The University of Vermont, Burlington, VT) filled with chilled, deoxygenated Krebs buffer, as described (Reese et al., 2009). Adult aortae (n=8) were similarly isolated, then placed in chambers perfused with oxygenated Krebs (21% O_2, 5% CO_2, balance N_2). Brachiocephalic, left carotid, and left subclavian arteries were tied off at their base; the ductus arteriosus was tied off in fetal tissues. The excised vessel preparation was positioned and secured on ~120 μm (fetal) to ~500 μm (adult) pipette tips.

Once mounted, the perfusion chamber was placed on an inverted microscope equipped with a video camera and an image-capture system (IonOptix, Milton, MA) to continuously record the intraluminal diameter of both the aAo and dAo simultaneously. Optical markers used to detect the lumen diameter were positioned at the narrowest point of the constricted vessel. Vessels were allowed to equilibrate at 37 °C for 30–40 minutes, then pressurized in a stepwise manner to 6 mm Hg (preterm), 20 mm Hg (term) or 80 mm Hg (adult). After equilibration, vessels were exposed to 50 mM KCl (×2) to ascertain vessel reactivity. Vasoconstrictive drugs and doses used for the subsequent myography experiments included: the thromboxane receptor agonist U-46619 (10^{-8} M; Cayman Chemical), phenylephrine (10^{-5} M, Sigma-Aldrich), endothelin-1 (ET-1; 10^{-7} M in acetic acid, Bachem). In some studies, the U-46619 preconstricted aorta was exposed to acetylcholine (10^{-5} M, Sigma-Aldrich) to assess endothelial-dependent vasodilatory responses. Aortae were also exposed to the NO-donor sodium nitroprusside (SNP; 10^{-5} M, Sigma-Aldrich) and the direct-acting vasodilator papaverine (10^{-4} M, Sigma-Aldrich).

Drugs were dissolved in Krebs buffer or ethanol, unless otherwise specified. Final solvent concentration in the bath was ≤0.04%. Vessels were exposed to each agent until a stable baseline diameter was reached (typically 20–30 min). Drug concentrations refer to their final molar concentration in the bath. Differences between the aAo and dAo lumen diameter were evaluated by paired Student's t-test.

VSMC Isolation

Aortae from Immorto 8 week-old adults or 16.5 dpc embryos were dissected to separate the aAo from the dAo. To dissect the aAo, the aorta was cut away from the heart and the arch transected at the level of the left subclavian artery to prevent inclusion of tissue from the dAo (Figure 2.1). YFP fluorescence in the *Wnt1-Cre; R26R*^{YFP} NC

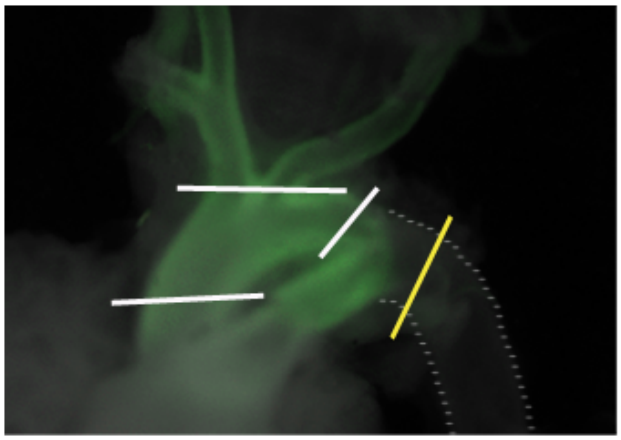

Figure 2.1 Lines of dissection to isolate aAo and dAo. Wnt1-Cre; R26R^{YFP} linage labeled aorta demonstrating the border between the aAo and dAo. White solid lines denote dissection to isolate aAo. Yellow solid line indicates dAo dissection. The vessel between the yellow and the rightmost white line was discarded. White dotted lines show the margins of the dAo.

lineage labeled mouse was also used to facilitate clean dissections of the aAo. The dAo was taken from the remaining tissue beginning just distal to the ductus arteriosus in embryos (the ligamentum arteriosum in adults) and continuing until the level of the diaphragm. Adult aortae were processed as previously described (Geisterfer et al., 1988). Embryonic aortae were processed by peeling the adventitia away from the vessel. Vessels were then cut open longitudinally and the endothelial cells gently scraped away. The remaining vessel was plated into a four well culture dish and cells migrated away from the explant over one week. The tissue was then discarded and the explanted cells were trypsinized and replated to start cell lines. Cells were cultured in DMEM, high glucose; 10% fetal calf serum, 1% penicillin/streptomycin. Cells were immortalized by changing the culture conditions to 33°C and adding 30 units/mL interferon gamma. Cells were removed from immortalizing conditions 48 hours prior to conducting experiments. Clonal cell lines were derived by dissociating aortic outgrowths with 0.25% trypsin, and plating cells at clonal cell densities. Isolated clones were selected with cloning rings and further propagated. Clonal lines of VSMCs were not cultured past 5 passages in order to ensure retention of smooth muscle characteristics. These cells maintained expression of characteristic VSMC markers smooth muscle actin (SMA) and smooth muscle myosin heavy chain (smMHC) both in the explant and as clonal cell lines (Figure 2.2). Three clonal lines from each region of the aorta were studied for both the embryonic and adult time points.

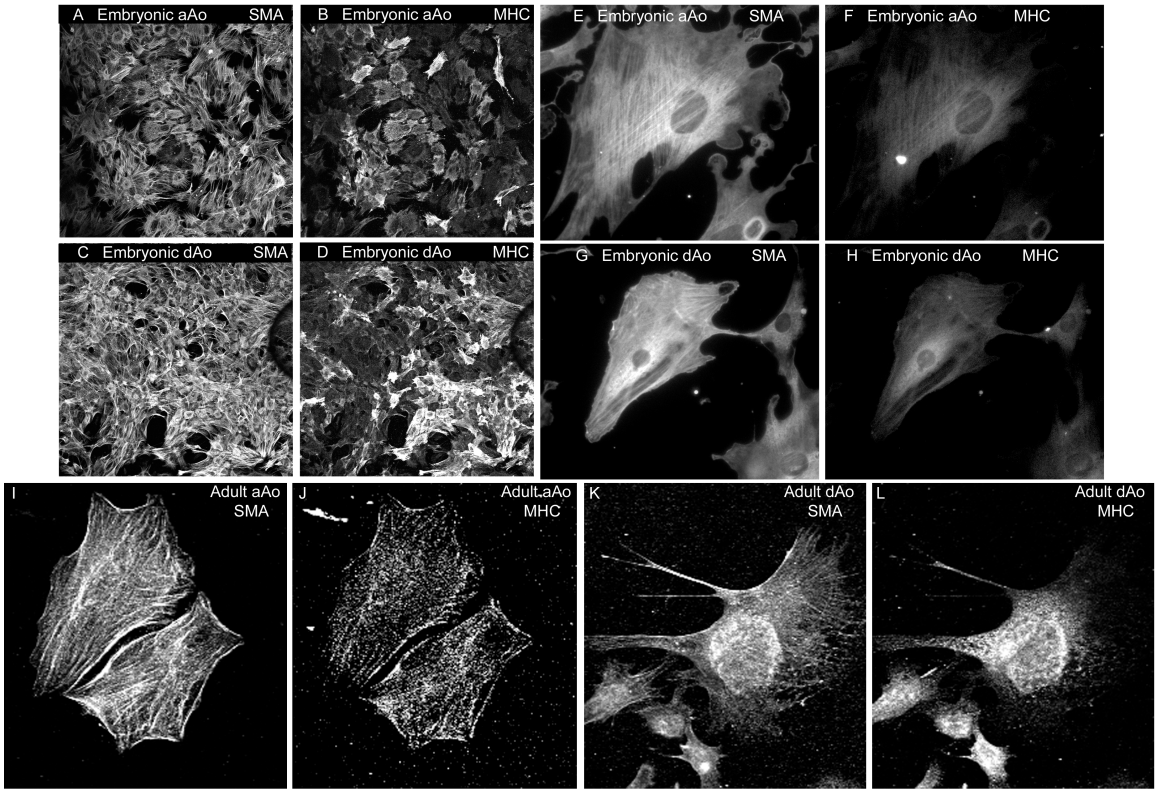

Figure 2.2 Isolated cells express VSMC markers smooth muscle actin (SMA) and smooth muscle myosin heavy chain (MHC). A-D) Explanted embryonic VSMCs three days after plating aorta. E-H) Expression of VSMC markers in clonal embryonic VSMC derived lines. I-L) Expression of VSMC markers in clonal adult VSMC derived lines.

Immunofluorescence and Imaging

Cells were fixed with 2% formaldehyde and 0.25% Triton-X in PBS. Antibodies used include: mouse anti- α smooth muscle actin (Sigma, 1:200), rabbit anti-smooth muscle myosin heavy chain (Biomedical Tech, 1:200), mouse anti-vinculin (Sigma, 1:200). Actin filaments were labeled with phalloidin 568nm (Invitrogen, 1:100), and DNA was labeled with DAPI (1:10,000). Imaging of immunofluorescence in isolated cells was performed on an Olympus FV_1000 inverted microscope in the Vanderbilt University Cell Imaging Shared Resource Core. Fluorescent images are z-projections

generated using ImageJ software. Quantification of the VSMC migration assay was conducted using ImageJ software. Whole mount imaging of aortae was performed using a Leica M165 FC dissecting microscope.

For quantification of focal adhesion area, fixed VSMCs on glass coverslips were blocked in 5% goat serum and 1% bovine serum albumin for 1 hr at RT. Cells were stained with α-vinculin antibody to label focal adhesions for 1 hr at RT and with anti-mouse IgG 488nm (Invitrogen, 1:500) and DAPI for 45 minutes at RT. Using ImageJ, background fluorescence and diffuse perinuclear labeling were removed using the threshold function. Focal adhesions were selected and analyzed using the "Analyze Particle" function. Focal adhesions were measured for area in pixels for both embryonic and adult VSMC derived lines. These data were analyzed with the Mann-Whitney U test.

***In vitro* assays**

Boyden chamber assays were completed with 8μm Millicell inserts. 40,000 cells were loaded into each well and four wells were assayed for each of three cell lines derived from the different regions of the aorta from both 16.5 dpc embryos and 8 week-old adults. After 24 hours, the filters were removed and cells on the underside of the filter were visualized by Giemsa staining. The number of cells per area were counted and then averaged. Student's paired t-tests were used to determine statistical significance.

Scratch assays were performed in 4 well chamber slides. Cells were plated at confluence ($5x10^5$ cells/well). 24 hours later, sheets of confluent cells were scratched with a p20 pipette tip with equal force applied to each well. Width of the wound at time 0 and after 6 hours was determined and the average percent wound closure was calculated

for each cell line. Four wells of each of three cell lines derived from the different regions of the aorta from both 16.5 dpc embryos and 8 week-old adults were quantified. Statistical significance was determined with a Student's paired t-test.

Results

Ascending and descending domains of the embryonic aorta exhibit distinct patterns of gene expression.

The aAo and dAo domains of the aorta are derived from NC and somitic mesoderm respectively. The aAo and dAo of 13.5dpc embryos were subjected to microarray analyses to explore whether distinct components of a single vessel derived from diverse progenitor pools have varied patterns of gene expression. This stage was chosen because it is the first day after reorganization of the truncus arteriosus into the aortic arch and pulmonary trunk. *Wnt-1-Cre; R26R*^{YFP} NC lineage labeled aortae were used to accurately dissect aortic regions containing NC and mesodermal derivatives within the developing aorta (Figure 2.3A). In comparing gene expression patterns of the aAo versus the dAo, we found a total of 1,475 significantly differentially hybridized probes. Significance was defined as expression of at least 1.5-fold difference and a B-H p value of <0.05. Of these 1,475 differentially hybridized probes, 459 genes were upregulated in the aAo and 597 genes were upregulated in the dAo (Figure 1B). Using the Database for Annotation, Visualization and Integrated Discovery (DAVID), we analyzed the gene ontology (GO) terms associated with each

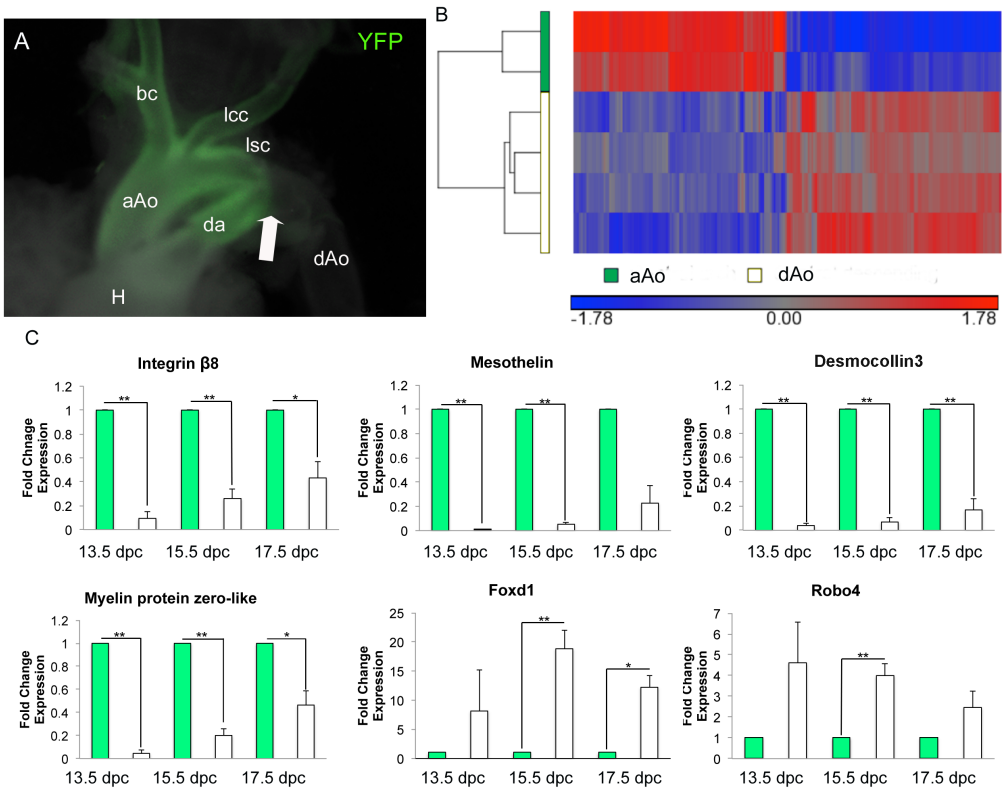

Figure 2.3 Embryonic regions of the aorta have distinct gene expression profiles. A) Wnt1-Cre; R26RYFP lineage labeled aorta demonstrating the border between the aAo and dAo. White arrow points to the border between the NC- and somitic-derived VSMCs. B) Hierarchical clustering of 1,475 probes detected as significantly different (at least 1.5-fold, B-H p value < 0.05) between control aAo and dAo samples. Values shown are log base 2, and bright red, bright blue, and gray indicate the highest, lowest, and median normalized signal values, respectively. Vertical dendrograms represent the individual samples, of which there are two to four replicates for each sample type. C) qRT-PCR on RNA taken from aorta samples throughout development. Abbreviations: aAo, ascending aorta; bc, brachiocephalic artery; da, ductus arteriosus; dAo, descending aorta; H, heart; lcc, left common carotid; lsc, left subclavian. Error bars represent SEM. *, $p \leq 0.05$; **, $p \leq 0.01$.

gene identified in the microarray (Table 2.2). Because we were interested in the smooth muscle characteristics of cell adhesion and cell migration, we focused on GO term categories related to those processes. One of the GO terms containing a number of genes highly expressed in the aAo was “cellular adhesion”. In the dAo, genes related to the GO

terms “cell migration” and “cell motion” were highly expressed in comparison with the aAo. The genes that were most differentially expressed in these categories were the ones we proceeded to verify. qRT-PCR of selected gene products identified by microarray verified their differential expression in the aAo versus dAo at 13.5, 15.5, and 17.5 dpc (Figure 2.3C). Sustained differences in gene expression patterns across the timeframe measured suggest that these data reflect definitive phenotypes in these embryonic structures.

Gene Ontology Category	aAo	dAo
Biological Process	**Number of Genes**	
G protein signaling	10	-
Ion transport	39	39
Cell adhesion	35	80
Ion homeostasis	22	29
Cell surface receptor linked signaling	-	95
Response to wounding	-	48
Cell migration	-	30
Cell motion	-	41
Immune response	-	46
Extracellular structure organization	-	18
Regulation of blood vessel size	-	8

Table 2.2 Example GO terms differentially regulated in different regions of embryonic aorta.

Microarray and gene expression studies suggested that developing aAo and dAo exhibit fundamental phenotypic differences in motility and contractility. We derived cells lines from distinct regions of the aorta of embryonic 16.5 dpc Immorto mice to assess these characteristics at the cellular level and determine whether gene expression variation observed *in vivo* was retained in VSMCs. Importantly, clonal cell lines derived from embryonic aAo and dAo maintained the differential expression of genes identified from the microarray of native tissue (Figure 2.4). In observing these cells,

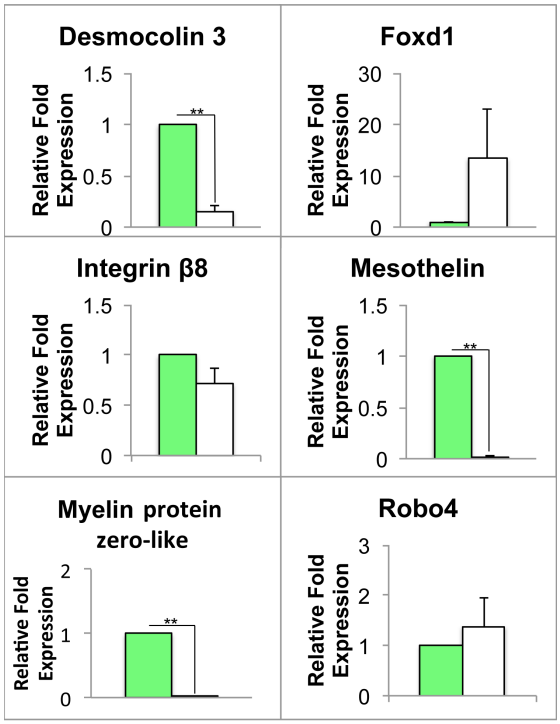

Figure 2.4 Isolated embryonic VSMCs differentially express genes related to cell adhesion and cell migration. qRT-PCR on RNA from cell lines demonstrating the relative expression of candidate genes. Green bars represent aAo VSMC line gene expression; white bars represent dAo VSMC line gene expression. Error bars represent SEM. *, $p \leq 0.05$; **, $p \leq 0.01$.

immediate and consistent differences were observed between lines derived from embryonic aAo versus dAo domains. First, when VSMC cell lines derived from the two domains were stained with phalloidin to highlight filamentous actin and an antibody against vinculin to visualize focal adhesions, significant and reproducible variation in the distribution of actin filaments and focal adhesions was revealed (Figure 2.5). Embryonic aAo VMSCs were relatively larger (4.5 times greater area, $p<0.05$) and had many focal adhesions scattered throughout the cell whereas the embryonic dAo VSMCs were consistently smaller and had significantly larger focal adhesions (Figure 2.5 A, D, and G). The localization of actin filaments also differed between embryonic aAo versus dAo cell lines with more organized parallel filaments evident in cells from the dAo (Figure 2.5 B and E). Importantly, while variation was observed in these cells, antibodies against SMA and MHC (Figure 2.2) confirmed that all derived cell lines maintained expression of markers of differentiated vascular smooth muscle.

These differences in cytoskeletal organization together with the gene expression profiles observed in intact vessels and clonal cell lines suggested that the embryonic aAo and dAo cells may also vary in migratory abilities (Chrzanowska-Wodnicka and Burridge, 1996). To test this hypothesis, scratch assays on confluent cell cultures were conducted to compare high-density cell migration in VSMCs from different embryonic origins. Six hours after injury, cell lines derived from embryonic dAo VSMCs moved at a significantly higher rate when compared to the migration of cell lines derived from embryonic aAo VSMCs (Figure 2.5 H-J). Next, single cell migratory properties were assessed using Boyden chamber assays. As predicted, and consistent with sheet

movement analyses, embryonic dAo VSMC-derived cell lines were consistently much more migratory when compared to aAo VSMCs-derived cell lines (Figure 2.5 K-M).

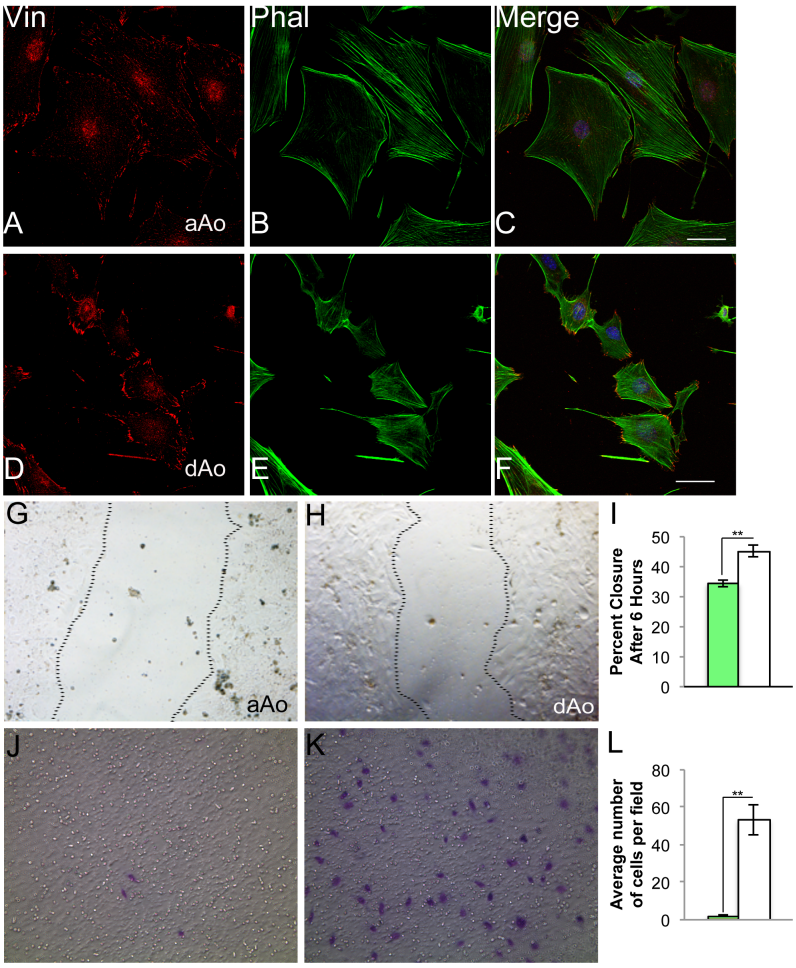

Figure II.5 Localization of cytoskeletal elements and migratory characteristics differ between cells derived from embryonic aAo versus dAo. A-C) Embryonic aAo VSMCs labeled with anti-vinculin antibody and phalloidin. D-F) Cells derived from the embryonic dAo labeled with anti-vinculin antibodies and phalloidin. DNA labeled with DAPI. G) Quantification of relative focal adhesion area. H, I) Scratch assay using embryonic aAo and dAo VSMC lines, 6 hours after scratch was applied. J) Quantification of percent wound closure in embryonic VSMC lines. K, L) Boyden chamber assay on embryonic VSMCs t=24 hours. Cells stained with Giemsa demonstrate the number of cell that invaded the membrane. M) Quantification of number of cells migrated after 24 hours. Scale bars represent 50μm. Abbreviations: Vin, vinculin; Phal, phalloidin. Error bars represent SEM. *, $p \leq 0.05$; **, $p \leq 0.01$.

Regions of the aorta have distinct contractile properties in the embryo.

We next determined whether the observed phenotypic differences extended to contractile properties in these two domains derived from NC and mesodermal progenitors. To test the relative contractility of the vessel, aortae from 15.5 and 19.5 dpc embryos were cannulated and the change in lumen diameter in response to applied vasoconstrictors was measured (Figure 2.6). Importantly, this myographic approach allowed for the simultaneous analysis of both domains within the same vessel. With the

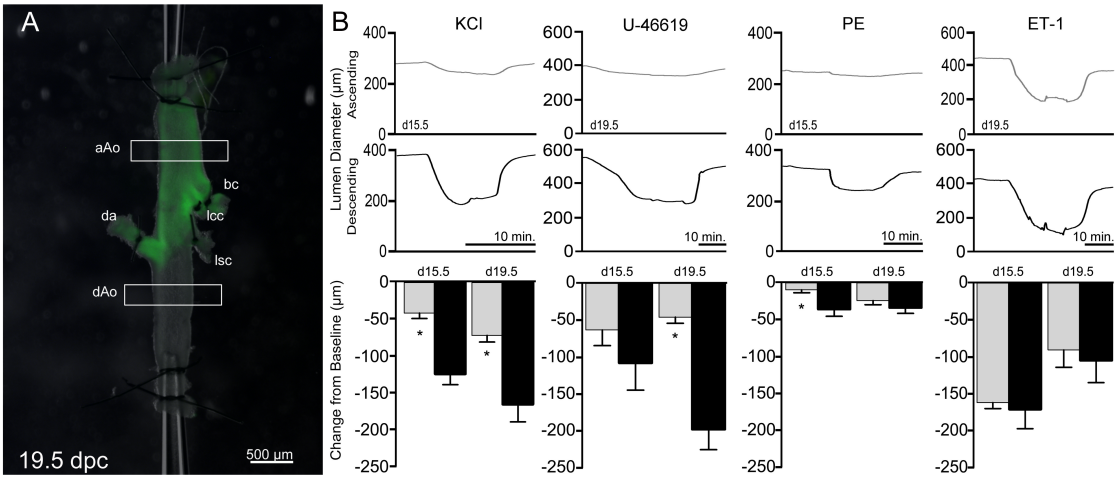

Figure 2.6 Region-specific contractile response of the embryonic aorta. A) Lineage labeled 19.5 dpc aorta mounted on cannula for experimental analysis. Boxes represent regions where lumen diameters are measured. B) Example traces from aAo (gray) and dAo (black) with the addition of different vasoconstrictors, PE (phenylephrine), ET-1 (endothelin-1). Abbreviations: aAo, ascending aorta; bc, brachiocephalic artery; da, ductus arteriosus; dAo, descending aorta; lcc, left common carotid; lsc, left subclavian. Error bars represent SEM. *, $p \leq 0.05$; **, $p \leq 0.01$.

addition of general (potassium chloride) and specific agonists (U46619 and phenylephrine), the embryonic dAo was significantly more contractile than the aAo counterpart at both gestational time points (Figure 2.6B). Taken together, these data

demonstrate that subdomains of an individual artery seeded by progenitors of varying origin exhibit distinct phenotypes in the embryonic state and these differences were maintained in cell lines derived from the regions of interest.

Phenotypic convergence of aAo and dAo domains in the adult aorta.

Given the phenotypic heterogeneity of ascending and descending domains of the embryonic aorta, microarray analysis was conducted on these same regions in the adult vessel to determine whether this divergence persisted. In turn, these results were compared to expression patterns observed for the superior mesenteric and coronary arteries whose myogenic components are derived from serosal and epicardial mesothelia respectively (Dettman et al., 1998; Landerholm et al., 1999; Wilm et al., 2005). Interestingly, while significant variation was observed between the aorta, mesenteric, and coronary vessels, expression profiles of the aAo and dAo of the adult did not vary. In these analyses, 1,496 probes were differentially hybridized across these four vessels (Figure 2.7A and B). Within this probe set, unique expression profiles for the superior mesenteric, coronary, and aorta as a whole were readily identified (Figure 2.7B). Surprisingly, of the 1,496 differentially hybridized probes, none were significantly differentially expressed between the ascending and descending aorta (Figure 2.7). Furthermore, the differentially expressed genes that were verified with qRT-PCR in embryonic vessels were either not expressed or expressed at very low levels in the adult aorta. While in the embryo the data suggested two distinct gene expression profiles in the aAo and dAo, the adult aorta has statistically uniform gene expression profiles.

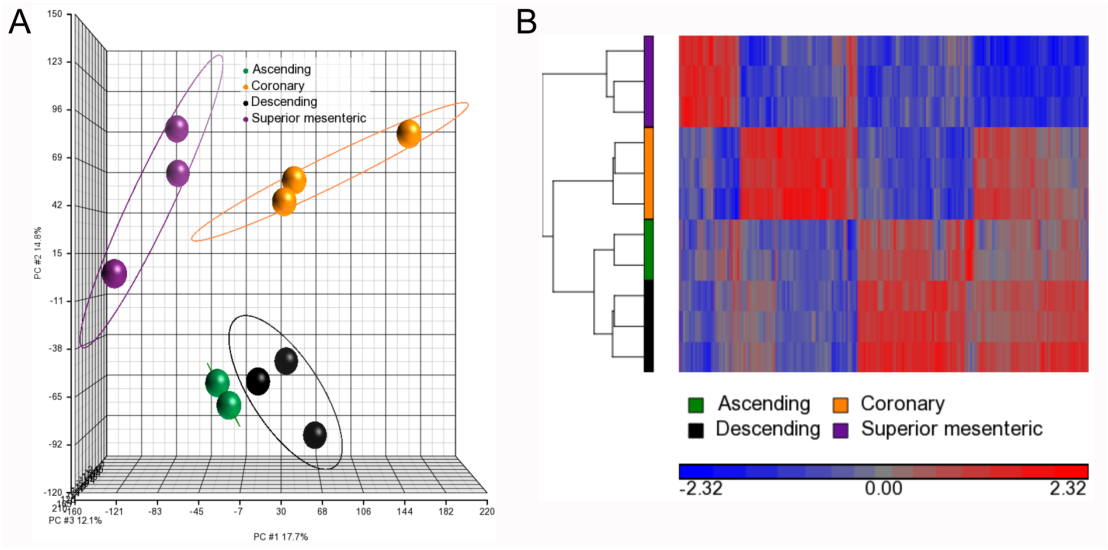

Figure 2.7 Adult vessels have different gene expression patterns, however the regions of the aorta have similar profiles. A) Principal components analysis of four different blood vessel tissues: ascending aorta (red), descending aorta (green), coronary artery (blue), and superior mesenteric artery (purple) is shown. The colors represent the different sample replicates, as indicated in the legend, and circles mark the ellipsoids (+/- standard a deviation of 2) for each group. The X-axis, Y-axis, and Z-axis components represent 17.7%, 14.8%, and 12.1%, respectively, of the total variability between experimental replicates. B) Hierarchical clustering of 1,496 probes detected as significantly different (at least 1.5-fold, B-H *p value* < 0.05) between ascending aorta, descending aorta, coronary, and superior mesenteric arteries. Values shown are log base 2, and bright red, bright blue, and gray indicate the highest, lowest, and median normalized signal values, respectively. Vertical dendrograms represent the individual samples, of which there are three replicates for each sample type (two replicates for ascending aortic tissue).

In light of this finding, we tested the other basic parameters that distinguish embryonic domains within the adult aorta. VSMC lines from the adult aAo and dAo were derived using the same methodologies employed on embryos. Interestingly, morphology and cytoskeletal characteristics of clonal VMSC-derived lines isolated from adult aAo and dAo domains were also remarkably similar (Figure 2.8 A-G). Additionally, migratory patterns of cell sheets after scratch injury and of single cells in Boyden chamber analyses from both adult domains were tested to probe phenotypic characteristics (Figure 2.8 H-M). In both settings, movement of cells derived from either domain was indistinguishable using quantitative analyses in contrast to those observed for their embryonic counterparts. Finally, analyses of vessel contractility were conducted on young adults using the same myographic modalities employed on embryonic counterparts. Here, we determined that the contractile properties of the aAo and dAo were remarkably similar with no significant difference in response to any of the antagonists cited above (Figure 2.9). The single exception to this pattern is endothelin-1, an endothelially-expressed gene product, which has potent non-region-specific effects in the fetal aorta, but only limited effects on the adult aAo and dAo. Application of vasodilators did not reveal any pattern of dilation in the different regions of the aorta in either the embryo or the adult (Figure 2.10).

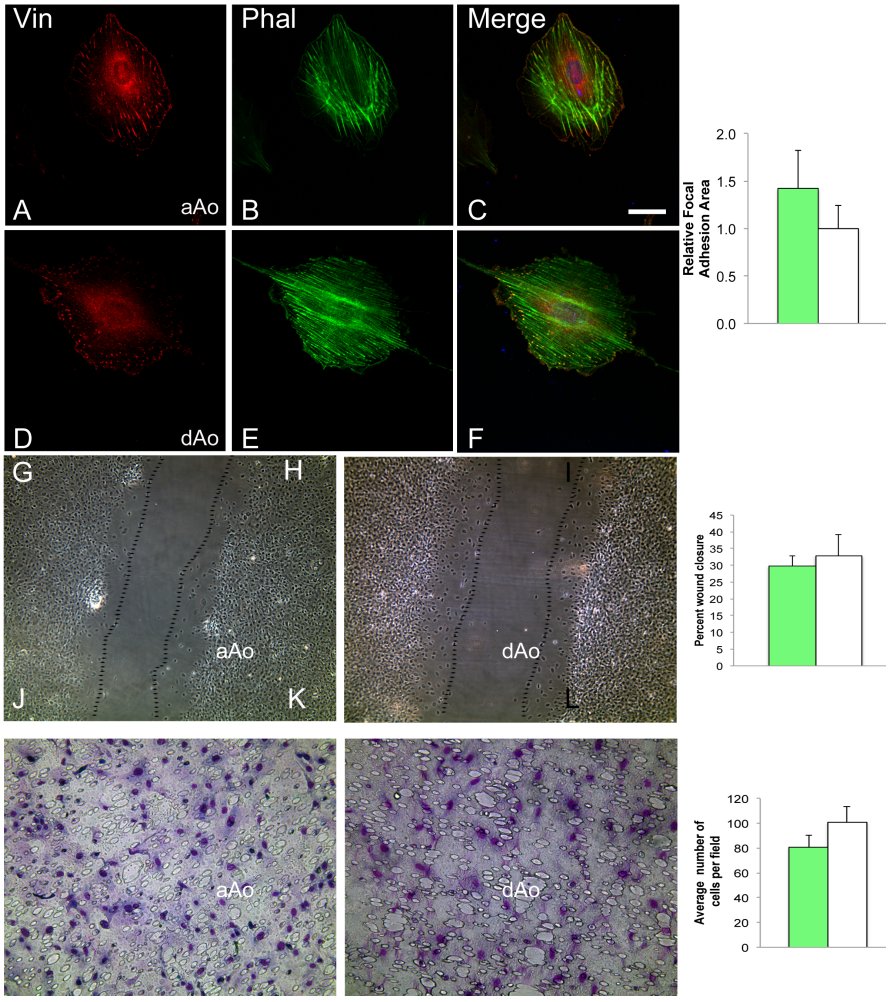

Figure 2.8 VSMC lines from adult aAo and dAo have similar localization of cytoskeletal elements and migratory characteristics. A-C) Representative adult aAo VSMCs labeled with anti-vinculin antibody and phalloidin. D-F) Representative adult dAo VSMC lines labeled with anti-vinculin antibodies and phalloidin. DNA labeled with DAPI. G) Quantification of relative focal adhesion area. H, I) Scratch assay of adult aAo and dAo VSMC lines after 6 hours. J) Quantification of percent wound closure in adult VSMC cultures. K, L) Boyden chamber assay on adult VSMC lines t=24 hours. M) Quantification of number of cells migrated after 24 hours. Scale bars represent 50μm. Abbreviations: aAo, ascending aorta; dAo, descending aorta; Vin, vinculin; Phal, phalloidin. Error bars represent SEM. *, $p \leq 0.05$; **, $p \leq 0.01$.

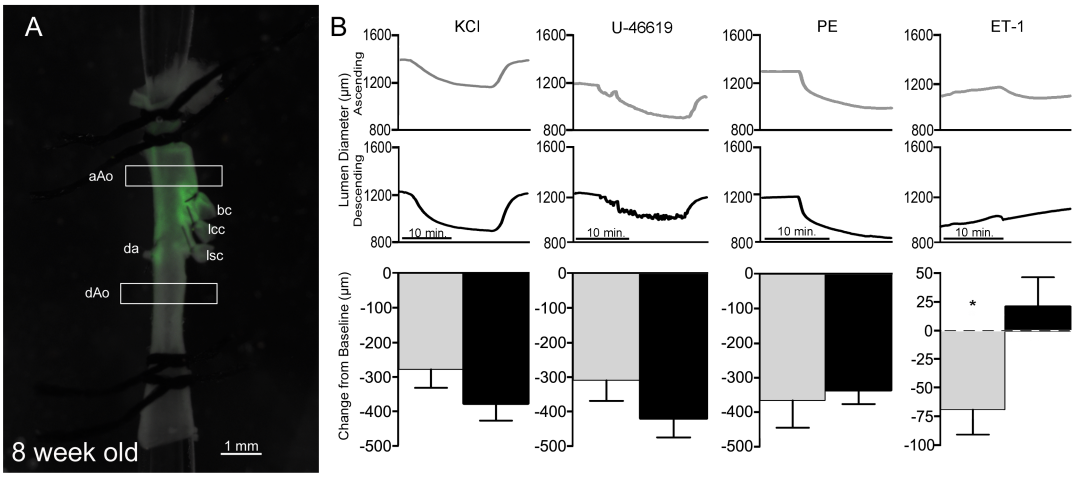

Figure 2.9 Regions of the adult aorta have similar contractile responses to vasoconstrictors. A) Lineage labeled 8 week old aorta on cannula. Boxes represent regions where lumen diameters are measured. B) Example traces from aAo (gray) and dAo (black) with the addition of different vasoconstrictors, PE (phenylephrine), ET-1 (endothelin-1). Abbreviations: aAo, ascending aorta; bc, brachiocephalic artery; da, ductus arteriosus; dAo, descending aorta; H, heart; lcc, left common carotid; lsc, left subclavian. Error bars represent SEM. *, $p \leq 0.05$.

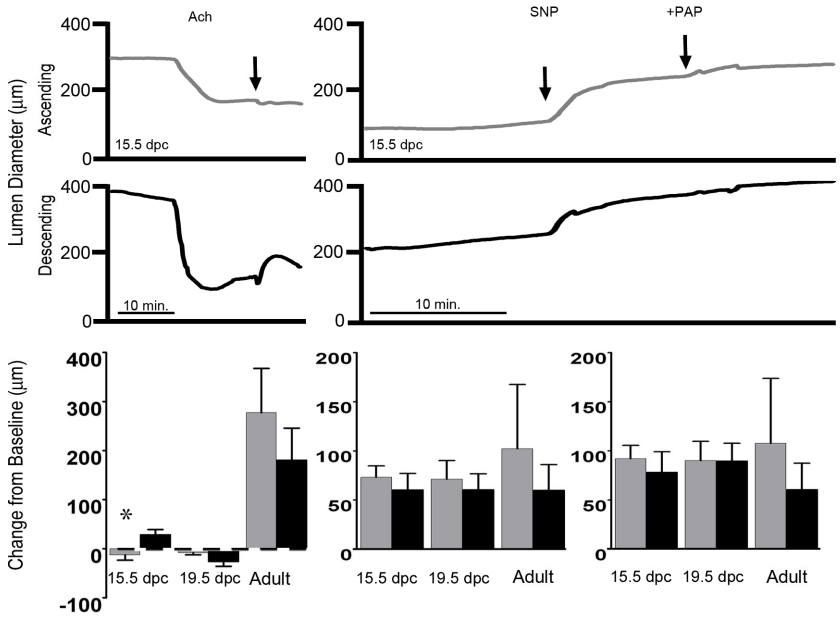

Figure 2.10 Vasodilators do not elicit a patterned response in the regions of the aorta. Whole vessel myography with the application of vascodilators. aAo (gray) and dAo (black) dilate to a similar degree in both embryonic and adult aortae. Ach, acetylcholine; SNP, sodium nitroprusside; PAP, papaverine.

Discussion

The data presented in this study conclusively demonstrate the unique characteristics of the embryonic regions of the aorta, which phenotypically converge in the adult. This is a novel finding that establishes a roadmap for future analyses to determine how this process of convergence occurs and what happens when the VMSCs of the aorta falter in patterning. Further investigation can now be done to examine the variables that influence convergence. One exciting manipulation would be to expose embryonic regions of the aorta to different flow conditions to change the biomechanical environment. It is possible that the change in blood pressure and flow that occurs at birth is the event that results in vascular convergence. These data firmly establish a platform on which a more complete understanding of vascular maturation can be built.

Additionally, these data may serve as a paradigm to explain how apparently homogeneous smooth muscle populations in the adult respond differently to injury or disease. For example, it is not uncommon for tissues in the adult to revert to embryonic characteristics when stressed. Similarly, cells of the nephron reactivate developmental programs to repair damage done to the kidney (Jiang et al., 2013; Lin et al., 2010). In this context, reverting to a developmental program allows the cells of the tissue to repair and maintain function. The heart is another example of an organ that reactivates developmental characteristics to protect against stress (Oka et al., 2007; Rajabi et al., 2007). It has been hypothesized, however, that long term these developmental characteristics may lead to disease in the adult (Rajabi et al., 2007). Therefore, one potential explanation for the difference in disease progression of these two regions of the aorta may be that, despite their similar adult characteristics, these domains revert to their

divergent embryonic state to cope with stress. This reversion may, over time, result in the differential pattern of disease found in different regions of the aorta including atherosclerosis and calcification as well as aortic aneurism at the junction between regions (Haimovici and Maier, 1971; Leroux-Berger et al., 2011; Majesky et al., 2011). We would predict that a metabolically stressed mouse model would exhibit the embryonic patterns we have described in the different regions of the aorta.

The plasticity of smooth muscle cells in culture has been well documented (Chamley-Campbell et al., 1979). VSMCs are easily manipulated by the conditions under which they are cultured. Therefore, it is entirely possible that the *in vitro* experiments described above do not perfectly replicate the *in vivo* setting. Due to the sensitivity of these cells, it was critical that all clones were treated the same. Based on the stability of both VSMC markers and the differential expression of genes identified from the microarray, these data clearly indicate significant differences between the embryonic cell lines derived from diverse origins and the maintenance of these differences over the timeframe studied *in vitro*.

Our studies lay the groundwork to determine whether the fundamental differences in embryonic VSMCs play a role in vascular diseases of the adult. The data described here lay the groundwork for the determination embryonic patterns converge in the adult and the role this plays in the context of disease.

CHAPTER III

LOSS OF CENP-F CAUSES MICROTUBULE HYPER-STABILIZATION AND DEFECTS IN FOCAL ADHESION DYNAMICS, CELL POLARITY, AND DIRECTIONAL MIGRATION

Abstract

Remodeling of the microtubule network is vital for a diverse range of cellular functions including intracellular transport, directional migration, and cell division. CENP-F is a large, multiple domain-containing protein with diverse nuclear and cytoplasmic functions. A common theme underlying these activities is CENP-F interaction with the microtubule network. Still, little is known concerning the role of CENP-F in regulation of microtubules. We have established a novel *CENP-F*$^{-/-}$ cell model and demonstrate that loss of CENP-F hyperstabilizes the microtubule network with accumulation of tubulin post-translational modifications. The overall stabilization of the microtubule network in *CENP-F*$^{-/-}$ cells prevents cell polarization and leads to strong defects in focal adhesion dynamics and cell motility. We conclude that CENP-F is a powerful regulator of the microtubule network, and that its loss of function impacts a broad array of cellular behaviors in development, homeostasis, and disease.

Introduction

Microtubules (MTs) are dynamic polymers assembled from α/β-tubulin that participate in many critical cellular functions including movement, division, and intracellular transport. The MT network governs a broad range of functions through association with protein factors that regulate the dynamic properties and organizational states of the MT network. CENP-F (previously named mitosin and LEK1) is a large protein (350/400 KDa) that directly interacts with MTs (Feng et al., 2006) and with other MT-associated proteins (Moynihan et al., 2009b; Soukoulis et al., 2005b; Vergnolle and Taylor, 2007). CENP-F was first identified in tumor cell lines through its interaction with the kinetochore (Rattner et al., 1993) and by its binding to retinoblastoma (RB) protein (Ashe et al., 2004; Papadimou et al., 2005; Zhu et al., 1995). Subsequent work demonstrated that CENP-F also interacts with the centrosome (Moynihan et al., 2009b), nuclear envelope (Zuccolo et al., 2007), and transfer vesicles (Pooley et al., 2008; Pooley et al., 2006). Additionally, subcellular localization of CENP-F is dynamic, changing throughout mitosis and interphase (Liao et al., 1995; Rattner et al., 1993). CENP-F is ubiquitously expressed in the embryo with greatest levels in the developing heart and anterior brain and in the adult, albeit at reduced levels (Dees et al., 2012b).

As might be expected from its multifaceted domain structure and its complex and dynamic localization, CENP-F function at the cellular level is multiple and diverse. Previous *in vitro* studies have shown that loss of CENP-F or dominant negative CENP-F results in mitotic delay and misaligned chromosomes demonstrating its importance in mitosis (Chan et al., 1998; Holt et al., 2005; Hussein and Taylor, 2002; Liao et al., 1995; Yang et al., 2005). Further, CENP-F interacts with Hook2 at the centrosome influencing

cell shape (Moynihan et al., 2009b), with SNARE proteins regulating vesicular transport pathway (Pooley et al., 2008; Pooley et al., 2006), and plays an important role in interphase regulating primary cilium length (Jodoin et al., 2013). Loss of function leads to seemingly diverse neurological and muscular diseases (Holth et al., 2013; Khairallah et al., 2012). Cardiac-specific loss of CENP-F in the embryo results in adult-onset dilated cardiomyopathy and death (Dees et al., 2012b). Importantly, CENP-F overexpression has been used as a proliferation-marker of various cancers (Clark et al., 1997; Erlanson et al., 1999; Hui et al., 2005; Liu et al., 1998; Rattner et al., 1997). Autoantibodies against CENP-F are a hallmark of specific cancers (Rattner et al., 1997; Tschernatsch et al., 2005), and *CENP-F* gene amplification is observed in squamous cell carcinomas (de la Guardia et al., 2001). Thus, CENP-F function has broad and varied impact at the level of organelles, cells, organs, and the organism itself.

While multiple laboratories have conclusively demonstrated that CENP-F has wide-ranging control of diverse functions, the critical impact of CENP-F loss of function on its most fundamental relationship, that with the MT network, has not been resolved. Determining the role of CENP-F in regulation of the MT network is important for a mechanistic understanding of protein function in the diverse downstream events seen with loss and gain of gene function in development and disease.

Here, we have developed a novel cell model to explore the role of this protein in regulation of the MT network. Our data show that ablation of the *CENP-F* gene leads to an unexpected hyper-stabilization of the MT network with a unique loss of dynamic instability. With disruption of MT dynamics, *CENP-F*$^{-/-}$ cells exhibit dramatic loss of directionally persistent migration, defects in focal adhesion disassembly and

lamellipodial formation/retraction, and loss of regulation of cell shape. Taken together, this work provides molecular mechanism for loss of CENP-F function and the foundation for analysis and intervention in the various developmental and pathological abnormalities seen with disruption of this complex gene product.

Materials and Methods

Mouse Lines

Mice were previously described in Moynihan et al, 2009. *CENP-F*$^{fl/-}$; CMV-CRE animals were crossed to generate *CENP-F*$^{-/-}$; CMV-CRE animals. *CENP-F*$^{+/+}$; CMV-CRE animals were used to generate control mouse embryonic fibroblasts (MEFs). Dams were monitored daily for the presence of a vaginal plug with noon on the day of the plug noted as 0.5 dpc.

MEF Isolation

Primary MEFs were isolated from E13.5 day embryos using standard procedures. MEFSs were isolated as in Moynihan et al 2009. MEFs were used within three passages to avoid replicative senescence.

Genotyping

PCR genotyping was based on three features to distinguish wild type from Cre-mediated *CENP-F* exon 1-5 deletion: presence of the 5' loxP site upstream of *CENP-F*,

generation of a DNA band only possible with recombination after Cre-mediated excision, and the presence of the *cTNT-Cre* gene. The primers are listed below.

Across 5' loxP site: 5' AATAATGAAGCTGACACCAAAAACT,

3' GAACCTACCGTCTGAGAACCACTG;

Recombination band: 5' AATAATGAAGCTGACACCAAAAACT,

3' GAGGAGCACAGGAGGGAAATG

CMV-Cre: 5' TCC GGG CTG CCA CGA CCA A,

3' GGC GCG GCA ACA CCA TTT TT

Imaging

For migration movies, cells were plated on 1ug/ml fibronectin on MatTek dishes and DIC images were acquired at 1-minute intervals on the Deltavision (Applied Precision) in the Epithelial Biology core. Fluorescent images were also acquired on the Deltavision. For MT dynamics movies frames were acquired every 3 seconds for 2 minutes on the Deltavision at 100x magnification. WT and *CENPF*$^{-/-}$ cells were transfected with 0.5ug 3xGFP-EMTB (Addgene plasmid 26741) using Fugene6 (Roche) according to standard protocols.

Images showing dynamic movie pixels were created by projecting pixel differences between movie frames using an Image J macro available at http://rsb.info.nih.gov/ij/macros/Slice-to-Slice%20Difference.txt

For quantification of focal adhesions (FAs), fixed MEFs on glass coverslips were blocked in 5% goat serum and 1% BSA for 1 hr at RT. FAs were stained with α-vinculin antibody (1:200) for 1 hr at RT and with anti-mouse IgG 488nm (1:500) and TOPRO

(1:1000) for 45 minutes at RT. Cells were imaged on Zeiss LSM 510 Meta inverted confocal microscope in the Vanderbilt Cell Imaging Shared Resource Core at 40x. Projections were created from 0.3 μm slices through full thickness of FAs. In ImageJ background fluorescence and diffuse perinuclear labeling were removed using the threshold function. FAs were selected and analyzed using the "Analyze Particle" function. FAs were measured for total and average fluorescence in arbitrary units and area in pixels for both WT and *CENP-F*$^{-/-}$ MEFs. WT and *CENP-F*$^{-/-}$ FAs were statistically analyzed with the Mann-Whitney U test.

For reference cell, cells were plated and fixed on fibronectin crossbow micropatterns (CYTOO, Inc.) and stained with vinculin antibody as above. Single images were taken as above. Cells which completely occupied micropatterns were stacked in ImageJ, and a reference cell was created for WT and *CENP-F*$^{-/-}$ MEFs by averaging vinculin fluorescence in each stack and applying an ImageJ LUT.

Western Blot

Western blotting was conducted according to Bader et al (27) using appropriate Odyssey secondary antibodies and imaging (Pierce).

FRAP

Cells were transfected with mCherry-Paxillin using Fugene-6 (Promega) 48 hours before imaging. Frames were acquired every 10 seconds for 10 minutes. An ROI was set in a region containing FAs. A 1 second 405 nm laser event was scheduled on the third frame. Movies were generated on the Deltavision at 40x magnification. Fluorescence

intensity in bleached and non-bleached FAs was measured using ImageJ software. Bleached areas were normalized to non-bleached areas both pre- and post-bleach in order to obtain fluorescence recovery values. Data represents fraction of fluorescence recovery in the bleached region. Immobile fraction was calculated using the following equation: fi=1-[f(f)/(f(p)] (fi=immobile fraction, f(f)=fluorescence intensity final, f(s)=fluorescence intensity prebleach).

Nocodazole Treatment

Nocodazole (NOC) was diluted into DMSO. Cells were treated with 0, 1ug/ml, 2.5 ug/ml for two hours before analysis.

Quantification of MT Array Asymmetry

Quantified as previously described(Miller et al., 2009). Representative images are shown.

Antibodies

Cells were fixed for 10' at RT in 2% PFA with 0.25% triton prior to antibody labeling.

DM1A: mouse monoclonal Abcam (ab7291)

Acetylated tubulin: mouse monoclonal Abcam (ab24610)

Anti-Tubulin Detyrosinated (Glu): rabbit polyclonal Millipore (AB3201)

Cyclophilin B Abcam (ab16045)

Vinculin Abcam (ab18058)

Alexa Fluor 488 phalloidin Invitrogen (A12379)

DAPI or TOPRO was used to visualize DNA

Results

CENP-F regulates cell size and MT distribution

Dynamic changes in the MT network are intricately related to cell shape, size, and polarity. Given the extensive association of CENP-F with the MT network and associated proteins, we first determined whether cell shape and overall pattern of the MT network changed with loss of CENP-F.

Comparing WT and *CENP-F*$^{-/-}$ MEFs, three distinct differences related to MT network function were immediately recognized. First, the *CENP-F*$^{-/-}$ MEFs were overall larger than WT MEFs (Figure 3.1A,C). Second, while WT MEFs exhibited a typically asymmetric distribution of tubulin across the cell, *CENP-F*$^{-/-}$ cells lacked this asymmetric array (Figure 3.1; visualized with DM1A, an antibody against alpha tubulin). Quantification of fluorescence intensity confirmed the lack of symmetric distribution of MTs in the *CENP-F*$^{-/-}$ cells (Figure 3.1B,D). Finally, we noted that *CENP-F*$^{-/-}$ MEFs have long "swirled" MTs near the cell periphery when compared to their WT counterparts (Figure 3.1A,C). Thus, the overall state of the cell and its MT network is dramatically altered with loss of CENP-F.

MTs in *CENP-F*$^{-/-}$ MEFs are hyper-stabilized.

Given that loss of CENP-F causes major changes in the MT network we postulated that altered MT dynamics may underlie this change in structure. While CENP-F has not been associated with regulation of MT post-translational modifications, the overall structure of the MT network in *CENP-F*$^{-/-}$ cells, especially with "swirling" MT extensions at the cell periphery, is suggestive of MT hyper-stabilization (Liu et al., 2005a; Liu et al., 2005b). Post-translational modifications, namely acetylation and proteolytic removal of the C-terminal tyrosine and glutamate residues, are a hallmark of long-lived, stable MTs (Infante et al., 2000; Webster et al., 1987). Acetylated and detyronsinated MTs are typically found in the perinuclear region where the "oldest" MTs reside (Li et al., 1996b; Webster and Borisy, 1989). Indeed, this concentration of modified tubulin is observed in the perinuclear region of the WT MEFs (Figure 3.1F,G). In sharp contrast, the entire length of the MT network, from perinuclear domain to cell periphery, was enriched in these post-translational modifications of tubulin in *CENP-F*$^{-/-}$ MEFs (Figure 3.1I,J). Western blotting demonstrated that while WT and *CENP-F*$^{-/-}$ MEFs contain the same amount of tubulin, *CENP-F*$^{-/-}$ MEFs were enriched in acetylated tubulin (Figure 3.1K). This reveals that *CENP-F*$^{-/-}$ MEFs contain an abundance of modified MTs compared to WT MEFs.

NOC is a dose-dependent, MT-depolymerizing agent used extensively to probe for changes in MT stability (Samson et al., 1979). To determine the relative stability of MTs in WT and *CENP-F*$^{-/-}$ MEFs, cells were treated with varying concentrations of NOC and assayed with immunofluorescence for the presence of MTs. After a two-hour treatment with 1μg/ml NOC, we observed a paucity of MTs in WT cells with only short

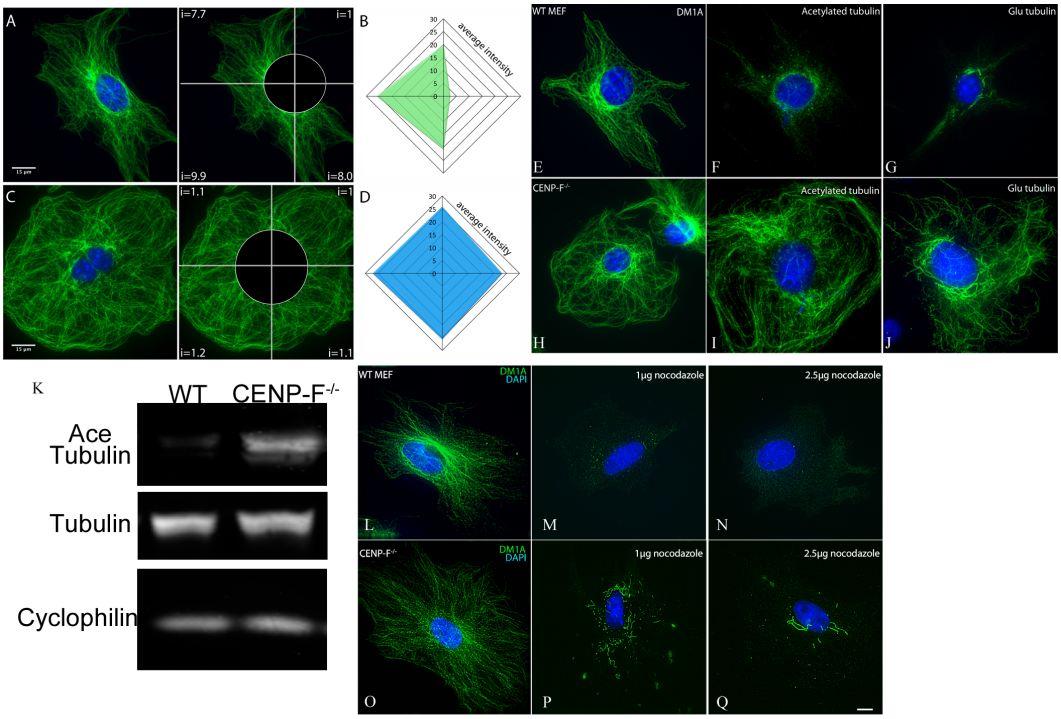

Figure 3.1 CENP-F is required for establishment of MT array asymmetry, and loss of CENP-F leads to an abundance of post-translational modifications and resistance to depolymerization by NOC. Immunostaining of MTs with DM1A antibody (green) and DAPI (blue) in WT (**A**) and *CENP-F*$^{-/-}$ (**C**) mouse embryonic fibroblasts. Scale bar = 15 microns. Schematic for fluorescence intensity quantification is shown in **(A, C left panels)** (see methods for detailed quantification description). Representative fluorescent intensity plots (N=30, each) of WT (**B**) and *CENP-F*$^{-/-}$ (**D**) are shown for each sample. For quantification purposes, cells were divided into four quadrants (L=left, R=right, F=front, B=back). Post-translational modifications of tubulin are indicative of MT stability. Immunostaining of MTs (green) in Wild-type MEFs (**E-G**) show minimal amounts of acetylated (**F**) and Glu (**G**) tubulin in relation to the typical staining of the complete MT network (**E**). In contrast, the MT network of *CENP-F*$^{-/-}$ MEFs (**H**) contain an abundance of post-translational modifications as indicated by immense acetylated (**I**) and Glu (**J**) tubulin staining. Scale bar=10 microns. Western blot demonstrating abundance of acetylated tubulin and tubulin in WT and *CENP-F*$^{-/-}$ MEFs (**K**). Immunofluorescence analysis of the MT network (green) in WT (**L-N**) and *CENP-F*$^{-/-}$ (**O-Q**) MEFs treated for 2 hours with no NOC (**L, O**), 1ug/ml NOC (**M, P**), or 2.5ug/ml NOC (**N, Q**). Numerous short MTs persist in *CENP-F*$^{-/-}$ MEFs (**P, Q**) as compared to full depolymerization of MTs in WT MEFs (**M, N**). N=25. Scale bar= 10 microns.

remnants persisting in the perinuclear domain (Figure 3.1M). Complete MT depolymerization was observed at 2.5 μg/mL NOC (Figure 3.1N). Conversely, the MT network of *CENP-F*$^{-/-}$ MEFs remained partially intact after two hours of 1μg/mL and even 2.5 μg/mL NOC, with intact, but shorter, segments in the perinuclear area (Figure 3.1P,Q) demonstrating the stability of these MTs.

CENP-F$^{-/-}$ MEFS lack directionally persistent migration

Stabilization of MTs at the leading edge of migrating cells promotes directionally persistent migration (Petrie et al., 2009). Given the lack of asymmetry in the MT network and the presence of hyper-stabilized MTs throughout *CENP-F*$^{-/-}$ cells, we postulated that these cells would lack directionally persistent migration. Live cell microscopy by DIC clearly demonstrated that WT cells exhibited directionally persistent migration over the one-hour time span tested (Figure 3.2A-D). In contrast, *CENP-F*$^{-/-}$ MEFs were unable to maintain migration in a sustained direction (Figure 3.2E-H), with quantification of directional persistence parameters showing a significant difference between WT (0.81) and *CENP-F*$^{-/-}$ (0.24) MEFs ($p=<0.001$) (Figure 3.2I). Additionally, generation and retention of lamellapodial extensions varied greatly in these cells. While lamellapodia were generated and retained along the axis of migration in WT cells, these structures appeared randomly and transiently around the circumference of *CENP-F*$^{-/-}$ cells (Supplemental movies 1 and 2). Finally, to explore the relationship between MT stabilization and the loss of directionally persistent migration, MEFs were treated with 1μg/mL NOC to chemically destabilize the MTs. NOC treatment did not significantly

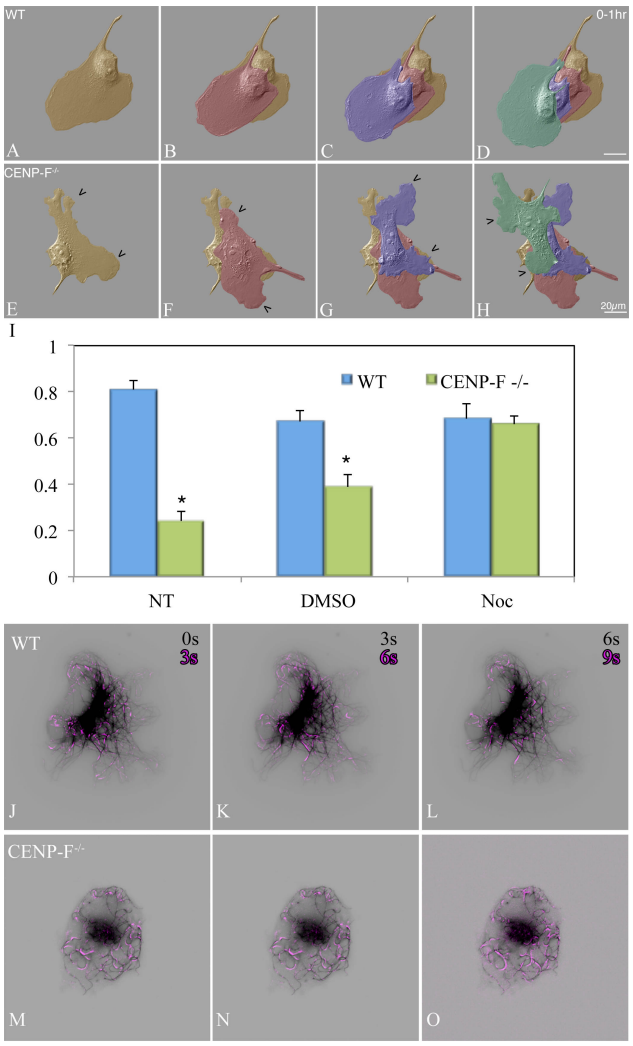

Figure 3.2 *CENP-F*$^{-/-}$ MEFs lack directionally persistent migratory patterns and have dramatically altered MT dynamics. Migration patterns of WT (A-D) and *CENP-F*$^{-/-}$ (E-H) acquired by DIC microscopy over a period of one hour. False-colored overlays of cells are shown in panels **A-H**. Orange= time zero, Red= 20 mins, Purple= 40 mins, Green= 60 mins. *CENP-F*$^{-/-}$ MEFs fail to establish directionally persistent migration patterns as quantified in **I**. When treated with DMSO there is not a statistically significant difference in directional persistence, but treatment with NOC restores *CENP-F*$^{-/-}$ directional persistence. A value of 1.0 corresponds to movement in a straight line whereas 0 equals random movement. WT= 0.81 and *CENP-F*$^{-/-}$= 0.24. N=20. p=<0.001. Error bars represent SEM. Time-lapse imaging of WT (**J-L**) and *CENP-F*$^{-/-}$ (**M-O**) MEFs expressing 3xEGFP-EMTB (black) to highlight the MT network. Images showing dynamic pixel differences were created by projecting pixel differences (purple) between sequential movie frames. Normal MT dynamic instability can be observed in WT (**J-L**) MEFS with periods of growth and shrinkage (in purple) primarily at the MT tips. In contrast, *CENP-F*$^{-/-}$ MEFs (**M-O**) show pixel differences (purple) along the entire length of the MT with very little pixel differences excluded to the cell periphery.

affect the directional persistent movement of the WT MEFs compared to control DMSO treatment (Figure 3.2I). Interestingly, treatment of *CENP-F*$^{-/-}$ MEFs with 1ug/mL NOC for two hours restored directed movement comparable to that observed WT MEFs (Figure 3.2I, Supplemental movies 3 and 4), consistent with the idea that CENP-F plays a role in MT destabilization or remodeling.

CENP-F$^{-/-}$ MTs have impaired dynamics

Hyper-stabilization of the MT network most often leads to a reduction in MT dynamics, visualized as stunting of growth and regression at MT plus ends (Gardner et al., 2012). As shown here, loss of CENP-F function leads to hyper-stabilization of the MT network with concurrent inability of the cell to move in a directionally persistent manner. A potential molecular mechanism linking these two phenomena is the disruption of MT dynamics.

To explore whether changes in MT dynamics occur with loss of CENP-F function, GFP-EMTB-labeled MTs in WT and *CENP-F*$^{-/-}$ cells were imaged in real time. In agreement with previous reports in several cell systems (Altinok et al., 2007; Garrison et al., 2012; Uchida et al., 2010), WT MEFs exhibited typical characteristics of MT dynamics with the majority of change occurring at the MT tips over time (Figure 3.2J-L, Supplemental movie 5). Interestingly, the MT network of *CENP-F*$^{-/-}$ MEFs demonstrated much greater movement than in WT cells but, in a completely different manner. In these cells, movement was greatest along the length of the MT and not associated the peripheral tips (Figure 3.2M-O, Supplemental movie 6). Rather than the typical extension/retraction dynamic seen in WT cells, MTs of *CENP-F*$^{-/-}$ MEFs exhibited a

"shaking" dynamic at mid-points of the network. Thus, an increase in MT pause duration and a decrease in average growth and shrink rates correlate with microtubules which are not undergoing regular dynamic instability (Table 3.1).

DYNAMIC PARAMATER	**WT n=15**	**CENP_F$^{-/-}$ n=15**
Growth Rate (μm/s)	0.2796 ± 0.025	0.15165 ± 0.00374
Shrink Rate (μm/s)	0.2714 ± 0.008	0.18591 ± 0.0191
Average pause duration (s)	12.242 ± 1.09757	43.2889 ± 2.5005

Table 3.1 Dynamic properties of WT and CENP-F$^{-/-}$ microtubules.

Focal Adhesion Dynamics

Directional migration is also dependent on the ability of the cell to turn over integrin-based focal adhesions (FAs) (Sastry and Burridge, 2000; Webb et al., 2002). Interestingly, MTs and FAs are intimately related, with MT dynamics playing an integral role in FA disassembly (Ezratty et al., 2005; Kaverina et al., 1999; Small et al., 2002) and directional migration (Kaverina and Straube, 2011). Given that *CENP-F$^{-/-}$* MEFs have altered MT dynamics and impaired migration, we postulated that FA disassembly would be altered in these cells. To explore this concept, WT and *CENP-F$^{-/-}$* MEFs were stained for vinculin, a FA component, and imaged with confocal microscopy. Over 3,700 FAs were analyzed in WT and *CENP-F$^{-/-}$* cells for area, mean fluorescence, and total fluorescence with ImageJ, employing the Mann-Whitney U test for statistical

significance. FAs in *CENP-F*$^{-/-}$ MEFs were significantly larger (p=0.001), had slightly higher mean fluorescence (p<5.1E-05), and higher total fluorescence (p<5.6E-05) (Figure 3.3A-C).

To more systematically compare FAs, a reference cell approach was used. By plating cells on a standardized fibronectin pattern, cells take identical shapes and can be compared using average fluorescence across many cells (Thery et al., 2006). The crossbow pattern has previously been used to simulate a polarized, migrating cell (Theisen et al., 2012). MEFs were plated on a standardized crossbow pattern, fixed, stained with vinculin, and imaged. Approximately 70 WT and *CENP-F*$^{-/-}$ cells were stacked and a visual average created. Using this approach, it is clear that *CENP-F*$^{-/-}$ MEFs have a much higher average fluorescence in the distribution of FAs (Figure 3.3F,I). Interestingly, *CENP-F*$^{-/-}$ MEFs on average had increased diffuse vinculin staining throughout the cell, as shown by a greater cytoplasmic fluorescence (Figure 3.3 H,I, Figure 3.4). To determine whether differences in FA size and density resulted from changes in FA dynamics, fluorescence recovery after photobleaching (FRAP) was employed to calculate the dynamics of on FA associated protein, Paxillin. WT and *CENP-F*$^{-/-}$ MEFs were transfected with mCherry-Paxillin and imaged before and after a photobleaching event (Supplemental movies 7 and 8). The fluorescence intensity of 30 FAs was measured in 10 cells for each condition. The resulting fluorescence recovery curve revealed that fluorescence in FAs in *CENP-F*$^{-/-}$ MEFs only recovers to approximately 60% while WT MEFs recovered to 91% (Figure 3.3J). This difference in fluorescence recovery could be due to differences in either the rate of diffusion or the immobile fraction in either the WT and *CENP-F*$^{-/-}$ MEFs. The half time (t ½) of the

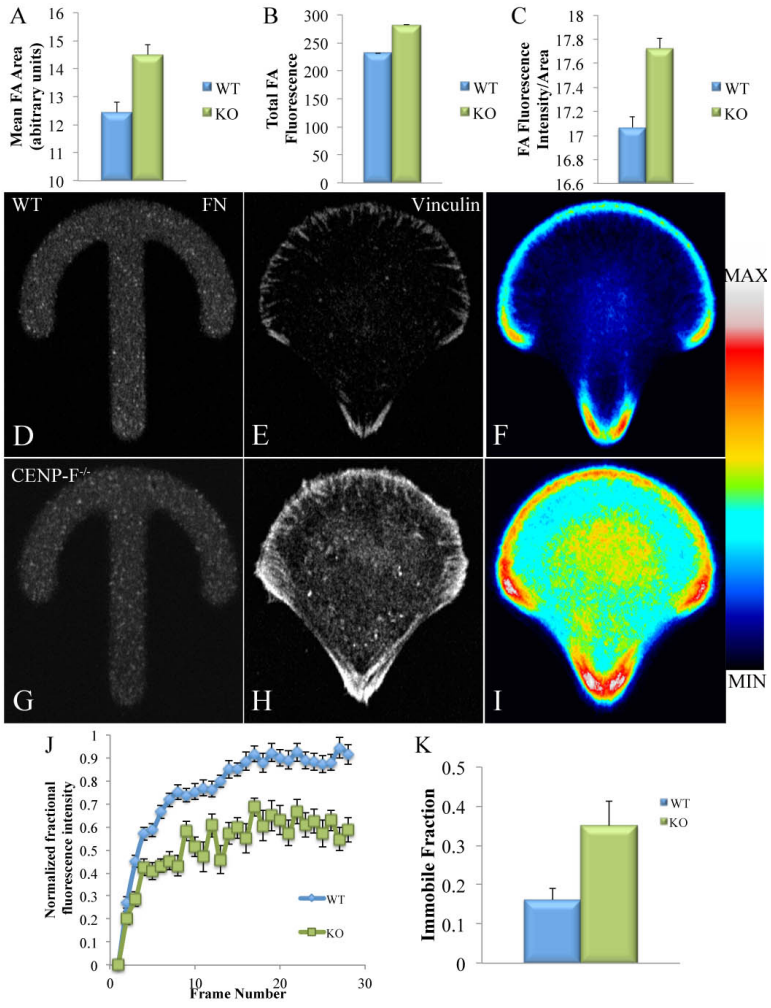

Figure 3.3 FAs of *CENP-F*$^{-/-}$ MEFs are larger, more dense, and disassemble more slowly than WT MEFs. Immunofluorescence using α-vinculin antibodies visualizing FAs in WT and *CENP-F*$^{-/-}$ MEFs. Quantification of mean size (A), total fluorescence intensity (B), and FA fluorescence intensity/area (C). N>1500. Immunofluorescence using vinculin antibodies in MEFs plated on fibronectin crossbows. Fluorescent fibronectin crossbows (D,G). vinculin staining in a representative WT and *CENP-F*$^{-/-}$ cell (E,H). When fluorescence of many cells is averaged, *CENP-F*$^{-/-}$ cells show greater FA and cytoplasmic vinculin fluorescence (D,I). N=78 WT, N=69 *CENP-F*$^{-/-}$. Fluorescence recovery curve from WT and *CENP-F*$^{-/-}$ MEFs. Error Bars represent SEM (J). Quantification of immobile fraction from fluorescence recovery curve (K). N=10

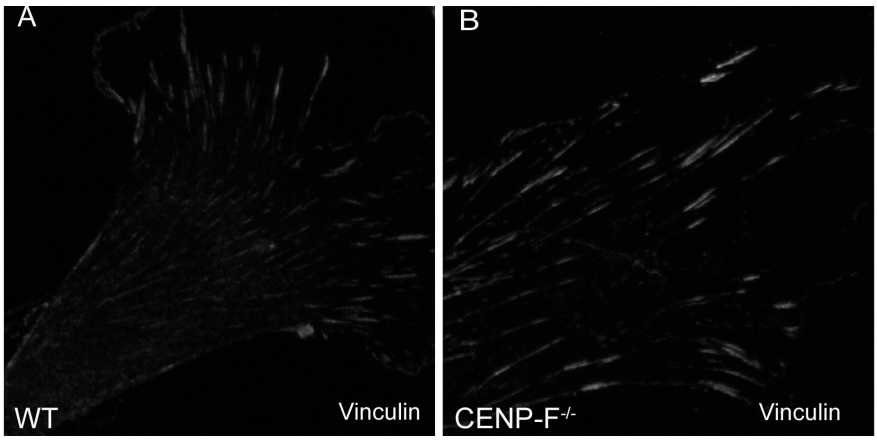

Figure 3.4 FAs of *CENP-F*$^{-/-}$ MEFs are larger and more dense. Immunofluorescence using α-vinculin antibodies visualizing FAs in WT and *CENP-F*$^{-/-}$ MEFs.

recovery curves between WT and *CENP-F*$^{-/-}$ were not statistically different (data not shown) suggesting that the rate of diffusion of Paxillin is not different between MEFs. However, there is a significant difference in the immobile fraction. The immobile fraction is a measurement of the proportion of bleached protein that fails to be turned over. The immobile fraction of the *CENP-F*$^{-/-}$ MEFs is twice that of the WT MEFs (Figure 3.3K). Taken together, these data demonstrate altered focal adhesion dynamics in *CENP-F*$^{-/-}$ cells.

Discussion

Importantly, previous loss of function analyses with CENP-F have clearly demonstrated delays in mitotic activity, mis-alignment of chromosomes, and multiple changes in functions related to the cytoplasm (Ashe et al., 2004; Holt et al., 2005; Liao et al., 1995; Moynihan et al., 2009b; Pooley et al., 2008; Pooley et al., 2006; Soukoulis et

al., 2005b; Varis et al., 2006; Vergnolle and Taylor, 2007; Yang et al., 2005), yet an underlying or unifying mechanism of disruption remains elusive. Here the dramatic changes in the overall structure of the cell and particularly in the MT network suggest broad, underlying effects that may influence all these properties. Taken together, our data determine that loss of CENP-F function leads to increased presence of modified tubulin and hyper-stabilization of the MT network. Given the broad importance of the MT network within cells, CENP-F has the potential to impact multiple cellular behaviors through its actions on the MT network.

Knowing the key role MTs play in cell migration (Petrie et al., 2009), it followed that *CENP-F*$^{-/-}$ cells would have migration defects. Directed migration is critical in development (Dees et al., 2012b; Goodwin et al., 1999; Wei et al., 1996) and disease (Dees et al., 2012b) and revealing a potential role for CENP-F in directed movement may bring insight into such events. Specifically, our finding that low levels of NOC ameliorate the migratory defect of *CENP-F*$^{-/-}$ MEFs is consistent with the idea that CENP-F works to either destabilize or remodel the MT network. Interestingly, loss of CENP-F function in the embryonic heart leads to defects in trabeculation (Dees et al., 2012b). Trabeculation, the inward growth of the ventricular wall, is dependent on myocyte migration through the burgeoning connective tissue space. Thus, understanding the essential role of CENP-F in regulation of directed cell movement potentially impacts myriad events in embryogenesis, tissue repair and cancer.

MTs not only affect cell migration directly through stabilization of the leading edge (Petrie et al., 2009) but also indirectly through their role in FA disassembly. Specifically, MTs go through lengthening and shortening cycles in order to target FAs

(Kaverina et al., 1998). Based on our findings of MT stabilization, it was likely that altered FA disassembly could additionally be playing a role in impairing cell migration. Our findings of larger FAs and increased FA fluorescence in *CENP-F*$^{-/-}$ cells are consistent with the hypothesis that the altered MT dynamics in *CENP-F*$^{-/-}$ cells and the decrease in MT turnover would decrease the ability of a cell to breakdown FAs, a vital step in directional migration. Paxillin transfected *CENP-F*$^{-/-}$ cells analyzed with FRAP had an immobile fraction twice that of WT cells, suggesting that the difference in the fluorescence recovery curves is due to the increased immobility of Paxillin in the FAs of *CENP-F*$^{-/-}$ MEFs. These data support our hypothesis that hyper-stabilization of MTs with loss of CENP-F function disrupts regulation of cell shape, size and migration.

Implications for the field

Disruption of CENP-F function leads to developmental abnormalities and disease outcomes in diverse cell types and models. Work from several groups has clearly demonstrated that CENP-F is critical in multiple processes influencing mitosis and interphase function. One concatenating feature in all these outcomes is the interaction of CENP-F with the MT network in regulating these diverse functions. Here, our data reveal a novel function, namely that CENP-F is a powerful destabilizing element of the MT network. This discovery has broad implications for the established roles of CENP-F in regulation of mitosis, chromosome pairing, migration, intracellular transport and cell shape in development, cancer, and disease.

CHAPTER IV

ISOLATION AND CULTURE OF NEURAL CREST CELLS FROM EMBRYONIC MURINE NEURAL TUBE

This chapter was published under this title in the *Journal of Visualized Experiments* in 2012. (Pfaltzgraff et al., 2012).

Abstract

The embryonic neural crest (NC) is a multipotent progenitor population that originates at the dorsal aspect of the neural tube, undergoes an epithelial to mesenchymal transition (EMT) and migrates throughout the embryo, giving rise to diverse cell types (Kulesa and Gammill, 2010; Le Douarin and Kalcheim, 1999; Saint-Jeannet, 2006). NC also has the unique ability to influence the differentiation and maturation of target organs (Freem et al., 2010; Nekrep et al., 2008; Plank et al., 2011). When explanted *in vitro*, NC progenitors undergo self-renewal, migrate and differentiate into a variety of tissue types including neurons, glia, smooth muscle cells, cartilage and bone.

NC multipotency was first described from explants of the avian neural tube (Baroffio et al., 1991; Cohen and Konigsberg, 1975; Sieber-Blum and Cohen, 1980). *In vitro* isolation of NC cells facilitates the study of NC dynamics including proliferation, migration, and multipotency. Further work in the avian and rat systems demonstrated that explanted NC cells retain their NC potential when transplanted back into the embryo (Bronner-Fraser et al., 1980; Morrison et al., 1999; Stemple and Anderson, 1992; White et al., 2001). Because these inherent cellular properties are preserved in explanted NC

progenitors, the neural tube explant assay provides an attractive option for studying the NC *in vitro*.

To attain a better understanding of the mammalian NC, many methods have been employed to isolate NC populations. NC-derived progenitors can be cultured from post-migratory locations in both the embryo and adult to study the dynamics of post-migratory NC progenitors (Biernaskie et al., 2009; Biernaskie et al., 2006; Chung et al., 2009; Corpening et al., 2011; Hagedorn et al., 1999; Heanue and Pachnis, 2011; Morrison et al., 2000; Morrison et al., 1999), however isolation of NC progenitors as they emigrate from the neural tube provides optimal preservation of NC cell potential and migratory properties (Etchevers, 2011; Ito et al., 1993; Stemple and Anderson, 1992). Some protocols employ fluorescence activated cell sorting (FACS) to isolate a NC population enriched for particular progenitors (Biernaskie et al., 2009; Corpening et al., 2011; Morrison et al., 1999; Stemple and Anderson, 1992). However, when starting with early stage embryos, cell numbers adequate for analyses are difficult to obtain with FACS, complicating the isolation of early NC populations from individual embryos. Here, we describe an approach that does not rely on FACS and results in an approximately 96% pure NC population based on a *Wnt1-Cre* activated lineage reporter (Mundell and Labosky, 2011).

The method presented here is adapted from protocols optimized for the culture of rat NC(Morrison et al., 1999; Stemple and Anderson, 1992). The advantages of this protocol compared to previous methods are that 1) the cells are not grown on a feeder layer, 2) FACS is not required to obtain a relatively pure NC population, 3) premigratory NC cells are isolated and 4) results are easily quantified. Furthermore, this protocol can be used for

isolation of NC from any mutant mouse model, facilitating the study of NC characteristics with different genetic manipulations. The limitation of this approach is that the NC is removed from the context of the embryo, which is known to influence the survival, migration and differentiation of the NC (Gammill et al., 2007; Gammill et al., 2006; Kasemeier-Kulesa et al., 2006; Kulesa and Gammill, 2010; Osborne et al., 2005; Schwarz et al., 2009).

1. Preparing plates

1.1) Use sterile technique at all times.

1.2) Prepare fibronectin (FN) by diluting 100 µL of human plasma FN stock into a final volume of 3.3 mL in Dulbecco's PBS (dPBS). Final concentration is 30 µg/mL and this can be stored at 4°C for 1 week.

1.3) Cover bottom of each well of a sterile tissue culture four well plate with FN solution and let sit for 15 minutes. Make sure the entire surface is covered. Make media during this time (steps 2 and 3).

1.4) Remove FN solution and allow plates to dry. Gently rinse wells with 500 µL DMEM, remove DMEM, and add 500 µL of Self-Renewal (SR) medium (see below). Incubate at 37°C in a humidified incubator containing 5 percent CO_2. Complete this approximately one hour before dissection so that the plates will be dry before use.

2. Preparing SR medium

2.1) For the culture of vagal and trunk NC from ten embryos (approximately one litter, depending on genetic background of the mouse line), prepare 25 mL of SR medium. Combine 12.5 mL low glucose DMEM, 7.5 mL Neurobasal

Medium, 25 µL retinoic acid (117 µM final concentration), and 25 µL 2-mercaptoethanol (50mM final concentration). Mix well.

2.2) Add 3.75 mL Chick Embryo Extract, 250 µL N2 salt supplement, 500 µL B27 supplement and 250 µL penicillin-streptomycin (1% final concentration). Filter the medium through a 0.22 µm filter.

2.3) Add 10 µL sterile IGF1 (20 µg/mL final concentration) and 20 µL sterile bFGF (20 µg/mL final concentration). Mix by inverting. Store at 4°C.

3. Preparing wash medium

3.1) For approximately 10 embryos prepare 50 mL of wash medium. Combine 50 mg BSA with 35 mL low glucose DMEM, 15 mL Neurobasal Medium, and 500 µL penicillin-streptomycin (1% final concentration). Sterile filter with a 0.22 µm filter.

4. Preparing collagenase/dispase

4.1) Add 50 µL of 100 mg/mL collagenase/dispase to 5 mL dPBS. Mix well.

4.2) Syringe filter with a 0.2 µm filter and add 1.5 mL into each of three wells of a twelve well plate. Pipette approximately 1 mL wash medium in the remaining wells. Store entire plate on ice until ready to digest dissected tissue.

4.3) Cut tips of a p20 and p1000 pipette filter tip with a sterile razor blade. Cut just below the beveled edge of the tip. The cut off p1000 will be used to transfer the whole embryo while the p20 will be used to transfer pieces of isolated tissue.

5. Isolating vagal and trunk neural tube from 9.5 dpc embryos

5.1) For timed pregnancies, dams with a vaginal plug are considered 0.5 dpc at noon the morning the plug is observed. Sacrifice and remove the uterus at 9.5 dpc.

5.2) Remove the decidua from uterus and gently remove the embryo from the decidua. Once experienced with this protocol, isolate 3-4 9.5 dpc embryos at a time in sterile dPBS. Use sterile technique and sterilized dissection instruments. Instruments can be sterilized by autoclaving, heat sterilization or by incubation in ethanol.

5.3) For anterior vagal NC: using insulin needles, cut the neural tube at the mid otic placode. Cut again at the posterior edge of the 4^{th} somite. Trim tissue ventral to the neural tube to remove the pharyngeal arches and heart.

5.4) For trunk NC: using insulin needles, remove the portion of the neural tube between somites 16-22 (or the last somite if embryos are developmentally earlier than the 22 somite stage).

5.5) Keep the yolk sac and any remaining embryonic tissue for genotyping.

6. Removal of non-neural ectoderm and mesoderm.

6.1) Place neural tube containing segments into collagenase/dispase at room temperature for 10 minutes. Immediately wash in wash medium.

6.2) Return tissue to sterile dPBS. Using sterile insulin needles, gently remove the non-neural ectoderm from the tissue and separate the somites away from the neural tube. The last remaining parts of the mesoderm from somite tissue can

be removed by triturating gently using a cut-down p20 tip. Be careful to not damage the neural tube. Observe this closely during trituration.

6.3) Place the isolated neural tube through a second and third 30 second wash of wash medium.

6.4) Wash once in SR medium, and place the isolated neural tube into the center of a FN-coated well that was prepared previously (Step 1.3). Humidify the hypoxia chamber with a dish of sterile water. Place the dish into the hypoxia chamber and flush the chamber with mixed gas to 3% O_2 (use a tank containing a mixture of 1% O_2, 6% CO_2, 93% N_2).

6.5) Always handle the chamber extremely carefully to ensure that explants are undisturbed and remain in the center of the wells.

6.6) Incubate at 37°C. Summary of steps 5-6 is shown in Figure 4.1.

7. Removal of neural tube

7.1) After 24 hours of incubation, remove the neural tube by gently teasing the edge of the neural tube away from the migrating cells using a sterile insulin needle. Remove and discard the neural tube from the medium using a sterile p20 cut as in step 6.2 and replace the medium with fresh SR medium (Figure 4.2). This is most easily done using an inverted microscope.

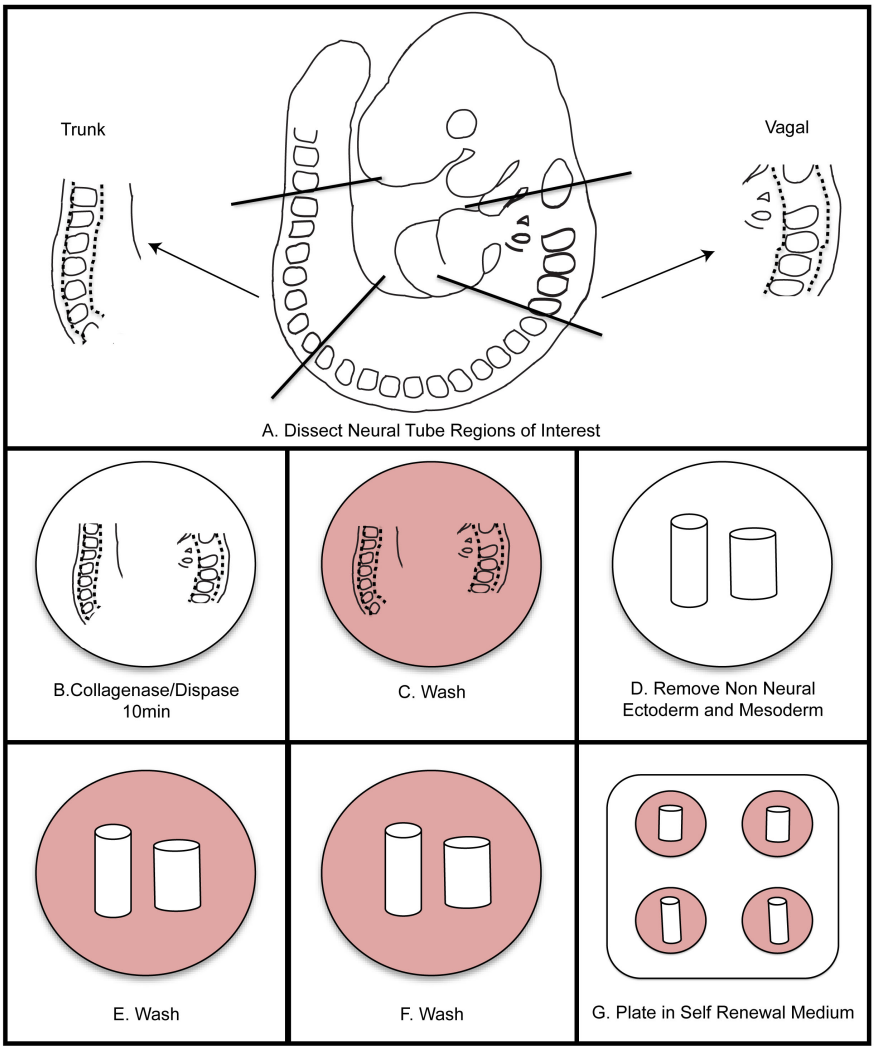

Figure 4.1 Overall schematic of NC isolation. A) Dissect regions of interest from the embryo. B) Digest neural tube in collagenase/dispase for ten minutes (do not exceed fifteen minutes). C) Wash in wash medium. D) Dissect away the non-neural ectoderm and mesoderm. E-F) Wash twice in wash medium. G) Plate in self renewal medium. Incubate at 37°C in 3% O_2 hypoxic conditions.

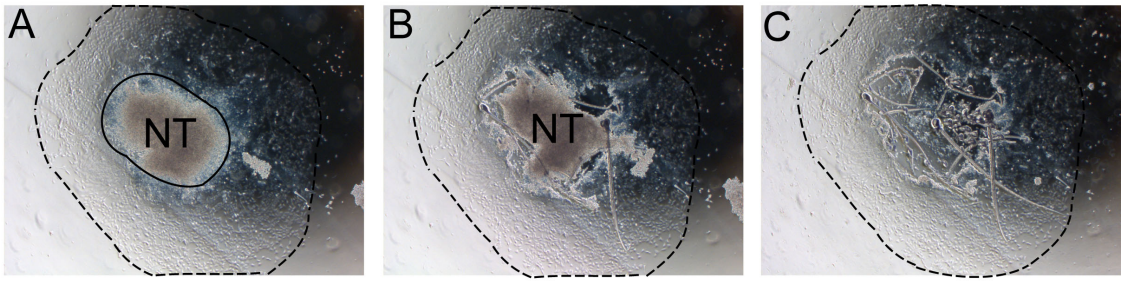

Figure 4.2 Stepwise removal of neural tube from explant. The neural tube must be removed after 24-48 hours to prevent contamination with non-NC cells. A) Notice the boundary between the neural tube and the NC outgrowth (solid line). B) Cut along the edge of the neural tube with an insulin needle. C) Discard the neural tube and replace medium with fresh self renewal medium. Dashed line indicates extent of the outgrowth. Abbreviation: NT, neural tube.

Representative Results

Following 24 hours of incubation at 37°C in hypoxic conditions, NC cells have migrated away from the neural tube in a nearly pure population (Figure 4.3a). Sometimes, less than ideal cultures will not yield robust outgrowths. For example, it is possible that after 24 hours the neural tube will have curled up upon itself and the NC will not migrate away from the neural tube (Figure 4.3b). Occasionally the neural tube will not attach to the fibronectin coated plates.

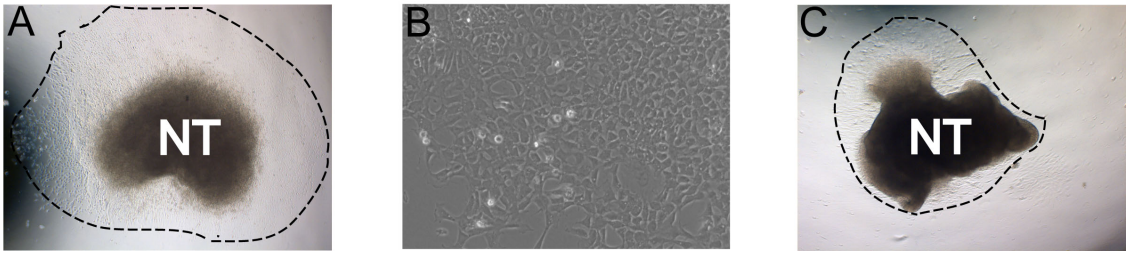

Figure 4.3 Examples of representative results. A) Typical explant outgrowth after 24 hours incubation in self renewal medium in hypoxic conditions (dashed line indicates extent of the outgrowth). B) Magnified view of NC outgrowth after 48 hours in culture. C) Less ideal culture with low outgrowth yield. A and C were cultured under the same conditions. Images demonstrate the natural range in culture robustness. This can be affected by efficiency of neural tube isolation, concentration of FN, hypoxic conditions, and time in collagenase/dispase digestions.

In our experience, sub-optimal NC migration or problems with attachment of the neural tube can be adversely affected by normoxia conditions or concentration of the fibronectin, respectively. Enzymatic activity of the collagenase/dispase varies slightly by batch and digestion time must be adjusted appropriately, however, do not digest the tissue longer than fifteen minutes. Overdigestion of the neural tube containing tissue in collagenase/dispase will also result in deficient outgrowths. If somite tissue is not easily removed from the neural tube after incubation in collagenase/dispase, the neural tube can be incubated for longer than ten minutes. Sometimes the neural tube will not attach to the substrate. If this is the case, double-check the fibronectin concentration and the hypoxia conditions.

While normoxic conditions can be used to culture wild-type NC, hypoxic conditions more closely mimic the *in vivo* environment (Ivanovic, 2009; Simon and Keith, 2008). In our experience, hypoxic conditions became critical when culturing mutant NC. For example, when *Foxd3* mutant NC were cultured in normoxic conditions, trunk NC had a greatly reduced cell outgrowth compared to controls. This disparity in outgrowth size was removed when the explants were cultured in hypoxic conditions (Figure 4.4). Furthermore, when wild-type neural tube explants were cultured in normoxia, the number of caspase-positive cells was greater then that of similar explants cultured in hypoxia (data not shown). By maintaining all NC culture in hypoxia, comparisons can more easily be made between dynamics of control and mutant cultures.

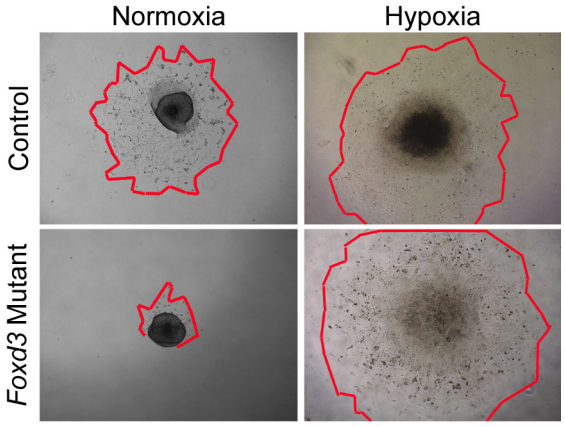

Figure 4.4 *In vitro* analyses of NC explant cultures in normoxia versus hypoxia. Control (wild type) NC cells migrated from neural tube explants after 48 hours in normoxic culture conditions. In contrast, *Foxd3* mutant NC had greatly reduced cell outgrowths in normoxia (red outlines mark edges of the NC outgrowths). When comparable explants were grown under hypoxic conditions, *Foxd3* mutant NC explants grew comparably to controls, allowing subsequent analyses. Note, this behavior correlated well with the behavior of *Foxd3* mutant NC *in vivo*.

Discussion

Careful attention should be paid to the developmental stage of embryo to ensure the success of this approach. Counting somites of early mouse embryos is critical both for stage matching embryos within a litter and determining the correct regions of neural tube for isolation. A variation of one or two somites between embryos is within a reasonable range of developmental timing, depending upon the resolution of the experiment conducted. An embryo between 9 and 9.5 dpc will have between 17 and 25 somites. If the embryo has more than 25 somites, the NC is further advanced in developmental time, and NC outgrowths will be less robust in culture. Staging embryos based on somite number facilitates precision in experiments when developmental stage of the embryo, and therefore NC, can influence the outcome of the experiments. In a 9.5 dpc embryo, the vagal NC migrates from the dorsal neural tube in defined anterior-posterior limits: from the mid-otic placode to somite 7. Similarly, trunk NC migrates from the neural tube at levels somite 8 to somite 24. To isolate distinct populations of NC progenitors as described in this protocol, discrete sub-regions within each of those domains are isolated. The region of the neural tube used will vary based upon the design of the experiment and the anterior-posterior region of the NC being studied.

The culture conditions described above, including the medium and incubation conditions, are specifically adapted for culture of murine NC. Similar SR medium was first used for the culture of rat NC (Morrison et al., 1999). In our hands, this rat medium, with the addition of Neurobasal Medium, produces a robust outgrowth of murine NC progenitors. Furthermore, unlike previous work culturing avian NC cells, a feeder layer is unnecessary for culture of the mammalian NC using this method (Etchevers, 2011; Ito et

al., 1993; Morrison et al., 1999; Stemple and Anderson, 1992). While there are numerous protocols detailing both avian and mammalian NC culture in normoxic conditions (Baroffio et al., 1991; Etchevers, 2011), we (Mundell and Labosky, 2011) (Figure 4.4), along with others in the field (Morrison et al., 2000), have found that culturing murine NC cells in hypoxic conditions as described here greatly aids survival and self-renewal, presumably because hypoxia more closely mimics physiological oxygen levels within the embryo (Ivanovic, 2009; Morrison et al., 2000; Simon and Keith, 2008).

Evaluation of the expression of molecular markers greatly facilitates the identification of NC cells and their differentiated derivatives. These include expression of Foxd3, p75, and Sox10 for NC stem cells. Markers of differentiated NC include smooth muscle alpha actin (SMA) for myofibroblasts, glial fibrillary acidic protein (GFAP) for glia, microphthalmia-associated transcription factor (MITF) for melanocytes, and beta-III tubulin, protein gene product 9.5 (PGP9.5), and peripherin for neurons. These markers can be used to determine explant efficiency and differentiation of NC progenitors.

Once this technique is mastered, cultured NC can be used in a variety of assays including quantification of proliferation, cell death, migration dynamics, and/or differentiation status. NC can also be clonally cultured to investigate self-renewal or multipotency of individual NC progenitors (Mundell and Labosky, 2011). After the neural tube is removed from the cultures, dissociate the NC cells in 100 µl Trypsin-EDTA (0.25%) for exactly 5 minutes at 37°C. Quench Trypsin-EDTA in excess wash medium (8-10 mls) by adding 800 µl per well and transferring to individual 15 ml tubes containing wash medium. Gently centrifuge cells at 150 x *g* for 3 minutes, remove supernatant and resuspend cell pellet in 1 ml SR medium. Count cells using a

hemocytometer and plate them at a density of 25 cells/cm^2. These colonies can be serially passaged to assay self-renewal. To assay multipotency, maintain the NC cells at clonal density in SR medium for 6 days and then switch to differentiation medium (10ng/ml bFGF and 1% chick embryo extract). Culture the cells in differentiation medium under hypoxia for 8 days before analyzing colony composition with molecular markers as above(Morrison et al., 1999).

In conclusion, this method for isolating NC cells from mouse embryos produces a feeder free adherent culture of premigratory NC cells without the use of FACS. Analysis of experiments using these cells can easily be quantified. While this technique is straightforward, its applications for the study of NC characteristics of migration, self-renewal, and differentiation are vast. Furthermore, isolating NC from genetically modified mouse embryos allows for the direct study of particular genes and pathways in the context of NC migration, survival, and/or differentiation.

Table 4.1 Table of Reagents

Reagent	**Company**	**Catalogue number**	**Comments**
DMEM (low glucose)	Gibco/Invitrogen	11885	
Neurobasal Medium	Gibco	21103	
BSA	Sigma	A3912-10G	
dPBS	Gibco	14190-144	
IGF1	BD Biosciences	354037	Store in 50 µg/mL

			aliquots at -20°C.
bFGF	BD Biosciences	354060	Store in 25 µg/mL aliquots at -20°C.
Fibronectin	Gibco	33016-015	Stored in 1mg/mL aliquots at -20°C.
Retinoic acid	Sigma	R2625	Store in 35 µg/ml aliquots after reconstituting in ethanol at -20°C.
2-mercaptoethanol	Sigma	D-5637	
N2 supplement	Gibco	17502-048	
B27 supplement	Gibco	17504-044	
Steriflip 0.22 µm filters	Millipore	SCGP00525	
Penicillin-streptomycin	Invitrogen	15140122	
0.20 µm filters	Corning	431219	
Syringes (for filtration)	BD Biosciences	301604	
Four well plates	Thermo Fisher Scientific	176740	
Collagenase/Dispase	Roche	269 638	Activity varies by batch. Store in 100 mg/mL aliquots at -

			20°C.
Insulin needles (29½ gage)	Becton Dickson	309306	
Hypoxia Chamber	Billups-Rothenberg		
Oxygen Analyzer	Billups-Rothenberg		
Forceps #5	Fine Science Tools		For removing uterus and decidua.
Trypsin-EDTA (0.25%)	Gibco	25200	

CHAPTER V

ISOLATION AND PHYSIOLOGICAL ANALYSIS OF MOUSE CARDIOMYOCYTES

This chapter was accepted under this title in the *Journal of Visualized Experiments* January, 2014.

Abstract

Cardiomyocytes, the workhorse cell of the heart, contain exquisitely organized cytoskeletal and contractile elements that generate the contractile force used to pump blood. Individual cardiomyocytes were first isolated over 40 years ago in order to better study the physiology and structure of heart muscle. Techniques have rapidly improved to include enzymatic digestion via coronary perfusion. More recently, analyzing the contractility and calcium flux of isolated myocytes has provided a vital tool in the cellular and sub-cellular analysis of heart failure. Echocardiography and EKGs provide information about the heart at an organ level only. Cardiomyocyte cell culture systems exist, but cells lack physiologically essential structures such as organized sarcomeres and t-tubules required for myocyte function within the heart. In the protocol presented here, cardiomyocytes are isolated via Langendorff perfusion. The heart is removed from the mouse, mounted via the aorta to a cannula, perfused with digestion enzymes, and cells are introduced to increasing calcium concentrations. Edge and sarcomere detection software is used to analyze contractility, and a calcium binding fluorescent dye is used to

visualize calcium transients of electrically paced cardiomyocytes; increasing understanding of the role cellular changes play in heart dysfunction. Traditionally used to test drug effects on cardiomyocytes, we employ this system to compare myocytes from WT mice and mice with a mutation that causes dilated cardiomyopathy. This protocol is unique in its comparison of live cells from mice with known heart function and known genetics. Many experimental conditions are reliably compared, including genetic or environmental manipulation, infection, drug treatment, and more. Beyond physiologic data, isolated cardiomyocytes are easily fixed and stained for cytoskeletal elements. Isolating cardiomyocytes via perfusion is an extremely versatile method, useful in studying cellular changes that accompany or lead to heart failure in a variety of experimental conditions.

Introduction

Cardiomyocytes provide the contractile force for the heart. Each myocyte contains organized cytoskeletal and contractile elements essential to contraction. The heart not only contains cardiomyocytes but also fibroblasts, connective tissue, and modified myocytes such as Purkinje fibers. Changes in any or all of these cell types can be seen in heart failure, making determination of the ultimate cause of heart dysfunction difficult. Decreased ventricular contractility of a failing heart is preceded by varying degrees of fibrous tissue build-up and hypertrophy and dysfunction of the cardiomyocytes (Babick and Dhalla, 2007). Arrhythmias can be caused by dysfunction in the conducting cells (Nogami, 2011), fibrosis interrupting cardiac conduction(Clancy et

al., 2004), or changes in the expression of ion channels in cardiomyocytes (Babick and Dhalla, 2007)(Splawski et al., 2004). Indeed, these problems often co-exist in a complicated fashion.

Isolating and studying cardiomyocytes allows one to examine contractile and electrical dysfunction of individual myocytes in the context of overall heart function. Techniques to isolate individual cardiac myocytes were developed over 40 years ago in an effort to better study physiology of this 'workhorse' cell of the heart. Isolation techniques have been improved to increase yield and quality of cells, with the vital development of coronary perfusion via cannulation of the aorta, first performed in 1970 (Berry et al., 1970). This article describes cardiomyocyte isolation followed by measurement of contractility and calcium transients using ratiometric fluorescence and cell dimensioning data acquisition software. In both genetic and environmental models of heart disease, utilizing this protocol provides key information about cell contractility, sarcomeric contractility and relaxation, calcium transients, and cytoskeletal disruption. This system is often used to test the effect of drugs on isolated cardiomyocytes (Fang et al., 2011; Feng et al., 2012). We employ the system to compare contractility and calcium transients of cardiomyocytes between wild type mice and mice with a mutation leading to dilated cardiomyopathy.

Studying individual cardiac myocytes has numerous advantages over other commonly used methods to study cardiac anatomy and physiology. Echocardiography and electrocardiography provide information about the contractile function and electrical conduction of the heart overall. Neither of these methods explains the cause or nature of the dysfunction below the level of the whole organ. Measuring contractility of individual

cardiomyocytes using edge-detection and sarcomere length algorithms can demonstrate that changes within the contractile cell of the heart are present within global heart dysfunction. Measuring calcium transients demonstrates the influence of changes in ion flux at a cellular level to contractile dysfunction or arrhythmias.

In addition to complementing whole organ studies, this protocol provides cells easily stained for sub-cellular components. It is possible to see cytoskeletal changes by staining tissue sections of the whole heart; however, one is only able to visualize a cross section of cells. A whole cardiomyocyte is thicker than the typical tissue section, and given the arrangement and length of the cardiomyocytes, it is difficult to see whole cells in a single section. Isolated cardiomyocytes can be fixed immediately and stained for a variety of cytoskeletal elements and ion channels. Confocal images can be compiled into full thickness z-stacks of the cell. Additionally, staining isolated cardiac myocytes allows for staining of components that are impossible to visualize in sections, such as the membrane invaginations known as t-tubules.

Cultured cell lines of cardiac myocytes do exist, some of which have similar transcriptional profiles and phenotypic features to cardiac myocytes. Some, such as the HL-1 cell line, even retain some sarcomeric organization and rudimentary contractile ability(Claycomb et al., 1998). Despite these qualities, cultured cells lack the “box car” shape and t-tubule structure of cardiomyocytes and have less sarcomeric organization. These components are essential to the function of cardiomyocytes *in vivo*. In addition, using cultured cells allows genetic manipulation but not *in vivo* physiologic manipulation. Isolated cardiomyocytes retain their cellular organization long enough to study but are still easily imaged and even transduced (Kaestner et al., 2009).

Isolated cardiomyocytes are extremely versatile, providing a substrate to identically analyze cells from varied experimental conditions. Isolation and physiological analysis of myocytes have been used by countless labs for a variety of experiments including studying the effect of drugs (Fang et al., 2011; Feng et al., 2012) or small molecules (Vainio et al., 2012), environmental stressors (Park et al., 2013), infection (Novaes et al., 2011), illness (Weltman et al., 2012), or genetic mutation (Despa et al., 2012; Papanicolaou et al., 2010) on contractility and/or calcium transients and studying the regulation of contractility and calcium release within a cardiomyocytes (Despa et al., 2012; Helmes et al., 2003; Touchberry et al., 2013). With the application of any of these stressors, changes in heart function could be due to any combination of changes in the cardiomyocytes themselves and changes in the surrounding environment of the heart, such as scarring, changes in conductivity, or changes to extracellular matrices. This is an ideal protocol for answering research questions regarding individual myocyte structure and function in the context of heart failure from any cause.

Although it has countless advantages over other techniques, physiological analysis of isolated cardiomyocytes is not ideal for every research question. Isolation is a terminal procedure, thus cardiomyocytes can only be assessed at one time in the mouse's life. This can be partially overcome using cohorts and sacrificing individual mice along the course of illness development or by monitoring the mouse to determine whether it has clinically significant heart failure before isolation. While this protocol can determine whether cardiomyocyte dysfunction has occurred, one cannot draw the conclusion that this dysfunction is the root cause of heart failure without additional experimental information. It is possible that cardiomyocyte dysfunction itself is secondary to other

changes in the heart. Despite these challenges, studying cardiomyocytes offers valuable information in determining the nature of dysfunction in the heart, especially when combined with other experiments.

The following protocol is adapted from one provided by Dr. Chee Lim, Vanderbilt University (Figure 5.1). Although contractility and calcium flux data are highly reproducible and useful in comparing hearts with genetic or environmental manipulation, isolation itself remains a technique dependent protocol, requiring

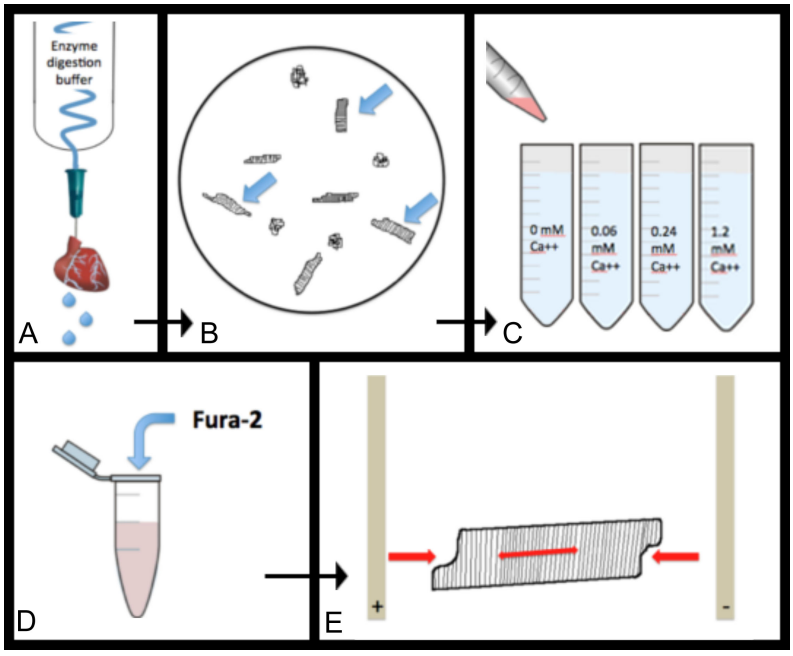

Figure 5.1 General overview of cardiomyocyte isolation. A) Heart is digested via coronary perfusion with enzyme digestion buffer. B) Cells are further dispersed into individual, healthy myocytes. C) Cells are sequentially transferred through increasing calcium concentrations so cells become calcium tolerant. D) Cells are loaded with the calcium dependent dye, Fura-2 AM. E) Loaded cells are electrically paced while sarcomere length, cell length, and fluorescence are recorded.

optimization. Minimizing the time between removing the heart from the mouse and perfusing the heart via aortic cannulation is essential for a quality digestion. In addition,

digestion time and enzyme concentration can be optimized for the highest quality myocytes. Steps likely requiring optimization, along with suggestions for optimization, are noted below.

Methods

Ensure all procedures involving animals are approved by the appropriate animal use and care body.

1) Prepare stock buffers in advance.

1.1) Prepare 2 L stock Ca^{++} free Tyrode's (Table 5.1). Adjust the pH to 7.4 with NaOH.

$Ca2^{++}$ free Tyrode	mM	FW/concentration	Amount for 2L solution
NaCl	135	58.44 g	15.8 g
KCl	4	74.56 g	0.596 g
$MgCl_2$	1	1 M	2 ml
HEPES	10	238.31 g	4.77 g
NaH_2PO_4	0.33	141.96 g	0.094 g

Table 5.1 Calcium-free Tyrode's solution. Reagents for 2L of stock Ca^{++}-free Tyrode's solution.

1.2) Prepare 2 L stock 1.2 mM Ca^{++} Tyrode's **(**Table 5.2). Adjust the pH to 7.4 with NaOH.

1.2 mM Ca^{++} Tyrode	mM	FW/concentration	Amount for 2L solution
NaCl	137	58.44 g	16 g
KCl	5.4	74.56 g	0.805 g
$MgCl_2$	0.5	1 M	1 ml
HEPES	10	238.31 g	4.77 g
$CaCl_2 \bullet 2H_2O$	1.2	147.01 g	0.353 g

Table 5.2 1.2 mM Calcium Tyrode's solution. Reagents for 2L of stock 1.2mM Ca^{++} solution.

2) On the day of the experiment, prepare perfusion, transfer, and digestion buffers.

2.1) Prepare 150 ml perfusion buffer in Ca^{++} free Tyrode's (Table B.3) and filter through a 0.2 μm filter.

Perfusion Buffer	mM	FW	amount in 150ml Ca^{++} free tyrode
Glucose	10	180.16 g	0.27 g
2,3-Butanedione-monoxime (BDM)	10	101.11 g	0.152 g
Taurine	5	125.16 g	0.094 g

Table 5.3 Perfusion Buffer. Reagents to prepare perfusion buffer on the day of experiment.

2.2) Prepare 35 ml Ca^{++} free transfer "Buffer A" (Table B.4) and 25 ml Ca^{++} containing "Buffer B" (Table B.5). Filter each through a 0.2 μm filter.

Buffer A	35 ml Perfusion Buffer
Bovine serum albumin (BSA)	0.175 g

Table 5.4 Buffer A. Reagents to prepare Buffer A on the day of experiment.

Buffer B	mM	FW	25 ml Ca2+ Tyrode buffer
Glucose	5	180.16 g	0.0225 g

Table 5.5 Buffer B. Reagents to prepare Buffer B on the day of experiment.

2.3) Prepare solutions of 0.06, 0.24, 0.6, and 1.2 mM Ca^{++} by mixing Buffer A and B per Table B.6.

Transfer Buffer	Buffer A (ml)	Buffer B (ml)
0.06 mM Ca^{++}	9.5	0.5
0.24 mM Ca^{++}	8	2
0.6 mM Ca^{++}	5	5
1.2 mM Ca^{++}	0	10

Table 5.6 Transfer Buffers. Reagents to prepare transfer buffers on the day of experiment.

2.4) Prepare 25 ml digestion buffer by dissolving digestion enzymes in 25 ml perfusion buffer (Table 5.7) based on the body weight (BW) of the mouse. Filter through a 0.2 μm filter before use.

Enzyme Digestion Buffer	25 ml Perfusion Buffer
Collagenase B	0.4 mg/g body weight
Collagenase D	0.3 mg/g body weight
Protease XIV	0.05 mg/g body weight

Table 5.7 Enzyme Digestion Buffer. Reagents to prepare enzyme digestion buffer on the day of experiment.

3) Experimental Setup

3.1) Assemble a constant flow Langendorff apparatus, available commercially or using a peristaltic pump, tubing, and a heat exchanger coil to allow a flow rate of 3ml/min of perfusate heated to 37°C. A simple schematic is provided in the 2011 review by Bell, *et al.*(Bell et al., 2011)

3.2) Set circulating water bath temperature (~47 °C) of the Langendorff apparatus so that outflow from the cannula is at 37 °C at a flow rate of 3 ml/min.

3.3) Run 70% ethanol through the perfusion system for 15 min, followed by 100 ml of ultrapure type I water. Run perfusion buffer through the system for 5 min while eliminating air bubbles.

3.4) Sterilize all surgical tools with a desired method.

3.5) Create cannula by attaching a short piece (about 3 mm) of PE-50 tubing to the tip of a 23G luer-stub adaptor. Heat tip of tubing to create a lip over which the aorta will be positioned.

4) Cardiomyocyte isolation

4.1) Inject mouse with 0.2 ml Heparin solution (1000 IU/ml), via intraperitoneal injection.

4.2) After 5 min, anesthetize mouse with isofluorane. When fully anesthetized (no response to strong foot pinch), spray chest with 70% EtOH. Open the chest, quickly excise the heart, being careful not to damage the aorta, and place in 4 °C perfusion buffer. Use curved forceps to grasp and lift under the heart. This creates space to trim attachments behind the heart with fine scissors.

4.3) Cannulate the heart by gently grasping the edge of the aorta with two pairs of fine forceps and carefully pulling the opening of the aorta over the lip of the cannula. Ensure the tip of the cannula is not past the aortic valve and into the ventricle, as this will inhibit perfusion of the heart via the coronary arteries.

4.4) Secure the aorta to the cannula by tying a loop of 5-0 silk suture around the aorta immediately above the lip of the cannula.

Note: Steps 4.2 through 4.4 should be completed as quickly as possible for best quality digestion.

Note: The heart can be hung directly onto the cannula already attached to the Langendorff Apparatus with flowing perfusion buffer. However, hanging the heart onto a cannula attached to a small syringe of perfusion buffer under a dissection microscope has been found to be most successful. This allows a small amount of perfusion buffer to be pushed through, watching for clearing of coronary arteries and ensuring heart is securely attached to cannula. The cannula is then hung on the Langendorff with running perfusion buffer.

4.5) Perfuse the heart with Ca^{++} free perfusion buffer at a flow of 3ml/min for 2-3 min.

4.6) Switch to enzyme digestion buffer and perfuse for 7-10 min, heart will become softer and lighter in color.

Note: Digestion time can be adjusted based on enzyme activity and heart size.

4.7) Once heart is palpably flaccid, remove heart from cannula and place in a sterile p60 dish with Buffer A (Ca^{++} free transfer buffer).

4.8) Remove atria and great vessels. Remove right ventricle if desired. With forceps, separate the ventricle into small pieces. Pipette several times with a sterile 5 ml transfer pipette to further disperse cells.

4.9) Filter the cell suspension into a 50 ml conical tube through a 250 μm nylon mesh filter.

4.10) Allow the suspension to pellet for about 10 min.

4.11) Transfer the pellet into the 0.06 mM Ca^{++} solution. Allow cells to pellet for 10 min. Healthy cells will pellet, while most dead cells will float.

4.12) Aspirate the supernatant, and transfer the pellet to the 0.24 mM Ca^{++} solution.

4.13) Repeat 10 min incubation, aspiration, and transfer through the remaining two Ca^{++} solutions until cells are in the 1.2 mM solution. At this point, a majority of the cells should be rod shaped myocytes.

5) Measuring Contractility and Calcium transients

Note: Both contractility and calcium transients can be measured simultaneously.

5.1) Prepare Fura-2 AM solution by resuspending in anhydrous DMSO to a concentration of 1 μg/μl. Fura-2 AM solution can be stored in a desiccator at -20 °C.

5.2) Load 1 ml of suspended cells with 1 μl Fura-2 AM. Allow cells to sit in dark 10 min then aspirate supernatant. Wash twice with Ca^{++} Tyrode's solution, allowing cells to pellet in the dark for 10 min between washes.

5.3) Place a glass coverslip in a stage insert that allows heated perfusion/aspiration and electrode pacing with a myocyte field stimulator. Place stage insert on inverted microscope set up for fluorescence measurement, adding a drop of oil to lens if using an oil immersion objective.

5.4) Set up heated gravity perfusion with 1.2 mM Ca^{++} Tyrode's solution so solution on stage reaches 37 °C. Attach aspiration to vacuum. Attach electrodes.

5.5) Turn on the microscope system, and open the ratiometric fluorescence and cell dimensioning data acquisition software.

5.6) Add a few drops of Fura-2 AM loaded cells to the stage insert, blocking perfusion momentarily to allow healthy cells to settle.

5.7) Use 40x objective to locate desired cell. A healthy cell should be rod shaped and not spontaneously contracting. It should visibly and uniformly contract when cell is paced at 5-20V.

Note: Physiological analysis requires a high quality digestion. It is possible to have cells that look healthy but do not pace well for physiological analysis. Digestion protocol may require refinement to get high quality, healthy myocytes. Additionally, mutant or diseased hearts may require modifications to the protocol.

5.8) Adjust lens rotation and change aperture so desired cell is lined up horizontally on screen and background is not visible.

5.9) Align edge detection bars to each end of myocyte and adjust threshold. Align sarcomere detection on a portion of cell with uniform sarcomeres. The longer you can make this bar, the more accurate the mathematical model of sarcomere length will be, so long as it is not on two populations of sarcomeres.

5.10) Pace cells at 2 Hz and 5-20 V for 10-15 sec before recording.

5.11) Record tracing. Ambient light should be minimized for best calcium transient recording.

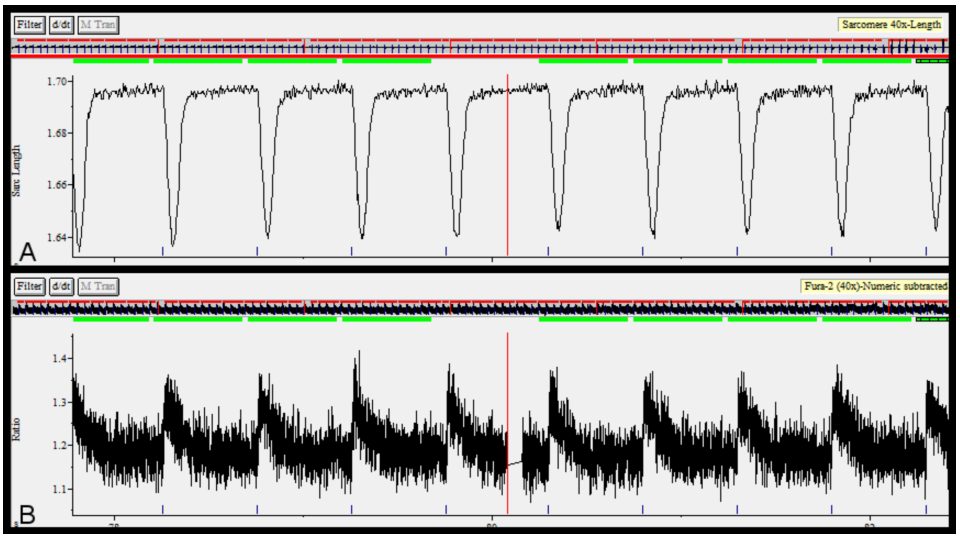

Figure 5.2 Example data capture. A) Sample contractility tracing represented by sarcomere length vs. time. B) Sample calcium transients represented by Fura-2 ratio vs. time.

6) Analysis.

6.1) Analyze traces using ratiometric fluorescence and cell dimensioning data acquisition software.

7) Further studies

7.1) This protocol provides excess cells which can be used for a variety of other experiments including: fixation and immunostaining, assessing direct drug effects, short term culture, and atomic force microscopy.

Representative Results

Once the contractility and transient tracings are collected (**Figure 5.2**), data are easily analyzed with the appropriate software. The whole tracing, or portions thereof can be averaged (**Figure 5.3**). Contractility can be analyzed in a variety of ways. For systolic function, one can assess the magnitude of contraction with fractional shortening, or speed

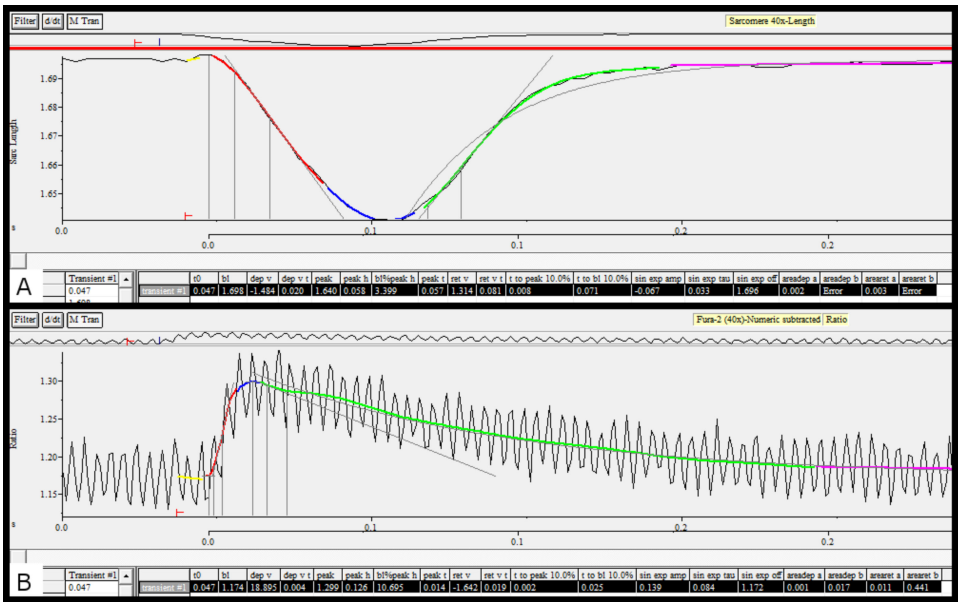

Figure 5.3 Example data analysis. A) Average contractility tracing after analysis. B) Average of calcium transients after analysis.

of contraction with time to peak shortening, and contraction velocity. Diastolic function can be analyzed similarly with time to 50% shortening and relaxation velocity. For calcium transients, similar data can be compared including baseline and peak Fura-2 ratios and time to peak or baseline (Table 5.8). These analyses provide comparable data from WT and KO hearts on systolic and diastolic cellular contractile function, as well as calcium flux, any of which could be altered in a heart with similar whole organ

dysfunction. Additionally, cells from the same isolation can be used for other experiments as listed in the protocol, including immunohistochemical staining (Figure 5.4).

Contractility	
Baseline	1.73 μm
Peak	1.64 μm
Fractional Shortening	4.70%
Time to peak	0.056 sec
Time to 50% baseline	0.043 sec
Calcium transients	
Baseline	1.18
Peak	1.32
Time to peak	0.021 sec
Time to 50% baseline	0.083 sec

Table 5.8 Contractility and calcium transient analyses. N = 5

Discussion

Isolation of quality cardiomyocytes requires some level of practice and optimization. This protocol contains key steps that can greatly affect the outcome of the digestion. These should be considered carefully when performing and troubleshooting the protocol. The time from removal of the heart to cannulation and perfusion should be minimized, ideally less than five minutes. Rinsing the heart immediately in ice-cold

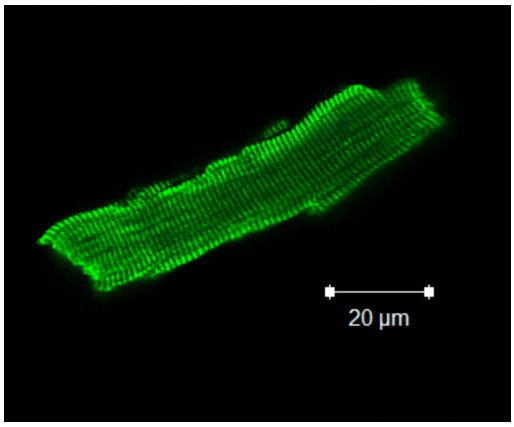

Figure 5.4 Immunofluorescent staining of cardiomyocyte cytoskeleton (α-actinin).

perfusion buffer after removing from the mouse and dissecting and cannulating the heart in ice-cold buffer will also increase the chances of a quality digestion. The cannulation itself is a critical step. The tip of the cannula must be placed below the first branches of the aorta but not through the aortic valve into the ventricle, as this will prevent perfusion of the coronary arteries. Coronary perfusion is essential to a quality digestion. In this laboratory, the cannula is attached to a syringe filled with perfusion buffer. Gently injecting a small amount of perfusion buffer after mounting and watching the coronary arteries clear of blood can test adequacy of the cannulation.

Troubleshooting this protocol involves carefully assessing the aforementioned critical steps. If the heart does not become palpably soft during the digestion, there are a few potential causes. First, during cannulation, the tip of the cannula may have been advanced beyond the aortic valve, preventing perfusion via the coronary arteries. This can be assessed before hanging the heart on the Langendorff apparatus but pushing a small amount of perfusion buffer through the cannula with a syringe and watching carefully for the coronary arteries to clear of blood. If perfusion is adequate but the heart does not digest well, consider purchasing different lots of enzymes. Because the enzymes

are actually mixtures, lots do not act identically. We recommend purchasing small amounts of each enzyme. When lots are found that digest well, purchase larger quantities of that lot for future use. As discussed, if dissection and cannulation of the heart take longer than 5-10 min, the quality of the digested cells can be poor. Consider completing isolations with wild type or untreated animals to master the dissection before moving on to knockout or treated animals. After digestion, cells must be slowly be made calcium tolerant. Cells should spend at least 10 min in each of the calcium solutions. Rushing these steps can decrease the yield and viability of cells.

Although reproducible, the physiological measurements depend on starting with a quality digestion. When selecting cells to measure, choose cells that are not spontaneously contracting, which indicates a leaky, damaged cell membrane. Cells should contract uniformly when paced. Consider pacing cells for 10-15 sec before recording measurements to ensure contractile consistency. If cell appears to be contracting uniformly, but the measurements of contraction magnitude varies drastically over time, first check to make sure that the region of interest defined covers only one population of sarcomeres. Occasionally two cells group together and the region of interest (ROI) may be measuring two different populations of sarcomere as one. If an appropriate ROI is chosen but contractility is variable within a single cell, the cell may be dying and another cell should be chosen. For calcium transients, it is critical to dilute Fura-2 AM in desiccated anhydrous DMSO as water changes the amount of Fura-2 AM that is functionally available. After loading, allow at least 20 min between the first wash and measuring transients to allow all Fura-2 AM to de-esterify within the cell. As with any fluorescent dye, protect the cells from light during and after loading. Some cells will

not uptake the dye, thus occasionally no calcium transients will be observed in a measured cell. Although contractility and calcium transients tracings may appear "cleaner" when the pacing rate is greatly reduced (0.5-1 Hz), measurements are more physiological at a rate closer to the mouse heart rate, thus a pace of at least 2 Hz is preferred.

The isolation itself can be modified if desired. This laboratory uses a constant flow method (3 ml/min for mice) during perfusion. Some groups have found a gravity flow more effective. Gravity flow perfusion allows for the digestion to be visualized more easily as the flow rate increases as the heart is digested.

As mentioned, these techniques do carry limitations. As the quality of the physiological measurements is dependent on quality of the digestion, it is prudent to measure myocytes from more than one heart for each experimental condition. Each heart will provide many myocytes to measure, but repeat digestions will ensure that results are consistent between hearts. Isolation is a terminal procedure, thus, if experimental design involves following the heart function of an animal over time, the cardiomyocytes can only be harvested once. More mice are required so a cohort can be followed longitudinally while individual mice are sacrificed to analyze cardiomyocytes.

Our focus has been studying contractility and cytoskeletal structure in a knockout mouse, however, isolated cardiomyocytes can be used for a variety of other experiments including live cell staining for t-tubules, studying cardiomyocytes from pressure or volume overloaded mice, examining the effects of pharmacological treatment, immunofluorescence, transfection (Kaestner et al., 2009), and transcriptional profiling (Flynn et al., 2011). This versatile technique provides countless advantages over other

methods used to study heart failure. Studying physiology of individual cells gives information that is not offered by whole organ studies such as echocardiography or electrocardiography, providing insight into the cellular changes that accompany whole organ failure. In addition, isolated cells are superior for imaging sub-cellular structures, as the whole cell can be easily stained and imaged. Isolating cardiomyocytes for analysis of contractility, calcium transients, and immunofluorescence is an extremely versatile technique that offers valuable information from a huge variety of experimental designs.

CHAPTER VI

DEVELOPMENTAL BIOLOGY BASED INTER-PROFESSIONAL PROJECTS PROMOTE AND STRENGTHEN INTERDISCIPLINARY COLLABORATIVE BEHAVIORS

Abstract

Basic science research and clinical practice frequently inform each other, but a persistent communication gap impedes collaborative efforts between clinicians and scientists. To date, a long-term effective strategy to ameliorate this deficit remains unknown. One approach is to foster inter-professional collaboration early in graduate and professional training. The curriculum proposed here utilizes this approach in order to promote communication between graduate and medical students and thus augment knowledge for both groups of students in regards to embryological development of human model organisms used in basic science research.

For this project, each collaborative interdisciplinary group consisted of one graduate student, one medical student, and a clinician. This group compared developmental features between model organisms and humans, which culminated in a collaborative poster presentation. All participants were surveyed at the beginning of the course, immediately after course completion, and four months after its completion. The survey instruments were used to measure the degree to which interdisciplinary communication, knowledge confidence in histology, and knowledge confidence in embryology increased due to participation in the course. Ultimately,

we were interested in assessing the longevity of these gains.

Overall, the curriculum proposed here may be adapted to facilitate interdisciplinary communication and collaboration for students or individuals from disparate professional backgrounds. We anticipate that this early collaboration for students will have long-lasting beneficial effects for these interactions.

Introduction

Although the translation of findings from basic biomedical research to clinical practice is integral for continuing advancements in patient care, communication barriers between scientists and physicians persist (Kong and Segre, 2010; McClain, 2010; Restifo and Phelan, 2011; von Roth et al., 2011). This interdisciplinary communication gap can potentially limit future innovation in the diagnosis, treatment, and prevention of human disease (Restifo and Phelan, 2011; von Roth et al., 2011). Basic science is often distanced both physically and organizationally from the clinical arena, thus potentially missing promising and clinically relevant avenues for research. Various contributing factors that have been outlined by other investigators include: (1) physicians' perception that research only has utility for the purposes of career advancement (Jayasundera et al., 2003), (2) insufficient time for physicians to assimilate the rapidly growing body of knowledge generated by biomedical studies (von Roth et al., 2011), and (3) different emphases on the acquisition and use of knowledge during formative training for basic scientists and physicians (Restifo and Phelan, 2011). However, several studies have illustrated the importance of bi-

directional information flow between basic scientific and patient-oriented research studies (Horig et al., 2005; Marincola, 2003; Rubio et al., 2010). Thus, a variety of approaches have been proposed for bridging the chasm between these two professions. Proposed strategies include using a dedicated translator who is facile in interpreting biomedical research findings (Sherwin, 2003), piloting physician-scientist partnerships (Kong and Segre, 2010), assigning biomedical graduate students to clinical rotations (von Roth et al., 2011), and promoting medical scientist training programs (Roberts et al., 2012).

Another potential approach for addressing the physician-scientist communication gap has been to develop inter-professional relationships early in the formal education of these students in their respective fields. Efforts have already been initiated to foster interdisciplinary learning and behaviors early in graduate and medical student education. As an example, the Baylor College of Medicine and the Cleveland Clinic independently created biomedical PhD programs that place an emphasis on clinically-oriented research by the graduate student and joint mentoring with basic scientists and clinicians (Smith et al., 2013). The Cleveland Clinic also developed a five-year program for medical students to learn techniques in basic and translational research (Fishleder et al., 2007). In a similar vein, inter-professional education has been employed as a means to improve the delivery of comprehensive care to patients (Hammick et al., 2007). In order to foster inter-professional relationships between basic scientists and medical professionals we established a collaborative research project rooted in developmental biology.

Here, we present novel curriculum changes to an elective course offered to graduate students in the Vanderbilt University Program in Developmental Biology. Specifically, the elective course's traditional content (the history and basic concepts of developmental biology) was supplemented with a research project on a model organ and organism. This project entailed collaboration between a graduate student, a medical student, and a clinical faculty member, with the dual goals of building interdisciplinary collaborations and enhancing knowledge in developmental biology. We

Developmental Model Organ	**Human Condition**
Xenopus Thyroid	Congenital Hypothyroidism
Xenopus Heart	Heterotaxia
Mouse Merkel Cells	Merkel Cell Tumors
Avian Palate	Cleft Palate
Mouse Cerebral Cortex	Tuberous Sclerosis
Avian Foregut	Intestinal Cancer
C. elegans Motor Neurons	Amyotrophic Lateral Sclerosis
Mouse Sympathetic Ganglion	Autonomic Orthostatic Tachycardia
Avian Melanocytes	Melanoma
Zebrafish Otic Placode	Cochlear Implantation
Mouse Lung	Pulmonary Hypertension
Xenopus Eye	Cataracts

Table 6.1 Examples of developmental model organisms and paired human conditions.

hypothesized that the facilitated communication between these three individuals would enhance the learning experience for each member of the team: graduate students learn human developmental biology concepts, medical students acquire similar knowledge in model organisms, and clinical faculty members gain experience in biological concepts

that are not applied on a daily basis in the course of clinical care. In order to test the efficacy of the inter-professional project in enhancing knowledge and interdisciplinary communication we asked participants to complete surveys reflecting on their experience.

Program Description

Twelve second year graduate students voluntarily enrolled into an elective course, Introduction to Developmental Biology CDB325. The course has traditional lecture/laboratory components focused on basic concepts in embryology through studying model organisms used in basic research. Organogenesis is not traditionally taught in the lecture component, so in an effort to promote independent study in this area, each student was randomly assigned to examine the development of a particular organ from a model organism. These assigned organs were chosen to complement ongoing clinical research being conducted by a second year medical student (Table 6.1). The goal of the course project was to teach graduate and medical students basic concepts in organogenesis by in-depth study of a particular structure and to consider the relative merits of using animal model systems to study human disease. The student pair was assigned a clinical faculty mentor whose area of practice corresponded to the students' assigned organ. Second year medical students volunteered to participate in this collaborative project.

The two students met first to discuss organ structure, function, and development. Later meetings with clinical faculty were designed to generate a conversation about the relationship between development and disease. The students

then accompanied their faculty mentor into the clinic to observe patients with the conditions discussed. Lastly, the students produced a poster presentation describing their model organism and assigned organ and the relevance of the model organ to the analysis of human disease. Input from the clinical faculty member was solicited throughout the project and clinical faculty attended the poster session.

Inter-Professional Project Time Line

Two months out:

Identify faculty interested in participating

One month out:

Match medical students with faculty members

Choose model organism and organ to match with medical faculty focus

Start of course:

Introduce graduate and medical students to each other

2-3 weeks in:

First meeting of faculty and students to discuss histology, gross anatomy, and physiology of the organ, with comparison of the human organ and organ in the model organism

5-6 weeks in:

Second meeting of faculty and students to discuss the contribution of the germ layers to this organ and tissue interactions during development with consideration of signaling between/within the tissue

7-8 weeks in:

Students accompany faculty into the clinic to see patients and discuss how developmental processes can lead to disease

End of week 8:

Students present their poster summarizing their experience and make a conclusion as to whether or not their particular model organ is a strong model of human disease

Program Evaluation

Anonymous surveys were used to analyze the effectiveness of this project in fostering both collaborative attitudes and knowledge of the topic. Students were surveyed before the course, immediately after the course, and 4 months after conclusion of the course. These surveys were designed to gather data concerning the relative level of comfort each student had interacting with a student in a different discipline, a scientist (a PhD faculty member), or a clinician (an MD faculty member). Students were also asked to report their self-assessed level of confidence in developmental biology concepts as outlined in the course learning objectives.

Statistical analysis was performed using a paired student's t-test. Faculty members were surveyed immediately after the conclusion of the course in order to determine how effective this project was in generating interest in developmental concepts relevant to their daily practice and whether they perceived the project to be worthwhile.

Research Electronic Data Capture (REDCap) (Harris et al., 2009) was used to administer surveys to student and faculty participants in the course. Participation in the survey had no influence on course grades. The project was considered exempt by the Vanderbilt Institutional Review Board. All students completed HIPPA training prior to visiting the clinic.

In general, the students described improved comfort levels in their inter-professional interactions over the course of the project. Graduate students reported a statistically significant increase in confidence talking to medical students and

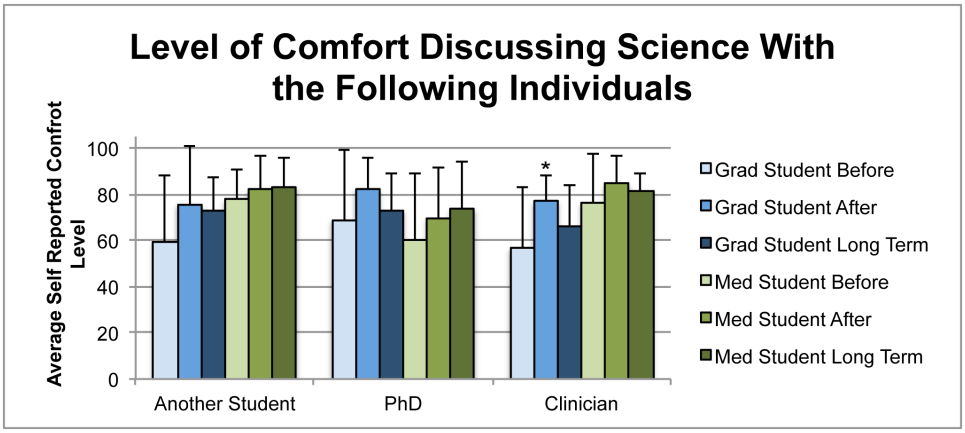

Figure 6.1 Collaborative project improved student comfort in discussing research with other professionals. Average reported level of comfort discussing science with different categories of people. Students were asked before and after the collaborative project to rate their level of comfort, between 0 and 100 with 100 being very comfortable, discussing their work with different categories of professionals. Error bars are one standard deviation. * $p<0.05$ n=12.

clinicians after participation in the program (Figure 6.1). There was a positive, but not significant, trend in the confidence of medical students in communicating with graduate students and clinicians. Interestingly, after a four month follow-up survey, the medical students had maintained their increase in comfort discussing science with other professionals and students, while the graduate students returned to their original comfort levels.

When asked to self-report their knowledge concerning material related to their project, students reported an increase in confidence across the board. Graduate students had a statistically significant improvement in their confidence with organogenesis concepts not covered in class or assigned readings after participation in

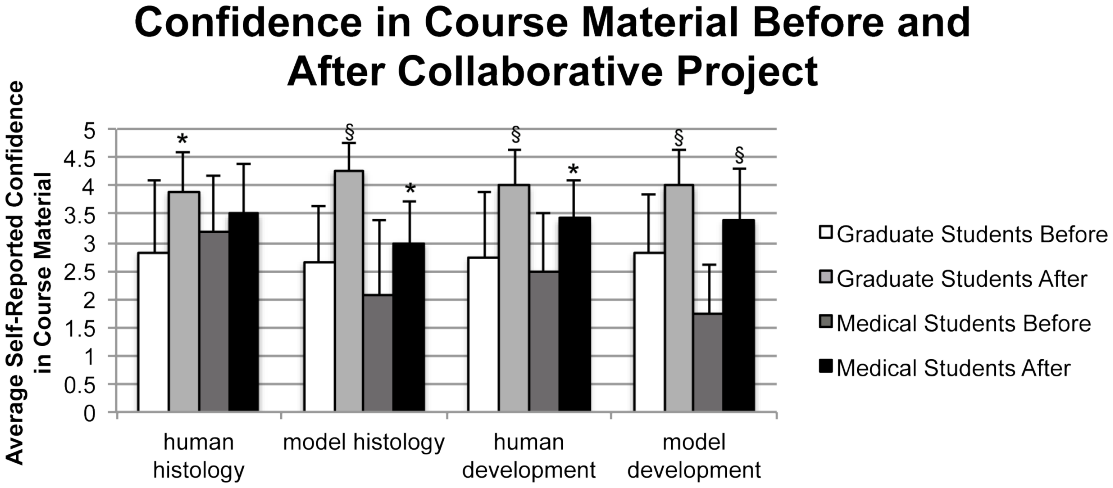

Figure 6.2 Collaborative project improved student confidence in material. Average reported level of confidence in material covered by group project. Students were asked before and after the collaborative project whether they strongly agreed (5) agreed (4), were neutral (3), disagreed (2), or strongly disagreed (1) with the statement "I feel confident in my knowledge of [histology or developmental concepts]". Error bars are one standard deviation. * $p<0.05$, § $p<0.01$, n=12.

the collaboration (Figure 6.2). The confidence of the medical students in the subject areas had a statistically significant increase in all areas with the exception of human histology (Figure 6.2). Excluding one group, which had confounding issues with communication and failed to complete all assigned meetings, 100% of the participants reported that they would recommend this course to peers. Taken together, these results indicate that students reported increased confidence in their developmental biology knowledge, their comfort communicating across disciplines, and their satisfaction with the course.

Finally, faculty reported enjoying the "opportunity to review those [developmental] processes in detail that [they] had not done prior to this." 60% of the faculty stated that this exercise enriched their understanding of developmental processes related to the diseases they see everyday (Figure 6.3). Therefore, these data suggest that both students and faculty had an enriching experience in the collaboration.

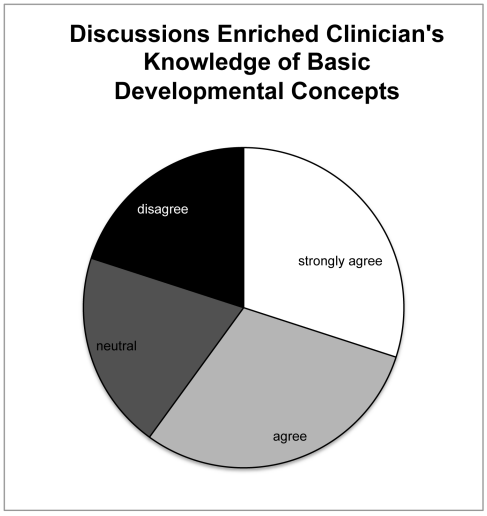

Figure 6.3 Collaborative project enriched knowledge of clinicians. Clinicians were asked after the collaborative project whether they agreed or disagree with the following statement "Discussions with the students enriched your knowledge of basic developmental concepts.", n=10.

Conclusions

Although a positive trend in self-reported confidence of the graduate and medical students exists, the curriculum only enhanced clinician-graduate student interactions on a statistically significant basis. There may be three explanations for this finding: 1) we were working with a small cohort of students and lacked extensive statistical power; 2) a basic science investigator was not introduced into the groups (since the project's aim was to introduce graduate students to clinically oriented concepts); and 3) the clinician-graduate student interaction is the pair with the least interaction in the conventional academic setting. Furthermore, four months after the course, the graduate students returned to their original level of comfort. This suggests that a future curriculum will need recurrent inter-professional interaction in order for this comfort level to have greater longevity and lasting effects on professional behaviors.

On the other hand, the curriculum demonstrated statistically significant increases of confidence in all course subject areas, except for human histology, in the medical student group. These data are reasonable since the medical students recently completed their first year of coursework, which included six months of human histology. Of note, both medical students and graduate students learned new information that was not a part of their traditional curricula during engagement in the collaborative project. We postulate that these inter-professional projects are an effective way to transmit scientific concepts through multiple groups of individuals.

However, further investigation of changes in student knowledge before and after the collaboration is needed to substantiate this conclusion.

There are limitations inherent to this study. First, we have a small sample size that was limited by the number of matriculating students in the Program in Developmental Biology. This pilot studies allows us to get a feel for what works for our students in future sections. Second, the project timeframe was limited to eight weeks, the duration of this course in developmental biology. Additional cohorts would add power to the study. Lastly, students were only asked to self report their level of comfort with other professionals and their confidence in course material. Designing individualized knowledge exams to test each unique project would not have been feasible due to the size of this endeavor. Ultimately, we decided that self-reporting would be a relative marker for student comfort in future interdisciplinary interactions.

Implemented curriculum changes enriched the learning of both students and faculty members. Students learned material in a new environment and were exposed to concepts they would not have otherwise encountered. For example, medical student understanding of model organism development increased substantially, likely improving a common deficit of knowledge with concepts in these areas, while faculty members were reacquainted with basic science concepts not routinely articulated in their clinical practice. Altogether, the participants were inspired to foster inter-professional relationships in their continuing research. As a testament to this persisting interest, the medical students volunteered for this project (they were not enrolled in the course) and maintained incentive-free participation. While inter-

professional relationships are not a substitute for didactic lectures on fundamental concepts, this is a well-received and effective model for supplemental learning. Graduate students observed the translational impact of their basic science research by spending time in the clinic, and medical students saw how questions asked at the bench can inform human health. Therefore, all students attained the ability to communicate with peers in other disciplines and appreciate the interplay between basic science research and clinical practice.

Supplemental Project Handouts

Student Instructions

Model Organ Project: There will be one major project that will continue throughout the time of the course. On the first day of class, each student will be given an organ from a model organism. The student will then develop knowledge about how this organ relates to analogous human development through independent reading, discussion with a medical student partner, and individual meetings with clinicians. When you are assigned your model organ, you will also be grouped with a student course director, who will monitor your progress and provide help when needed.

There are 3 aspects to this project:

1. Collaboration with medical student

To bridge medical education with graduate education at Vanderbilt, you will be working with a medical student on the project. It is still *your* project, with you completing the bulk of the work; the medical student will simply be a source of

discussion from a different perspective. Specifically, each medical student has an emphasis project to complete over the summer, and we have paired him/her to an appropriate model organism that will relate to his/her work. The student will also be present in the clinician meetings to both add to the discussion and provide a bridge to facilitate discussion. We envision this process to be a learning experience for everyone involved. On the first day of class, we will provide an opportunity for you to meet your partner to begin discussing this collaboration. There is one required meeting between you and your partner which should be completed within the first two weeks of class. This should be a 30-60 minute meeting for you to discuss what you've learned about your model organ and the medical student to discuss how his emphasis project relates. Then you will both schedule the clinician meetings. Additional meetings with the medical student can be completed at your discretion.

2. Three meetings with clinician

a. You have two weeks to complete each of these meetings; you will e-mail the clinician to set up meeting times between you, your medical student partner, and the clinician. After each meeting, e-mail your student leader to let them know you have completed the meeting and whether or not you feel you accomplished the goals of the meeting. The due dates for sending these e-mails are listed in the schedule. While the discussion during each of these meetings will vary with the conversation, there are goals that should be accomplished. The student may prepare slides to aid in the discussion, but it is important to remain concise and highlight the most important/interesting points. Foremost, it is your job to make sure the goals are accomplished and try to direct this meeting. Each meeting should last about an hour.

b. The goals for these meetings are as follows:

i. First meeting: Introduction to the clinician and discussion of adult organ in both model organism and human. This meeting should cover histology, gross anatomy, and physiology of the organ, with comparison of the human organ and organ in the model organism.

ii. Second meeting: Discussion of the development of the organ in human and model organism. Some points to include in this discussion are: contribution of the germ layers to this organ, tissue interactions during development with consideration of signaling between/within the tissue, functional and structural differences between human and model organism development. From this meeting, the student should also have a clinical problem or congenital disorder that relates to the organ he/she is studying to research for the next meeting.

iii. Third meeting: discussion of the mechanism of the disease in human, whether the model organism is appropriate to model the disease, and why or why not.

c. The clinician will be given an evaluation form in order to provide us feedback as to how you have accomplished the goals of the meeting.

3. Poster

Based on the student's research and discussions with the clinician, the students will present a final poster on their model organ. The poster should include the same information that was discussed with the clinician, but it should remain concise enough for a brief presentation to students/professors/clinician who visit. These visitors will be given an evaluation form on this presentation

Inter-Professional Project Poster and Abstract Instructions

You must submit an abstract for your poster by Friday, July 20th (2 weeks before the poster presentation). Because you will collaborate with your medical student partner to organize and design the poster, you should also coordinate to write the abstract.

The poster abstract should be organized into five sections in the style of the journal 'Circulation Research':

- Histology, anatomy, and function
    - Give a brief overview of the organ in the adult animal. Discuss physiology only if relevant.

- Descriptive embryology
    - Describe the morphogenetic processes that form the organ during development. Potential points of discussion include cell behaviors (such as migration, intercalation, epithelial-to-mesenchymal transition, etc.), tissue behaviors (growth, retraction, folding, etc.), and tissue interactions (proximity of one cell-type or tissue relative to another). Use appropriate terminology for orientation and anatomy (dorsal/ventral, rostral/caudal, etc.). Do not include molecular or genetic discussions in this section.

- Similarities and differences to human organ
    - Compare and contrast the organ in the animal system you have been assigned to the human homolog. Points of discussion include comparisons of structure, function, tissue interactions, germ layer contributions, etc. This section should be focused in being informative to the clinical correlation section. You may include brief discussions of molecular or genetic developmental biology, but only if this is relevant to the clinical correlation section below.

- Clinical correlation
    - Critically assess the appropriateness of using the animal model system to study a clinical disease related to the organ. You and your partner will coordinate with a clinical mentor to choose the disease.

- Relation to emphasis project
    - Discuss how this research has been informative to the medical student's summer emphasis project. Include discussion of how the animal model system can be used to address a specific research question pertaining to the emphasis project.

Format: Abstract may not be longer than one half page, single-spaced, with half inch margins and 11 point Arial font. Do not use abbreviations or acronyms. Include abstract title and authors (graduate student, medical student, and clinical mentor).

CHAPTER VII

FUTURE DIRECTIONS

Role of Embryonic Origin and Environment in VSMC Biology

By exploring the molecular and physiological characteristics of the regions of the aorta we have been able to describe the convergence of regional embryonic vascular characteristics in the adult. What is still unclear however, is the process through which this convergence occurs. Is there a single stimulus that triggers convergence or is it a gradual postnatal change?

One possible environmental trigger for this convergence is the closing of the ductus arteriosus. By closing the ductus, blood is now forced into the lungs, to the left ventricle, and through the aAo for the first time. This exposes the aAo to sheer and stretch forces soon after birth, which could account for the convergence of regional phenotypes. To begin to test this hypothesis, I exposed endothelial cells to different types of flow stress: no flow, sheer flow (to replicate conditions of the adult dAo), and oscillatory flow (to replicate conditions of the adult aAo). The conditioned medium from these endothelial cells was then harvested and spun to remove any endothelial cells. Embryonic VSMCs were grown in the conditioned medium for 48 hours. After this time

mRNA was harvested from these cells and qRT-PCR was performed to see if flow alone is enough to change the regional gene expression to resemble that of the adult aorta. While the no flow conditioned medium did not have an effect on VSMC gene expression, both the sheer and oscillatory flow conditions altered expression of the embryonic VSMC. The data suggest that while conditioned medium from endothelial cells exposed to different flow conditions is sufficient to alter gene expression, it does not recreate the adult VSMC gene expression profile (Figure 7.1). A better experiment would be to co-culture endothelial cells and VSMCs while exposing them to different flow conditions.

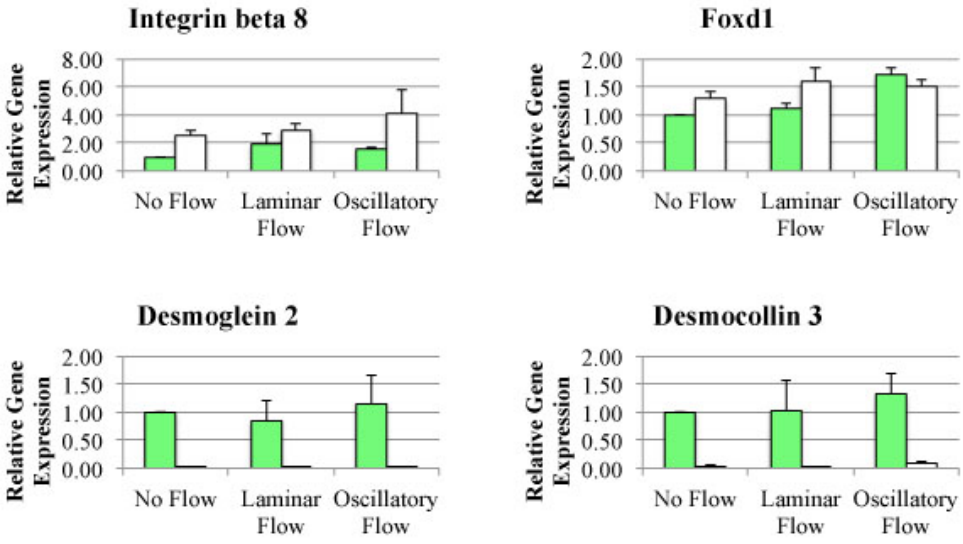

Figure 7.1 Endothelial cell conditioned medium alters embryonic VSMC gene expression. qRT-PCR data demonstrating gene expression patterns in embryonic aAo (green) and dAo (white) VSMCs exposed to endothelial cell conditioned medium. While the laminar and oscillatory flow conditioned medium slightly alters gene expression, it alone does not force embryonic VSMC gene expression to mimic that of the adult.

The best approach for testing the hypothesis that the closing of the ductus results in convergence of the regional differences would be to examine aortae of newly born pups with closed ductus arteriosus. If the regions of the newborn aorta resemble those of the adult regions, this establishes an association between these two events. To test if ductus closure is required for regional differences to converge, we could examine the aorta in genetic models of patent ductus arteriosus (PDA) such as prostaglandin E receptor 4 null ($EP4^{-/-}$) mice in which the ductus remains patent after birth. The aortae of these PDA animals could then be compared to the embryonic, postnatal, and adult aorta. If ductus closure is sufficient to trigger phenotypic convergence then we would expect to see a rapid convergence of characteristics in the aAo and dAo of WT mice while $EP4^{-/-}$ aAo and dAo would retain their embryonic phenotype.

If the closure of the ductus is not necessary for phenotypic convergence then perhaps a molecular cue related to vessel maturation is required. If we see a gradual transition from embryonic to adult phenotype, then perhaps the change is a consequence of vessel maturation and is not linked to any particular developmental event.

Further studies examining different vessels with VSMCs from the same embryonic origin would give insight both into environmental influences and the role of subregionality in embryonic origin. Some such studies have been performed comparing two vessels each with NC VSMC origin, the ductus arteriosus and the aAo (Shelton et al.,

2014). Subdivisions within a single embryonic origin could have very different vascular phenotypes. For example, *Hox* codes could provide additional position information about vascular origin. In fact, *Hox* expression has been directly linked to vascular phenotypes (Pruett et al., 2012; Pruett et al., 2008; Trigueros-Motos et al., 2013). While we demonstrated a regional embryonic phenotype that correlates with embryonic origin, perhaps subdomains of the aorta can be identified based on a combination of *Hox* code expression as well as embryonic origins.

Role of Embryonic VSMC Phenotypes on Vascular Physiology and Disease

Our data suggest that in healthy young adults, the regions of the aorta have very similar characteristics. If embryonic origin has consequences for physiology and disease in the adult, then we would expect to see some embryonic characteristics reemerge in diseased adult vessels. One possible direction would be to describe the vascular characteristics of the different regions of the aorta from an $apoE^{-/-}$ mouse (Meir and Leitersdorf, 2004). The $apoE^{-/-}$ mouse readily develops atherosclerosis and could be used as a model of vascular disease to test if regions of the aorta take on their embryonic characteristics under vascular stress. One study focusing on the role of *Hox* codes in atherosclerosis heterogeneity found that *HoxA9* plays an important role in establishing

athero-resistance in the dAo (Trigueros-Motos et al., 2013). While this study focused on genes that did not change between WT and apoE$^{-/-}$ conditions, we would be interested to see if the embryonic expression pattern reemerges in times of vascular stress. Another example of a genetic model for vascular stress would be the diabetes prone leptin-deficient (ob/ob) mouse model (Drel et al., 2006). Leptin-deficient mice provide a model for diabetes and obesity, which causes vascular stress. Based on our hypothesis that the embryonic profile reemerges in stressed or diseased tissue, we would predict that the aAo and dAo would have distinct characteristics in an adult suffering from vascular stress.

Cellular Localization of CENP-F

Loss of CENP-F has been shown to influence a number of cellular processes that all converge on the microtubule network. We therefore hypothesize that loss of CENP-F results in a direct change in microtubule dynamics accounting for the phenotype we describe (Moynihan et al., 2009a; Soukoulis et al., 2005a). However data demonstrating the mechanism through which CENP-F alters MT dynamics are lacking. To fill this gap in knowledge we must first generate a CENP-F specific antibody that faithfully binds to endogenous murine protein. To this end we have taken two routes, a rabbit polyclonal antibody and a mouse monoclonal antibody. The rabbit polyclonal was made against a 20 amino acid section of the amino terminus (NT). When we overexpress GFP tagged NT-CENP-F in COS cells we can see colocalization with the rabbit polyclonal primary

antibodies (Figure 7.2). The mouse monoclonal was made against the first 500 amino acids of CENP-F and its localization has not yet been evaluated.

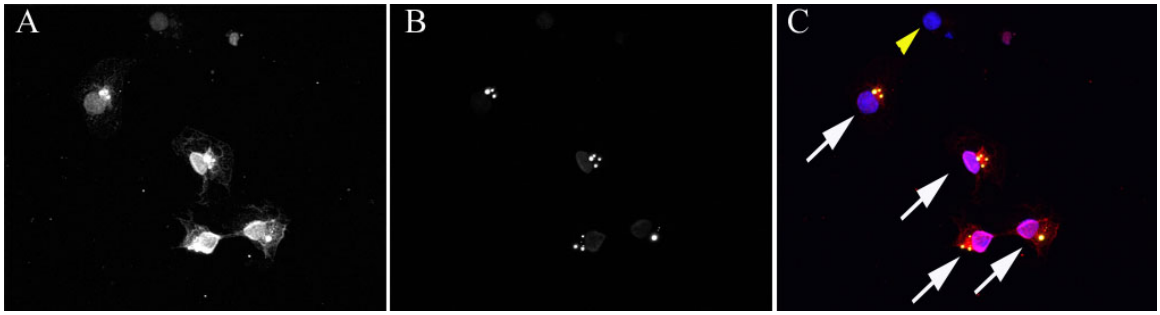

Figure 7.2 NT-CENP-F polyclonal antibodies are specific to CENP-F NT. A) Cos cells transfected with NT-CENP-F-GFP plasmid stained with affinity purified rabbit anti-NT-CENP-F antibody. B) Same cells demonstrating the native GFP fluorescence. C) Merge, NT-CENP-F (red), NT-CENPF-GFP (green), dapi (blue). Only cells transfected with NT-CENP-F-GFP are recognized by the affinity purified rabbit anti-NT-CENP-F antibody.

Sensitivity of CENP-F Mutant Mice to Cardiac Stress

While *CENP-F*$^{-/-}$ mice develop dilated cardiomyopathy, *CENP-F*$^{+/-}$ animals are asymptomatic. We hypothesized, however, that the heterozygous mice would be more sensitive to cardiac stress. The first stress that we examined was treatment with paclitaxel, a MT stabilizing chemotherapy agent. Preliminary data suggests that heterozygotes are particularly sensitive to MT specific cardiac stress. Future studies will test whether this result is statistically significant, and also include other chemotherapeutics with diverse mechanisms of action. In addition to paclitaxel we will investigate the effects of vinca alkaloids, MT destabilizers; doxorubicin, a DNA intercalator; and trastuzumab, a Her2 inhibitor. This panel of drugs will help us determine

if loss of CENP-F and stabilization of MTs results in a heart that is sensitive to all forms of cardiac stress or specifically stresses that act on the MT network.

Traditional chemotherapeutics are designed to take advantage of the machinery cells use to divide. Thus, common targets are the microtubule network, DNA damage, and pathways that arrest cell growth. A common concern is that these drugs will have negative side effects in cell populations that actively divide. While these side effects do occur, side effects in non-mitotic tissues also occur. Clinical heart failure occurs in 1-5% of people who receive chemotherapy, while drops in ejection fraction are seen in 5-20% of patients (Shakir and Rasul, 2009). The ability to identify genetic modulators of cardiotoxicity risk would be a powerful tool for predicting which patients may have a more severe reaction to certain chemotherapeutics.

Based on our data, we hypothesize that some single nucleotide polymorphisms (SNPs) associated with proteins that modulate MT dynamics will correlate with discrete cardiac outcomes of chemotherapy treatment, such as ejection fraction. We have identified 767 patients who have had their DNA sequenced and their charts contain record of paclitaxel, doxorubicin, trastuzumab, and/or vincristine treatment. These charts will be further mined for information on the dose and dates of chemotherapy treatment as well as echocardiographic data. Based on these data, we can group the patients according to drug dosage and change in ejection fraction. We can then determine whether there are SNPs that associate with either cardioprotection or decreased ejection fraction. Furthermore, association of SNPs with cardiac outcomes can be validated in other patient data sets.

Once we identify SNPs we will further investigate the role of the associated genes in MT biology in the heart. Using the zebrafish morpholino knock down system we can manipulate the expression of candidate genes and determine the implications for cardiac toxicity. Additionally, it could be that these MT SNPs are associated with disease in other organ systems that rely heavily on MT function, such as the nervous system. Once meaningful SNPs are identified, answering these additional questions would be the next viable step.

Conclusions

The data presented in this dissertation, while providing specific answers to some questions about vascular development and function, leave us with an array of new questions to follow up on. What stimuli cause the convergence of regional embryonic vascular characteristics in the aorta? What causes regions of the vasculature derived from the same embryonic origin to be divergent in function? What role does the microtubule network play in cardiac development and disease? Further investigation into these questions will generate a more comprehensive understanding of cardiovascular development and disease.

REFERENCES

Alimi, Y.S., Barthelemy, P., and Juhan, C. (1994). Venous pump of the calf: a study of venous and muscular pressures. J Vasc Surg *20*, 728-735.

Altinok, A., Kiris, E., Peck, A.J., Feinstein, S.C., Wilson, L., Manjunath, B.S., and Rose, K. (2007). Model based dynamics analysis in live cell microtubule images. BMC Cell Biol *8 Suppl 1*, S4.

Andersen, M.R., and Stender, S. (2000). Endothelial nitric oxide synthase activity in aorta of normocholesterolemic rabbits: regional variation and the effect of estrogen. Cardiovasc Res *47*, 192-199.

Arnal, J.F., Dinh-Xuan, A.T., Pueyo, M., Darblade, B., and Rami, J. (1999). Endothelium-derived nitric oxide and vascular physiology and pathology. Cell Mol Life Sci *55*, 1078-1087.

Ashe, M., Pabon-Pena, L., Dees, E., Price, K.L., and Bader, D. (2004). LEK1 is a potential inhibitor of pocket protein-mediated cellular processes. J Biol Chem *279*, 664-676.

Babick, A.P., and Dhalla, N.S. (2007). Role of Subcellular Remodeling in Cardiac Dysfunction due to Congestive Heart Failure. Medical Principles and Practice *16*, 81-89.

Baldwin, A.L., and Thurston, G. (2001). Mechanics of endothelial cell architecture and vascular permeability. Crit Rev Biomed Eng *29*, 247-278.

Baroffio, A., Dupin, E., and Le Douarin, N.M. (1991). Common precursors for neural and mesectodermal derivatives in the cephalic neural crest. Development *112*, 301-305.

Bazigou, E., and Makinen, T. (2013). Flow control in our vessels: vascular valves make sure there is no way back. Cell Mol Life Sci *70*, 1055-1066.

Bell, R.M., Mocanu, M.M., and Yellon, D.M. (2011). Retrograde heart perfusion: The Langendorff technique of isolated heart perfusion. Journal of Molecular and Cellular Cardiology *50*, 940-950.

Berry, M.N., Friend, D.S., and Scheuer, J. (1970). Morphology and Metabolism of Intact Muscle Cells Isolated from Adult Rat Heart. Circulation Research *26*, 679-687.

Biernaskie, J., Paris, M., Morozova, O., Fagan, B.M., Marra, M., Pevny, L., and Miller, F.D. (2009). SKPs derive from hair follicle precursors and exhibit properties of adult dermal stem cells. Cell stem cell *5*, 610-623.

Biernaskie, J.A., McKenzie, I.A., Toma, J.G., and Miller, F.D. (2006). Isolation of skin-derived precursors (SKPs) and differentiation and enrichment of their Schwann cell progeny. Nat Protoc *1*, 2803-2812.

Blatnik, J.S., Schmid-Schonbein, G.W., and Sung, L.A. (2005). The influence of fluid shear stress on the remodeling of the embryonic primary capillary plexus. Biomech Model Mechanobiol *4*, 211-220.

Bolstad, B.M., Irizarry, R.A., Astrand, M., and Speed, T.P. (2003). A comparison of normalization methods for high density oligonucleotide array data based on variance and bias. Bioinformatics *19*, 185-193.

Bronner-Fraser, M., Sieber-Blum, M., and Cohen, A.M. (1980). Clonal analysis of the avian neural crest: migration and maturation of mixed neural crest clones injected into host chicken embryos. The Journal of comparative neurology *193*, 423-434.

Chamley-Campbell, J., Campbell, G.R., and Ross, R. (1979). The smooth muscle cell in culture. Physiol Rev *59*, 1-61.

Chan, G.K., Schaar, B.T., and Yen, T.J. (1998). Characterization of the kinetochore binding domain of CENP-E reveals interactions with the kinetochore proteins CENP-F and hBUBR1. J Cell Biol *143*, 49-63.

Chen, Z., and Tzima, E. (2009). PECAM-1 is necessary for flow-induced vascular remodeling. Arterioscler Thromb Vasc Biol *29*, 1067-1073.

Cheung, C., Bernardo, A.S., Trotter, M.W., Pedersen, R.A., and Sinha, S. (2012). Generation of human vascular smooth muscle subtypes provides insight into embryological origin-dependent disease susceptibility. Nat Biotechnol *30*, 165-173.

Chien, S., Li, S., and Shyy, Y.J. (1998). Effects of mechanical forces on signal transduction and gene expression in endothelial cells. Hypertension *31*, 162-169.

Chrzanowska-Wodnicka, M., and Burridge, K. (1996). Rho-stimulated contractility drives the formation of stress fibers and focal adhesions. J Cell Biol *133*, 1403-1415.

Chung, I.H., Yamaza, T., Zhao, H., Choung, P.H., Shi, S., and Chai, Y. (2009). Stem cell property of postmigratory cranial neural crest cells and their utility in alveolar bone regeneration and tooth development. Stem cells *27*, 866-877.

Cines, D.B., Pollak, E.S., Buck, C.A., Loscalzo, J., Zimmerman, G.A., McEver, R.P., Pober, J.S., Wick, T.M., Konkle, B.A., Schwartz, B.S.*, et al.* (1998). Endothelial cells in physiology and in the pathophysiology of vascular disorders. Blood *91*, 3527-3561.

Clancy, R.M., Kapur, R.P., Molad, Y., Askanase, A.D., and Buyon, J.P. (2004). Immunohitologic Evidence Supports Apoptosis, IgG Deposition, and Novel Macrophage/Fibroblast Crosstalk in the Pathologic Cascade Leading to Congenital Heart Block. Arthritis Rheum *50*, 173-182.

Clark, G.M., Allred, D.C., Hilsenbeck, S.G., Chamness, G.C., Osborne, C.K., Jones, D., and Lee, W.H. (1997). Mitosin (a new proliferation marker) correlates with clinical outcome in node-negative breast cancer. Cancer Res *57*, 5505-5508.

Claycomb, W.C., Nicholas A Lanson, J., Stallworth, B.S., Egeland, D.B., Delcarpio, J.B., Bahinski, A., and Nicholas J Izzo, J. (1998). HL-1 cells: A cardiac muscle cell line that contracts and retains phenotypic characteristics of the adult cardiomyocyte. Proceedings of the National Academy of Science *95*, 2979-2984.

Clyman, R.I., Chan, C.Y., Mauray, F., Chen, Y.Q., Cox, W., Seidner, S.R., Lord, E.M., Weiss, H., Waleh, N., Evans, S.M.*, et al.* (1999). Permanent anatomic closure of the ductus arteriosus in newborn baboons: the roles of postnatal constriction, hypoxia, and gestation. Pediatr Res *45*, 19-29.

Cohen, A.M., and Konigsberg, I.R. (1975). A clonal approach to the problem of neural crest determination. Dev Biol *46*, 262-280.

Corpening, J.C., Deal, K.K., Cantrell, V.A., Skelton, S.B., Buehler, D.P., and Southard-Smith, E.M. (2011). Isolation and live imaging of enteric progenitors based on Sox10-Histone2BVenus transgene expression. Genesis *49*, 599-618.

Culver, J.C., and Dickinson, M.E. (2010). The effects of hemodynamic force on embryonic development. Microcirculation *17*, 164-178.

de la Guardia, C., Casiano, C.A., Trinidad-Pinedo, J., and Baez, A. (2001). CENP-F gene amplification and overexpression in head and neck squamous cell carcinomas. Head Neck *23*, 104-112.

Dees, E., Miller, P.M., Moynihan, K.L., Pooley, R.D., Hunt, R.P., Galindo, C.L., Rottman, J.N., and Bader, D.M. (2012a). Cardiac-specific deletion of the microtubule-binding protein CENP-F causes dilated cardiomyopathy. Disease models & mechanisms *5*, 468-480.

Dees, E., Miller, P.M., Moynihan, K.L., Pooley, R.D., Hunt, R.P., Galindo, C.L., Rottman, J.N., and Bader, D.M. (2012b). Cardiac-specific deletion of the microtubule-binding protein CENP-F causes dilated cardiomyopathy. Dis Model Mech.

Despa, S., Lingrel, J.B., and Bers, D.M. (2012). Na+/K+-ATPase a2-isoform preferntially modulates Ca2+ transients and sarcoplasmic reticulum Ca2+ release in cardiac myocytes. Cardiovasc Res *95*, 480-486.

Dettman, R.W., Denetclaw, W., Jr., Ordahl, C.P., and Bristow, J. (1998). Common epicardial origin of coronary vascular smooth muscle, perivascular fibroblasts, and intermyocardial fibroblasts in the avian heart. Dev Biol *193*, 169-181.

Dilley, R.J., and Schwartz, S.M. (1989). Vascular remodeling in the growth hormone transgenic mouse. Circ Res *65*, 1233-1240.

Dimitrow, P.P., Dudek, D., and Dubeil, J.S. (2001). The risk of alcohol leakage into the left anterior descending coronary artery during non-surgical myocardial reduction in patients with obstructive hypertrophic cardiomyopathy. Eur Heart J *22*, 437-438.

Drel, V.R., Mashtalir, N., Ilnytska, O., Shin, J., Li, F., Lyzogubov, V.V., and Obrosova, I.G. (2006). The leptin-deficient (ob/ob) mouse: a new animal model of peripheral neuropathy of type 2 diabetes and obesity. Diabetes *55*, 3335-3343.

Drozdz, D., and Kawecka-Jaszcz, K. (2013). Cardiovascular changes during chronic hypertensive states. Pediatr Nephrol.

Durand, J.B., Bachinski, L.L., Bieling, L.C., Czernuszewicz, G.Z., Abchee, A.B., Yu, Q.T., Tapscott, T., Hill, R., Ifegwu, J., Marian, A.J.*, et al.* (1995). Localization of a gene responsible for familial dilated cardiomyopathy to chromosome 1q32. Circulation *92*, 3387-3389.

Eralp, I., Lie-Venema, H., DeRuiter, M.C., van den Akker, N.M., Bogers, A.J., Mentink, M.M., Poelmann, R.E., and Gittenberger-de Groot, A.C. (2005). Coronary artery and orifice development is associated with proper timing of epicardial outgrowth and correlated Fas-ligand-associated apoptosis patterns. Circ Res *96*, 526-534.

Erlanson, M., Casiano, C.A., Tan, E.M., Lindh, J., Roos, G., and Landberg, G. (1999). Immunohistochemical analysis of the proliferation associated nuclear antigen CENP-F in non-Hodgkin's lymphoma. Mod Pathol *12*, 69-74.

Esner, M., Meilhac, S.M., Relaix, F., Nicolas, J.F., Cossu, G., and Buckingham, M.E. (2006). Smooth muscle of the dorsal aorta shares a common clonal origin with skeletal muscle of the myotome. Development *133*, 737-749.

Etchevers, H. (2011). Primary culture of chick, mouse or human neural crest cells. Nat Protoc *6*, 1568-1577.

Ezratty, E.J., Partridge, M.A., and Gundersen, G.G. (2005). Microtubule-induced focal adhesion disassembly is mediated by dynamin and focal adhesion kinase. Nat Cell Biol *7*, 581-590.

Fang, F., Li, D., Pan, H., Chen, D., Qi, L., Zhang, R., and Sun, H. (2011). Luteolin Inhibits Apoptosis and Improves Cardiomyocyte Contractile Function through the PI3K/Akt pathway in Simulated Ischemia/Reperfusion. Pharmacology *88*, 149-158.

Faury, G., Pezet, M., Knutsen, R.H., Boyle, W.A., Heximer, S.P., McLean, S.E., Minkes, R.K., Blumer, K.J., Kovacs, A., Kelly, D.P.*, et al.* (2003). Developmental adaptation of the mouse cardiovascular system to elastin haploinsufficiency. J Clin Invest *112*, 1419-1428.

Fawcett, D.W., Bloom, W., and Raviola, E. (1994). A textbook of histology, 12th edn (New York, Chapman & Hall).

Felker, G.M., Hu, W., Hare, J.M., Hruban, R.H., Baughman, K.L., and Kasper, E.K. (1999). The spectrum of dilated cardiomyopathy. The Johns Hopkins experience with 1,278 patients. Medicine (Baltimore) *78*, 270-283.

Feng, J., Huang, H., and Yen, T.J. (2006). CENP-F is a novel microtubule-binding protein that is essential for kinetochore attachments and affects the duration of the mitotic checkpoint delay. Chromosoma *115*, 320-329.

Feng, W., Hwang, H.S., Kryshtal, D.O., Yang, T., Padilla, I.T., Tiwary, A.K., Puschner, B., Pessah, I.N., and Knollmann, B.C. (2012). Coordinated Regulation of Murin Cardiomyocyte Contractility by Nanomolar (-)-Epigallocatechin-3-Gallate, the Major Green Tea Catechin. Mol Pharmacol *82*, 993-1000.

Fishleder, A.J., Henson, L.C., and Hull, A.L. (2007). Cleveland Clinic Lerner College of Medicine: an innovative approach to medical education and the training of physician investigators. Academic medicine : journal of the Association of American Medical Colleges *82*, 390-396.

Flaim, S.F., Ress, R.J., and Mest, S. (1985). Regional variation in norepinephrine-stimulated calcium uptake in rabbit aorta. Pharmacology *30*, 1-11.

Flynn, J.M., Santana, L.F., and Melov, S. (2011). Single Cell Transcriptional Profiling of Adult Mouse Cardiomyocytes. J Vis Exp, e3302.

Freem, L.J., Escot, S., Tannahill, D., Druckenbrod, N.R., Thapar, N., and Burns, A.J. (2010). The intrinsic innervation of the lung is derived from neural crest cells as shown by optical projection tomography in Wnt1-Cre;YFP reporter mice. J Anat *217*, 651-664.

Gadson, P.F., Jr., Dalton, M.L., Patterson, E., Svoboda, D.D., Hutchinson, L., Schram, D., and Rosenquist, T.H. (1997). Differential response of mesoderm- and neural crest-derived smooth muscle to TGF-beta1: regulation of c-myb and alpha1 (I) procollagen genes. Exp Cell Res *230*, 169-180.

Gadson, P.F., Jr., Rossignol, C., McCoy, J., and Rosenquist, T.H. (1993). Expression of elastin, smooth muscle alpha-actin, and c-jun as a function of the embryonic lineage of vascular smooth muscle cells. In Vitro Cell Dev Biol Anim *29A*, 773-781.

Galli, D., Dominguez, J.N., Zaffran, S., Munk, A., Brown, N.A., and Buckingham, M.E. (2008). Atrial myocardium derives from the posterior region of the second heart field, which acquires left-right identity as Pitx2c is expressed. Development *135*, 1157-1167.

Gammill, L.S., Gonzalez, C., and Bronner-Fraser, M. (2007). Neuropilin 2/semaphorin 3F signaling is essential for cranial neural crest migration and trigeminal ganglion condensation. Developmental neurobiology *67*, 47-56.

Gammill, L.S., Gonzalez, C., Gu, C., and Bronner-Fraser, M. (2006). Guidance of trunk neural crest migration requires neuropilin 2/semaphorin 3F signaling. Development *133*, 99-106.

Gardner, M.K., Zanic, M., and Howard, J. (2012). Microtubule catastrophe and rescue. Curr Opin Cell Biol.

Garrison, A.K., Shanmugam, M., Leung, H.C., Xia, C., Wang, Z., and Ma, L. (2012). Visualization and analysis of microtubule dynamics using dual color-coded display of plus-end labels. PLoS One *7*, e50421.

Geisterfer, A.A., Peach, M.J., and Owens, G.K. (1988). Angiotensin II induces hypertrophy, not hyperplasia, of cultured rat aortic smooth muscle cells. Circ Res *62*, 749-756.

Gimona, M., Herzog, M., Vandekerckhove, J., and Small, J.V. (1990). Smooth muscle specific expression of calponin. FEBS Lett *274*, 159-162.

Gittenberger-de Groot, A.C., DeRuiter, M.C., Bergwerff, M., and Poelmann, R.E. (1999). Smooth muscle cell origin and its relation to heterogeneity in development and disease. Arterioscler Thromb Vasc Biol *19*, 1589-1594.

Goodwin, R.L., Pabon-Pena, L.M., Foster, G.C., and Bader, D. (1999). The cloning and analysis of LEK1 identifies variations in the LEK/centromere protein F/mitosin gene family. J Biol Chem *274*, 18597-18604.

Hagedorn, L., Suter, U., and Sommer, L. (1999). P0 and PMP22 mark a multipotent neural crest-derived cell type that displays community effects in response to TGF-beta family factors. Development *126*, 3781-3794.

Haimovici, H., and Maier, N. (1971). Experimental canine atherosclerosis in autogenous abdominal aortic grafts implanted into the jugular vein. Atherosclerosis *13*, 375-384.

Hammick, M., Freeth, D., Koppel, I., Reeves, S., and Barr, H. (2007). A best evidence systematic review of interprofessional education: BEME Guide no. 9. Medical teacher *29*, 735-751.

Harris, P.A., Taylor, R., Thielke, R., Payne, J., Gonzalez, N., and Conde, J.G. (2009). Research electronic data capture (REDCap)--a metadata-driven methodology and workflow process for providing translational research informatics support. J Biomed Inform *42*, 377-381.

Heanue, T.A., and Pachnis, V. (2011). Prospective identification and isolation of enteric nervous system progenitors using Sox2. Stem cells *29*, 128-140.

Helmes, M., Lim, C.C., Liao, R., Bharti, A., Cui, L., and Sawyer, D.B. (2003). Titin Determines the Frank-Starling Relation in Early Diastole. The Journal of General Physiology *121*, 97-110.

Hoglund, V.J., and Majesky, M.W. (2012). Patterning the artery wall by lateral induction of Notch signaling. Circulation *125*, 212-215.

Holt, S.V., Vergnolle, M.A., Hussein, D., Wozniak, M.J., Allan, V.J., and Taylor, S.S. (2005). Silencing Cenp-F weakens centromeric cohesion, prevents chromosome alignment and activates the spindle checkpoint. J Cell Sci *118*, 4889-4900.

Holth, J.K., Bomben, V.C., Reed, J.G., Inoue, T., Younkin, L., Younkin, S.G., Pautler, R.G., Botas, J., and Noebels, J.L. (2013). Tau loss attenuates neuronal network hyperexcitability in mouse and Drosophila genetic models of epilepsy. J Neurosci *33*, 1651-1659.

Horig, H., Marincola, E., and Marincola, F.M. (2005). Obstacles and opportunities in translational research. Nature medicine *11*, 705-708.

Houser, J.W., Ackerman, G.A., and Knouff, R.A. (1961). Vasculogenesis and erythropoiesis in the living yolk sac of the chick embryo. A phase microscopic study. Anat Rec *140*, 29-43.

Hui, D., Reiman, T., Hanson, J., Linford, R., Wong, W., Belch, A., and Lai, R. (2005). Immunohistochemical detection of cdc2 is useful in predicting survival in patients with mantle cell lymphoma. Mod Pathol *18*, 1223-1231.

Hussein, D., and Taylor, S.S. (2002). Farnesylation of Cenp-F is required for G2/M progression and degradation after mitosis. J Cell Sci *115*, 3403-3414.

Infante, A.S., Stein, M.S., Zhai, Y., Borisy, G.G., and Gundersen, G.G. (2000). Detyrosinated (Glu) microtubules are stabilized by an ATP-sensitive plus-end cap. J Cell Sci *113 (Pt 22)*, 3907-3919.

Irizarry, R.A., Bolstad, B.M., Collin, F., Cope, L.M., Hobbs, B., and Speed, T.P. (2003). Summaries of Affymetrix GeneChip probe level data. Nucleic Acids Res *31*, e15.

Ito, K., Morita, T., and Sieber-Blum, M. (1993). In vitro clonal analysis of mouse neural crest development. Dev Biol *157*, 517-525.

Ivanovic, Z. (2009). Hypoxia or in situ normoxia: The stem cell paradigm. J Cell Physiol *219*, 271-275.

Ivens, E. (2004). Hypertrophic cardiomyopathy. Heart Lung Circ *13 Suppl 3*, S48-55.

Jacobs, M.L., Chin, A.J., Rychik, J., Steven, J.M., Nicolson, S.C., and Norwood, W.I. (1995). Interrupted aortic arch. Impact of subaortic stenosis on management and outcome. Circulation *92*, II128-131.

Jayasundera, T., Fisk, M., and McGhee, C.N. (2003). Attitudes to research and research training among ophthalmologists and ophthalmology trainees in New Zealand. Clinical & experimental ophthalmology *31*, 294-299.

Jiang, X., Rowitch, D.H., Soriano, P., McMahon, A.P., and Sucov, H.M. (2000). Fate of the mammalian cardiac neural crest. Development *127*, 1607-1616.

Jiang, Y.S., Jiang, T., Huang, B., Chen, P.S., and Ouyang, J. (2013). Epithelial-mesenchymal transition of renal tubules: divergent processes of repairing in acute or chronic injury? Med Hypotheses *81*, 73-75.

Jin, S.W., Beis, D., Mitchell, T., Chen, J.N., and Stainier, D.Y. (2005). Cellular and molecular analyses of vascular tube and lumen formation in zebrafish. Development *132*, 5199-5209.

Jodoin, J.N., Shboul, M., Albrecht, T.R., Lee, E., Wagner, E.J., Reversade, B., and Lee, L.A. (2013). The snRNA-processing complex, Integrator, is required for ciliogenesis and dynein recruitment to the nuclear envelope via distinct mechanisms. Biol Open *2*, 1390-1396.

Kaestner, L., Scholz, A., Hammer, K., Vecerdea, A., Ruppenthal, S., and Lipp, P. (2009). Isolation and Genetic Manipulation of Adult Cardiac Myocytes for Confocal Imaging. J Vis Exp, e1433.

Kamisago, M., Sharma, S.D., DePalma, S.R., Solomon, S., Sharma, P., McDonough, B., Smoot, L., Mullen, M.P., Woolf, P.K., Wigle, E.D.*, et al.* (2000). Mutations in sarcomere

protein genes as a cause of dilated cardiomyopathy. The New England journal of medicine *343*, 1688-1696.

Kasemeier-Kulesa, J.C., Bradley, R., Pasquale, E.B., Lefcort, F., and Kulesa, P.M. (2006). Eph/ephrins and N-cadherin coordinate to control the pattern of sympathetic ganglia. Development *133*, 4839-4847.

Katora, M.E., and Hollis, T.M. (1976). Regional variation in rat aortic endothelial surface morphology: relationship to regional aortic permeability. Exp Mol Pathol *24*, 23-34.

Kaverina, I., Krylyshkina, O., and Small, J.V. (1999). Microtubule targeting of substrate contacts promotes their relaxation and dissociation. J Cell Biol *146*, 1033-1044.

Kaverina, I., Rottner, K., and Small, J.V. (1998). Targeting, capture, and stabilization of microtubules at early focal adhesions. J Cell Biol *142*, 181-190.

Kaverina, I., and Straube, A. (2011). Regulation of cell migration by dynamic microtubules. Semin Cell Dev Biol *22*, 968-974.

Kawabe, J.I., and Hasebe, N. (2014). Role of the Vasa Vasorum and Vascular Resident Stem Cells in Atherosclerosis. Biomed Res Int *2014*, 701571.

Kelly, R.G., Brown, N.A., and Buckingham, M.E. (2001). The arterial pole of the mouse heart forms from Fgf10-expressing cells in pharyngeal mesoderm. Dev Cell *1*, 435-440.

Khairallah, R.J., Shi, G., Sbrana, F., Prosser, B.L., Borroto, C., Mazaitis, M.J., Hoffman, E.P., Mahurkar, A., Sachs, F., Sun, Y.*, et al.* (2012). Microtubules underlie dysfunction in duchenne muscular dystrophy. Sci Signal *5*, ra56.

Kinder, S.J., Loebel, D.A., and Tam, P.P. (2001). Allocation and early differentiation of cardiovascular progenitors in the mouse embryo. Trends Cardiovasc Med *11*, 177-184.

Kinsella, M.G., and Fitzharris, T.P. (1980). Origin of cushion tissue in the developing chick heart: cinematographic recordings of in situ formation. Science *207*, 1359-1360.

Kirby, M.L., Gale, T.F., and Stewart, D.E. (1983). Neural crest cells contribute to normal aorticopulmonary septation. Science *220*, 1059-1061.

Ko, Y.S., Coppen, S.R., Dupont, E., Rothery, S., and Severs, N.J. (2001). Regional differentiation of desmin, connexin43, and connexin45 expression patterns in rat aortic smooth muscle. Arterioscler Thromb Vasc Biol *21*, 355-364.

Komiyama, M., Ito, K., and Shimada, Y. (1987). Origin and development of the epicardium in the mouse embryo. Anat Embryol (Berl) *176*, 183-189.

Kong, H.H., and Segre, J.A. (2010). Bridging the translational research gap: a successful partnership involving a physician and a basic scientist. The Journal of investigative dermatology *130*, 1478-1480.

Kulesa, P.M., and Gammill, L.S. (2010). Neural crest migration: patterns, phases and signals. Dev Biol *344*, 566-568.

Kuro-o, M., Nagai, R., Nakahara, K., Katoh, H., Tsai, R.C., Tsuchimochi, H., Yazaki, Y., Ohkubo, A., and Takaku, F. (1991). cDNA cloning of a myosin heavy chain isoform in embryonic smooth muscle and its expression during vascular development and in arteriosclerosis. J Biol Chem *266*, 3768-3773.

Landerholm, T.E., Dong, X.R., Lu, J., Belaguli, N.S., Schwartz, R.J., and Majesky, M.W. (1999). A role for serum response factor in coronary smooth muscle differentiation from proepicardial cells. Development *126*, 2053-2062.

Le Douarin, N., and Kalcheim, C. (1999). The neural crest, 2nd edn (Cambridge, UK ; New York, NY, USA, Cambridge University Press).

Le Lievre, C.S., and Le Douarin, N.M. (1975). Mesenchymal derivatives of the neural crest: analysis of chimaeric quail and chick embryos. Journal of embryology and experimental morphology *34*, 125-154.

Leroux-Berger, M., Queguiner, I., Maciel, T.T., Ho, A., Relaix, F., and Kempf, H. (2011). Pathological calcification of adult vascular smooth muscle cells differs upon their crest or mesodermal embryonic origin. J Bone Miner Res.

Li, L., Miano, J.M., Cserjesi, P., and Olson, E.N. (1996a). SM22 alpha, a marker of adult smooth muscle, is expressed in multiple myogenic lineages during embryogenesis. Circ Res *78*, 188-195.

Li, W., Zhao, Y., and Chou, I.N. (1996b). Nickel (Ni2+) enhancement of alpha-tubulin acetylation in cultured 3T3 cells. Toxicol Appl Pharmacol *140*, 461-470.

Liao, H., Winkfein, R.J., Mack, G., Rattner, J.B., and Yen, T.J. (1995). CENP-F is a protein of the nuclear matrix that assembles onto kinetochores at late G2 and is rapidly degraded after mitosis. J Cell Biol *130*, 507-518.

Lie-Venema, H., van den Akker, N.M., Bax, N.A., Winter, E.M., Maas, S., Kekarainen, T., Hoeben, R.C., deRuiter, M.C., Poelmann, R.E., and Gittenberger-de Groot, A.C. (2007). Origin, fate, and function of epicardium-derived cells (EPDCs) in normal and abnormal cardiac development. ScientificWorldJournal *7*, 1777-1798.

Lin, S.L., Li, B., Rao, S., Yeo, E.J., Hudson, T.E., Nowlin, B.T., Pei, H., Chen, L., Zheng, J.J., Carroll, T.J.*, et al.* (2010). Macrophage Wnt7b is critical for kidney repair and regeneration. Proc Natl Acad Sci U S A *107*, 4194-4199.

Liu, L., Vo, A., Liu, G., and McKeehan, W.L. (2005a). Distinct structural domains within C19ORF5 support association with stabilized microtubules and mitochondrial aggregation and genome destruction. Cancer Res *65*, 4191-4201.

Liu, L., Vo, A., and McKeehan, W.L. (2005b). Specificity of the methylation-suppressed A isoform of candidate tumor suppressor RASSF1 for microtubule hyperstabilization is determined by cell death inducer C19ORF5. Cancer Res *65*, 1830-1838.

Liu, S.C., Sauter, E.R., Clapper, M.L., Feldman, R.S., Levin, L., Chen, S.Y., Yen, T.J., Ross, E., Engstrom, P.F., and Klein-Szanto, A.J. (1998). Markers of cell proliferation in normal epithelia and dysplastic leukoplakias of the oral cavity. Cancer Epidemiol Biomarkers Prev *7*, 597-603.

Luk, A., Ahn, E., Soor, G.S., and Butany, J. (2009). Dilated cardiomyopathy: a review. J Clin Pathol *62*, 219-225.

Majesky, M.W., Dong, X.R., and Hoglund, V.J. (2011). Parsing aortic aneurysms: more surprises. Circ Res *108*, 528-530.

Manabe, I., and Owens, G.K. (2001). The smooth muscle myosin heavy chain gene exhibits smooth muscle subtype-selective modular regulation in vivo. J Biol Chem *276*, 39076-39087.

Marincola, F.M. (2003). Translational Medicine: A two-way road. Journal of translational medicine *1*, 1.

Markwald, R.R., Fitzharris, T.P., and Manasek, F.J. (1977). Structural development of endocardial cushions. Am J Anat *148*, 85-119.

McClain, D.A. (2010). Bridging the gap between basic and clinical investigation. Trends in biochemical sciences *35*, 187-188.

Meir, K.S., and Leitersdorf, E. (2004). Atherosclerosis in the apolipoprotein-E-deficient mouse: a decade of progress. Arterioscler Thromb Vasc Biol *24*, 1006-1014.

Meissner, M.H., Moneta, G., Burnand, K., Gloviczki, P., Lohr, J.M., Lurie, F., Mattos, M.A., McLafferty, R.B., Mozes, G., Rutherford, R.B.*, et al.* (2007). The hemodynamics and diagnosis of venous disease. J Vasc Surg *46 Suppl S*, 4S-24S.

Mikawa, T., and Gourdie, R.G. (1996). Pericardial mesoderm generates a population of coronary smooth muscle cells migrating into the heart along with ingrowth of the epicardial organ. Dev Biol *174*, 221-232.

Miller, P.M., Folkmann, A.W., Maia, A.R., Efimova, N., Efimov, A., and Kaverina, I. (2009). Golgi-derived CLASP-dependent microtubules control Golgi organization and polarized trafficking in motile cells. Nat Cell Biol *11*, 1069-1080.

Minakata, K., Dearani, J.A., Schaff, H.V., O'Leary, P.W., Ommen, S.R., and Danielson, G.K. (2005). Mechanisms for recurrent left ventricular outflow tract obstruction after septal myectomy for obstructive hypertrophic cardiomyopathy. Ann Thorac Surg *80*, 851-856.

Mizia-Stec, K., Gasior, Z., Wojnicz, R., Haberka, M., Mielczarek, M., Wierzbicki, A., Pstras, K., and Hartleb, M. (2008). Severe dilated cardiomyopathy as a consequence of Ecstasy intake. Cardiovasc Pathol *17*, 250-253.

Morrison, S.J., Csete, M., Groves, A.K., Melega, W., Wold, B., and Anderson, D.J. (2000). Culture in reduced levels of oxygen promotes clonogenic sympathoadrenal differentiation by isolated neural crest stem cells. J Neurosci *20*, 7370-7376.

Morrison, S.J., White, P.M., Zock, C., and Anderson, D.J. (1999). Prospective identification, isolation by flow cytometry, and in vivo self-renewal of multipotent mammalian neural crest stem cells. Cell *96*, 737-749.

Moynihan, K.L., Pooley, R., Miller, P.M., Kaverina, I., and Bader, D.M. (2009a). Murine CENP-F regulates centrosomal microtubule nucleation and interacts with Hook2 at the centrosome. Mol Biol Cell *20*, 4790-4803.

Moynihan, K.L., Pooley, R., Miller, P.M., Kaverina, I., and Bader, D.M. (2009b). Murine CENP-F regulates centrosomal microtubule nucleation and interacts with Hook2 at the centrosome. Mol Biol Cell *20*, 4790-4803.

Mundell, N.A., and Labosky, P.A. (2011). Neural crest stem cell multipotency requires Foxd3 to maintain neural potential and repress mesenchymal fates. Development *138*, 641-652.

Muretta, J.M., and Thomas, D.D. (2013). Mutation that causes hypertrophic cardiomyopathy increases force production in human beta-cardiac myosin. Proc Natl Acad Sci U S A *110*, 12507-12508.

Nekrep, N., Wang, J., Miyatsuka, T., and German, M.S. (2008). Signals from the neural crest regulate beta-cell mass in the pancreas. Development *135*, 2151-2160.

Nogami, A. (2011). Prukinje-Related Arrhythmias Part I: Monomorphic Ventricular Tachycardias. Pacing and Clinical Electrophysiology *34*, 624-250.

Novaes, R.D., Penitente, A.R., Goncalves, R.V., Talvani, A., Neves, C.A., Maldonado, I.R.S.C., and Natali, A.J. (2011). Effects of Trypanosoma cruzi infection on myocardial morphology, single cardiomyocyte contractile function and exercise tolerance in rats. Int J Exp Pathol *92*, 299-307.

O'Sullivan, J.J., Derrick, G., and Darnell, R. (2002). Prevalence of hypertension in children after early repair of coarctation of the aorta: a cohort study using casual and 24 hour blood pressure measurement. Heart *88*, 163-166.

Oka, T., Xu, J., and Molkentin, J.D. (2007). Re-employment of developmental transcription factors in adult heart disease. Semin Cell Dev Biol *18*, 117-131.

Olley, P.M., and Coceani, F. (1981). Prostaglandins and the ductus arteriosus. Annu Rev Med *32*, 375-385.

Osborne, N.J., Begbie, J., Chilton, J.K., Schmidt, H., and Eickholt, B.J. (2005). Semaphorin/neuropilin signaling influences the positioning of migratory neural crest cells within the hindbrain region of the chick. Developmental dynamics : an official publication of the American Association of Anatomists *232*, 939-949.

Owens, G.K. (1995). Regulation of differentiation of vascular smooth muscle cells. Physiol Rev *75*, 487-517.

Owens, G.K., Kumar, M.S., and Wamhoff, B.R. (2004). Molecular regulation of vascular smooth muscle cell differentiation in development and disease. Physiol Rev *84*, 767-801.

Papadimou, E., Menard, C., Grey, C., and Puceat, M. (2005). Interplay between the retinoblastoma protein and LEK1 specifies stem cells toward the cardiac lineage. Embo J *24*, 1750-1761.

Papanicolaou, K.N., Streicher, J.M., Ishikawa, T.-o., Herschman, H., Wang, Y., and Walsh, K. (2010). Preserved heart function and maintained response to cardiac stresses in a genetic model of cardiomyocyte-targeted deficiency of cyclooxygenase-2. J Mol Cell Cardiol *49*, 196-209.

Park, M., Vatner, S.F., Yan, L., Gao, S., Yoon, S., Lee, G.J.A., Xie, L.-H., Kitsis, R.N., and Vatner, D.E. (2013). Novel mechanisms for caspase inhibition protecting cardiac function wth chronic pressure overload. Basic Res Cardiol *108*.

Passman, J.N., Dong, X.R., Wu, S.P., Maguire, C.T., Hogan, K.A., Bautch, V.L., and Majesky, M.W. (2008). A sonic hedgehog signaling domain in the arterial adventitia supports resident Sca1+ smooth muscle progenitor cells. Proc Natl Acad Sci U S A *105*, 9349-9354.

Perez-Pomares, J.M., Carmona, R., Gonzalez-Iriarte, M., Atencia, G., Wessels, A., and Munoz-Chapuli, R. (2002). Origin of coronary endothelial cells from epicardial mesothelium in avian embryos. Int J Dev Biol *46*, 1005-1013.

Petrie, R.J., Doyle, A.D., and Yamada, K.M. (2009). Random versus directionally persistent cell migration. Nat Rev Mol Cell Biol *10*, 538-549.

Pfaltzgraff, E.R., Mundell, N.A., and Labosky, P.A. (2012). Isolation and culture of neural crest cells from embryonic murine neural tube. J Vis Exp, e4134.

Pfaltzgraff, E.R., Shelton, E.L., Galindo, C.L., Nelms, B.L., Hooper, C.W., Poole, S.D., Labosky, P.A., Bader, D.M., and Reese, J. (2014). Embryonic domains of the aorta derived from diverse origins exhibit distinct properties that converge into a common phenotype in the adult. J Mol Cell Cardiol *69*, 88-96.

Piano, M.R. (2002). Alcoholic cardiomyopathy: incidence, clinical characteristics, and pathophysiology. Chest *121*, 1638-1650.

Plank, J.L., Mundell, N.A., Frist, A.Y., LeGrone, A.W., Kim, T., Musser, M.A., Walter, T.J., and Labosky, P.A. (2011). Influence and timing of arrival of murine neural crest on pancreatic beta cell development and maturation. Dev Biol *349*, 321-330.

Pooley, R.D., Moynihan, K.L., Soukoulis, V., Reddy, S., Francis, R., Lo, C., Ma, L.J., and Bader, D.M. (2008). Murine CENPF interacts with syntaxin 4 in the regulation of vesicular transport. J Cell Sci *121*, 3413-3421.

Pooley, R.D., Reddy, S., Soukoulis, V., Roland, J.T., Goldenring, J.R., and Bader, D.M. (2006). CytLEK1 is a regulator of plasma membrane recycling through its interaction with SNAP-25. Mol Biol Cell *17*, 3176-3186.

Pruett, N.D., Hajdu, Z., Zhang, J., Visconti, R.P., Kern, M.J., Wellik, D.M., Majesky, M.W., and Awgulewitsch, A. (2012). Changing topographic Hox expression in blood vessels results in regionally distinct vessel wall remodeling. Biol Open *1*, 430-435.

Pruett, N.D., Visconti, R.P., Jacobs, D.F., Scholz, D., McQuinn, T., Sundberg, J.P., and Awgulewitsch, A. (2008). Evidence for Hox-specified positional identities in adult vasculature. BMC Dev Biol *8*, 93.

Que, J., Wilm, B., Hasegawa, H., Wang, F., Bader, D., and Hogan, B.L. (2008). Mesothelium contributes to vascular smooth muscle and mesenchyme during lung development. Proc Natl Acad Sci U S A *105*, 16626-16630.

Rajabi, M., Kassiotis, C., Razeghi, P., and Taegtmeyer, H. (2007). Return to the fetal gene program protects the stressed heart: a strong hypothesis. Heart Fail Rev *12*, 331-343.

Rattner, J.B., Rao, A., Fritzler, M.J., Valencia, D.W., and Yen, T.J. (1993). CENP-F is a .ca 400 kDa kinetochore protein that exhibits a cell-cycle dependent localization. Cell Motil Cytoskeleton *26*, 214-226.

Rattner, J.B., Rees, J., Whitehead, C.M., Casiano, C.A., Tan, E.M., Humbel, R.L., Conrad, K., and Fritzler, M.J. (1997). High frequency of neoplasia in patients with autoantibodies to centromere protein CENP-F. Clin Invest Med *20*, 308-319.

Reese, J., O'Mara, P.W., Poole, S.D., Brown, N., Tolentino, C., Eckman, D.M., and Aschner, J.L. (2009). Regulation of the fetal mouse ductus arteriosus is dependent on interaction of nitric oxide and COX enzymes in the ductal wall. Prostaglandins Other Lipid Mediat *88*, 89-96.

Ren, X., Gomez, G.A., Zhang, B., and Lin, S. (2010). Scl isoforms act downstream of etsrp to specify angioblasts and definitive hematopoietic stem cells. Blood *115*, 5338-5346.

Rensen, S.S., Doevendans, P.A., and van Eys, G.J. (2007). Regulation and characteristics of vascular smooth muscle cell phenotypic diversity. Neth Heart J *15*, 100-108.

Reslan, O.M., Yin, Z., do Nascimento, G.R., and Khalil, R.A. (2013). Subtype-Specific Estrogen Receptor-Mediated Vasodilator Activity in the Cephalic, Thoracic and Abdominal Vasculature of Female Rat. J Cardiovasc Pharmacol.

Restifo, L.L., and Phelan, G.R. (2011). The cultural divide: exploring communication barriers between scientists and clinicians. Disease models & mechanisms *4*, 423-426.

Rich, S., and Brundage, B.H. (1987). High-dose calcium channel-blocking therapy for primary pulmonary hypertension: evidence for long-term reduction in pulmonary arterial pressure and regression of right ventricular hypertrophy. Circulation *76*, 135-141.

Rinkevich, Y., Mori, T., Sahoo, D., Xu, P.X., Bermingham, J.R., Jr., and Weissman, I.L. (2012). Identification and prospective isolation of a mesothelial precursor lineage giving rise to smooth muscle cells and fibroblasts for mammalian internal organs, and their vasculature. Nat Cell Biol *14*, 1251-1260.

Roberts, S.F., Fischhoff, M.A., Sakowski, S.A., and Feldman, E.L. (2012). Perspective: Transforming science into medicine: how clinician-scientists can build bridges across research's "valley of death". Academic medicine : journal of the Association of American Medical Colleges *87*, 266-270.

Rosenquist, T.H., Beall, A.C., Modis, L., and Fishman, R. (1990). Impaired elastic matrix development in the great arteries after ablation of the cardiac neural crest. Anat Rec *226*, 347-359.

Rubio, D.M., Schoenbaum, E.E., Lee, L.S., Schteingart, D.E., Marantz, P.R., Anderson, K.E., Platt, L.D., Baez, A., and Esposito, K. (2010). Defining translational research: implications for training. Academic medicine : journal of the Association of American Medical Colleges *85*, 470-475.

Ruckman, J.L., Luvalle, P.A., Hill, K.E., Giro, M.G., and Davidson, J.M. (1994). Phenotypic stability and variation in cells of the porcine aorta: collagen and elastin production. Matrix Biol *14*, 135-145.

Saga, Y., Miyagawa-Tomita, S., Takagi, A., Kitajima, S., Miyazaki, J., and Inoue, T. (1999). MesP1 is expressed in the heart precursor cells and required for the formation of a single heart tube. Development *126*, 3437-3447.

Saint-Jeannet, J.-P. (2006). Neural crest induction and differentiation (New York, N.Y. Georgetown, Tex., Springer Science+Business Media ;
Landes Bioscience/Eurekah.com).

Samson, F., Donoso, J.A., Heller-Bettinger, I., Watson, D., and Himes, R.H. (1979). Nocodazole action on tubulin assembly, axonal ultrastructure and fast axoplasmic transport. J Pharmacol Exp Ther *208*, 411-417.

Sastry, S.K., and Burridge, K. (2000). Focal adhesions: a nexus for intracellular signaling and cytoskeletal dynamics. Exp Cell Res *261*, 25-36.

Sato, Y., Watanabe, T., Saito, D., Takahashi, T., Yoshida, S., Kohyama, J., Ohata, E., Okano, H., and Takahashi, Y. (2008). Notch mediates the segmental specification of angioblasts in somites and their directed migration toward the dorsal aorta in avian embryos. Dev Cell *14*, 890-901.

Schmidt, A., Brixius, K., and Bloch, W. (2007). Endothelial precursor cell migration during vasculogenesis. Circ Res *101*, 125-136.

Schwarz, Q., Maden, C.H., Vieira, J.M., and Ruhrberg, C. (2009). Neuropilin 1 signaling guides neural crest cells to coordinate pathway choice with cell specification. Proc Natl Acad Sci U S A *106*, 6164-6169.

Shakir, D.K., and Rasul, K.I. (2009). Chemotherapy induced cardiomyopathy: pathogenesis, monitoring and management. J Clin Med Res *1*, 8-12.

Shelton, E.L., Ector, G., Galindo, C.L., Hooper, C., Brown, N., Wilkerson, I., Pfaltzgraff, E.R., Paria, B.C., Cotton, R.B., Stoller, J.Z.*, et al.* (2014). Transcriptional profiling reveals ductus arteriosus-specific genes that regulate vascular tone. Physiol Genomics.

Sherwin, T. (2003). In search of the clinical scientist. Clinical & experimental ophthalmology *31*, 284-285.

Shirwany, N.A., and Zou, M.H. (2010). Arterial stiffness: a brief review. Acta Pharmacol Sin *31*, 1267-1276.

Sieber-Blum, M., and Cohen, A.M. (1980). Clonal analysis of quail neural crest cells: they are pluripotent and differentiate in vitro in the absence of noncrest cells. Dev Biol *80*, 96-106.

Simon, M.C., and Keith, B. (2008). The role of oxygen availability in embryonic development and stem cell function. Nat Rev Mol Cell Biol *9*, 285-296.

Small, J.V., Geiger, B., Kaverina, I., and Bershadsky, A. (2002). How do microtubules guide migrating cells? Nat Rev Mol Cell Biol *3*, 957-964.

Smith, C.L., Jarrett, M., and Bierer, S.B. (2013). Integrating Clinical Medicine Into Biomedical Graduate Education to Promote Translational Research: Strategies From Two New PhD Programs. Acad Med *88*, 137-143.

Soukoulis, V., Reddy, S., Pooley, R.D., Feng, Y., Walsh, C.A., and Bader, D.M. (2005a). Cytoplasmic LEK1 is a regulator of microtubule function through its interaction with the LIS1 pathway. Proc Natl Acad Sci U S A *102*, 8549-8554.

Soukoulis, V., Reddy, S., Pooley, R.D., Feng, Y., Walsh, C.A., and Bader, D.M. (2005b). Cytoplasmic LEK1 is a regulator of microtubule function through its interaction with the LIS1 pathway. Proc Natl Acad Sci U S A *102*, 8549-8554.

Splawski, I., Timothy, K.W., Sharpe, L.M., Decher, N., Kumar, P., Bloise, R., Napolitano, C., Schwartz, P.J., Joseph, R.M., Condouris, K.*, et al.* (2004). CaV1.2 Calcium Channel Dysfunction Causes a Multisystem Disorder Including Arrhythmia and Autism. Cell *119*, 19-31.

Stankunas, K., Hang, C.T., Tsun, Z.Y., Chen, H., Lee, N.V., Wu, J.I., Shang, C., Bayle, J.H., Shou, W., Iruela-Arispe, M.L.*, et al.* (2008). Endocardial Brg1 represses ADAMTS1 to maintain the microenvironment for myocardial morphogenesis. Dev Cell *14*, 298-311.

Steinherz, L.J., Steinherz, P.G., Tan, C.T., Heller, G., and Murphy, M.L. (1991). Cardiac toxicity 4 to 20 years after completing anthracycline therapy. Jama *266*, 1672-1677.

Stemple, D.L., and Anderson, D.J. (1992). Isolation of a stem cell for neurons and glia from the mammalian neural crest. Cell *71*, 973-985.

Stenmark, K.R., and Mecham, R.P. (1997). Cellular and molecular mechanisms of pulmonary vascular remodeling. Annu Rev Physiol *59*, 89-144.

Steudel, W., Scherrer-Crosbie, M., Bloch, K.D., Weimann, J., Huang, P.L., Jones, R.C., Picard, M.H., and Zapol, W.M. (1998). Sustained pulmonary hypertension and right ventricular hypertrophy after chronic hypoxia in mice with congenital deficiency of nitric oxide synthase 3. J Clin Invest *101*, 2468-2477.

Subbiah, M.T., Bale, L.K., Dinh, D.M., Kottke, B.A., and Deitemeyer, D. (1981). Regional aortic differences in atherosclerosis-susceptibility: changes in prostaglandin biosynthesis and cholesterol accumulation in response to desoxycorticosterone (DOCA)-salt induced hypertension. Virchows Arch B Cell Pathol Incl Mol Pathol *37*, 309-315.

Sufka, K.J., Stratton, D.B., and Giordano, J. (1990). Regional differences in serotonergic contractile sensitivity mediated by 5-HT2 receptors in rat aorta. Artery *18*, 47-53.

Swain, S.M., Whaley, F.S., and Ewer, M.S. (2003). Congestive heart failure in patients treated with doxorubicin: a retrospective analysis of three trials. Cancer *97*, 2869-2879.

Tanous, D., Benson, L.N., and Horlick, E.M. (2009). Coarctation of the aorta: evaluation and management. Curr Opin Cardiol *24*, 509-515.

Theisen, U., Straube, E., and Straube, A. (2012). Directional persistence of migrating cells requires Kif1C-mediated stabilization of trailing adhesions. Dev Cell *23*, 1153-1166.

Thery, M., Racine, V., Piel, M., Pepin, A., Dimitrov, A., Chen, Y., Sibarita, J.B., and Bornens, M. (2006). Anisotropy of cell adhesive microenvironment governs cell internal organization and orientation of polarity. Proc Natl Acad Sci U S A *103*, 19771-19776.

Thieszen, S.L., Dalton, M., Gadson, P.F., Patterson, E., and Rosenquist, T.H. (1996). Embryonic lineage of vascular smooth muscle cells determines responses to collagen matrices and integrin receptor expression. Exp Cell Res *227*, 135-145.

Tomanek, R.J. (2005). Formation of the coronary vasculature during development. Angiogenesis *8*, 273-284.

Touchberry, C.D., Green, T.M., Tchikrozov, V., Mannix, J.E., Mao, T.F., Carney, B.W., Girgis, M., Vincent, R.J., Wetmore, L.A., Dawn, B.*, et al.* (2013). FGF23 is a novel regulator of intracellular calcium and cardiac contractility in addition to cardiac hypertophy. American Journal of Physiology - Endocrinology and Metabolism.

Traub, O., and Berk, B.C. (1998). Laminar shear stress: mechanisms by which endothelial cells transduce an atheroprotective force. Arterioscler Thromb Vasc Biol *18*, 677-685.

Trigueros-Motos, L., Gonzalez-Granado, J.M., Cheung, C., Fernandez, P., Sanchez-Cabo, F., Dopazo, A., Sinha, S., and Andres, V. (2013). Embryological-Origin-Dependent Differences in Hox Expression in Adult Aorta: Role in Regional Phenotypic Variability and Regulation of NF-kappaB Activity. Arterioscler Thromb Vasc Biol.

Tschernatsch, M., Stolz, E., Strittmatter, M., Kaps, M., and Blaes, F. (2005). Antinuclear antibodies define a subgroup of paraneoplastic neuropathies: clinical and immunological data. J Neurol Neurosurg Psychiatry *76*, 1702-1706.

Uchida, M., Mourino-Perez, R.R., and Roberson, R.W. (2010). Live-cell imaging of microtubule dynamics in hyphae of Neurospora crassa. Methods Mol Biol *638*, 259-268.

Vainio, L., Perjes, A., Ryti, N., Magga, J., Alakoski, T., Serpi, R., Kaikkonen, L., Piuhola, J., Szokodi, I., Ruskoaho, H.*, et al.* (2012). Neronostatin, a Novel Peptide Encoded by Somatostatin Gene, Regulates Cardiac Contractile Function and Cardiomyocytes Survival. J Biol Chem *287*, 4572-4580.

Van Assche, T., Hendrickx, J., Crauwels, H.M., Guns, P.J., Martinet, W., Fransen, P., Raes, M., and Bult, H. (2011). Transcription profiles of aortic smooth muscle cells from

atherosclerosis-prone and -resistant regions in young apolipoprotein E-deficient mice before plaque development. J Vasc Res *48*, 31-42.

van Meurs-van Woezik, H., Klein, H.W., Markus-Silvis, L., and Krediet, P. (1983). Comparison of the growth of the tunica media of the ascending aorta, aortic isthmus and descending aorta in infants and children. J Anat *136*, 273-281.

VanderLaan, P.A., Reardon, C.A., and Getz, G.S. (2004). Site specificity of atherosclerosis: site-selective responses to atherosclerotic modulators. Arterioscler Thromb Vasc Biol *24*, 12-22.

Varis, A., Salmela, A.L., and Kallio, M.J. (2006). Cenp-F (mitosin) is more than a mitotic marker. Chromosoma *115*, 288-295.

Vergnolle, M.A., and Taylor, S.S. (2007). Cenp-F links kinetochores to Ndel1/Nde1/Lis1/dynein microtubule motor complexes. Curr Biol *17*, 1173-1179.

Vokes, S.A., and Krieg, P.A. (2002). Endoderm is required for vascular endothelial tube formation, but not for angioblast specification. Development *129*, 775-785.

von Roth, P., Canny, B.J., Volk, H.D., Noble, J.A., Prober, C.G., Perka, C., and Duda, G.N. (2011). The challenges of modern interdisciplinary medical research. Nat Biotechnol *29*, 1145-1148.

Wagenseil, J.E., and Mecham, R.P. (2009). Vascular extracellular matrix and arterial mechanics. Physiol Rev *89*, 957-989.

Wagner, M., and Siddiqui, M.A. (2007). Signal transduction in early heart development (II): ventricular chamber specification, trabeculation, and heart valve formation. Exp Biol Med (Maywood) *232*, 866-880.

Wasteson, P., Johansson, B.R., Jukkola, T., Breuer, S., Akyurek, L.M., Partanen, J., and Lindahl, P. (2008). Developmental origin of smooth muscle cells in the descending aorta in mice. Development *135*, 1823-1832.

Webb, D.J., Parsons, J.T., and Horwitz, A.F. (2002). Adhesion assembly, disassembly and turnover in migrating cells -- over and over and over again. Nat Cell Biol *4*, E97-100.

Webster, D.R., and Borisy, G.G. (1989). Microtubules are acetylated in domains that turn over slowly. J Cell Sci *92 (Pt 1)*, 57-65.

Webster, D.R., Gundersen, G.G., Bulinski, J.C., and Borisy, G.G. (1987). Assembly and turnover of detyrosinated tubulin in vivo. J Cell Biol *105*, 265-276.

Wei, Y., Bader, D., and Litvin, J. (1996). Identification of a novel cardiac-specific transcript critical for cardiac myocyte differentiation. Development *122*, 2779-2789.

Weltman, N.Y., Wang, D., Redetzke, R.A., and Gerdes, A.M. (2012). Longstanding Hyperthyroidism is Associated with Normal or Enhanced Intrinsic Cardiomyocyte Function despite Decline in Global Cardiac Function. PLoS One *7*, e46655.

White, P.M., Morrison, S.J., Orimoto, K., Kubu, C.J., Verdi, J.M., and Anderson, D.J. (2001). Neural crest stem cells undergo cell-intrinsic developmental changes in sensitivity to instructive differentiation signals. Neuron *29*, 57-71.

Wilm, B., Ipenberg, A., Hastie, N.D., Burch, J.B., and Bader, D.M. (2005). The serosal mesothelium is a major source of smooth muscle cells of the gut vasculature. Development *132*, 5317-5328.

Winters, N.I., Williams, A.M., and Bader, D.M. (2014). Resident progenitors, not exogenous migratory cells, generate the majority of visceral mesothelium in organogenesis. Dev Biol.

Wolinsky, H., and Glagov, S. (1964). Structural Basis for the Static Mechanical Properties of the Aortic Media. Circ Res *14*, 400-413.

Wolinsky, H., and Glagov, S. (1967). A lamellar unit of aortic medial structure and function in mammals. Circ Res *20*, 99-111.

Woo, K.V., Qu, X., Babaev, V.R., Linton, M.F., Guzman, R.J., Fazio, S., and Baldwin, H.S. (2011). Tie1 attenuation reduces murine atherosclerosis in a dose-dependent and shear stress-specific manner. J Clin Invest *121*, 1624-1635.

Yang, Z., Guo, J., Chen, Q., Ding, C., Du, J., and Zhu, X. (2005). Silencing mitosin induces misaligned chromosomes, premature chromosome decondensation before anaphase onset, and mitotic cell death. Mol Cell Biol *25*, 4062-4074.

Yutzey, K.E., Rhee, J.T., and Bader, D. (1994). Expression of the atrial-specific myosin heavy chain AMHC1 and the establishment of anteroposterior polarity in the developing chicken heart. Development *120*, 871-883.

Zaffran, S., Kelly, R.G., Meilhac, S.M., Buckingham, M.E., and Brown, N.A. (2004). Right ventricular myocardium derives from the anterior heart field. Circ Res *95*, 261-268.

Zhang, H., Gu, S., Al-Sabeq, B., Wang, S., He, J., Tam, A., Cifelli, C., Mathalone, N., Tirgari, S., Boyd, S.*, et al.* (2012). Origin-specific epigenetic program correlates with vascular bed-specific differences in Rgs5 expression. Faseb J *26*, 181-191.

Zhou, B., and Pu, W.T. (2011). Epicardial epithelial-to-mesenchymal transition in injured heart. J Cell Mol Med *15*, 2781-2783.

Zhu, X., Mancini, M.A., Chang, K.H., Liu, C.Y., Chen, C.F., Shan, B., Jones, D., Yang-Feng, T.L., and Lee, W.H. (1995). Characterization of a novel 350-kilodalton nuclear phosphoprotein that is specifically involved in mitotic-phase progression. Mol Cell Biol *15*, 5017-5029.

Zuccolo, M., Alves, A., Galy, V., Bolhy, S., Formstecher, E., Racine, V., Sibarita, J.B., Fukagawa, T., Shiekhattar, R., Yen, T.*, et al.* (2007). The human Nup107-160 nuclear pore subcomplex contributes to proper kinetochore functions. Embo J *26*, 1853-1864.